

Supplementary Information for

Tantalum Ureate Complexes for Photocatalytic Hydroaminoalkylation

Han Hao^{§a}, Manfred Manßen^{§b}, Laurel L. Schafer^{c*}

[§] *These authors contributed equally.*

^a Department of Chemistry, University of Toronto, Toronto, Ontario M5S 3H6, Canada

^b Institut für Anorganische Chemie, Eberhard Karls Universität Tübingen, Auf der Morgenstelle 18, 72076, Tübingen, Germany.

^c Department of Chemistry, University of British Columbia, Vancouver, British Columbia V6T 1Z4, Canada

Contact: Prof. Laurel L. Schafer (schafer@chem.ubc.ca)

Table of Contents

S1.	General information	3
S2.	Synthesis of Metal Complexes and Substrates	4
S3.	General Procedure for Photocatalytic Hydroaminoalkylation Using Tantalum Ureate Photo Catalyst	6
S4.	Mechanistic Investigations	7
S4.1	Reaction with Tertiary Amines	7
S4.2	Amine Radical clock Experiment	7
S4.3	Alkene Radical Clock Experiment	7
S4.4	TEMPO Initiation Experiment	8
S4.5	Kinetic Isotope Effect	9
S5.	DFT Studies and Discussion	11
S6.	Photophysical Results	15
S7.	NMR Spectra	21
S8.	GC-MS Reports	73
S9.	Literature	78

S1. General information

All reactions were performed under a N₂ atmosphere using Schlenk or glovebox techniques, unless otherwise stated. All chemicals without a detailed synthesis description here were purchased from commercial sources (Sigma Aldrich, Alfa Aesar, TCI and Strem) and used without further purification, unless otherwise noted. All amines and alkenes were dried over CaH₂, distilled and degassed prior to use in catalytic experiments. Solvents were dried according to standard procedures and stored over activated molecular sieves (4 Å). Toluene-*d*₈ and C₆D₆ were purchased from Cambridge Isotope Laboratories, dried over sodium/ketyl and distilled prior to use. CDCl₃ was purchased from Cambridge Isotope Laboratories and used directly. Experiments conducted on an NMR tube scale were performed in J. Young NMR tubes (8" x 5 mm) sealed with screw-type Teflon caps. All glassware was dried in a 180 °C oven overnight before use.

¹H and ¹³C NMR spectra were recorded on Bruker 300 MHz and 400 MHz Avance spectrometers at ambient temperature. Chemical shifts (δ) are given relative to residual protons of the solvent and are reported in parts per million (ppm). Coupling constants *J* are given in Hertz (Hz). The following abbreviations are used to indicate signal multiplicity: s = singlet, d = doublet, t = triplet, q = quartet, m = multiplet, and br = broad. GC/MS analyses were conducted on an Agilent 7890B GC with an Agilent 5977 inert CI mass detector, utilizing methane as the ionization gas.

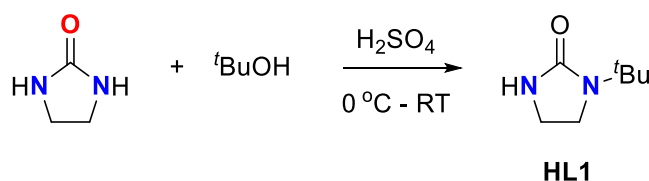
Calculations were performed using Gaussian 09 D.01 software.¹ The hybrid function M06L was used on all systems.² Def2-SVP basis sets were applied to all geometric optimizations and frequency calculations.³ Def2-TZVP basis sets were then applied for single point calculations. Solvent (toluene) effects were included using the SMD model.⁴ Orbital analysis was performed using Multiwfn,⁵ and molecular orbitals were illustrated using VMD.⁶

S2. Synthesis of Metal Complexes and Substrates

Tantalum Complexes and Ligands

Tantalum complexes and corresponding proteo ligands were prepared according to literature.⁷⁻¹⁰

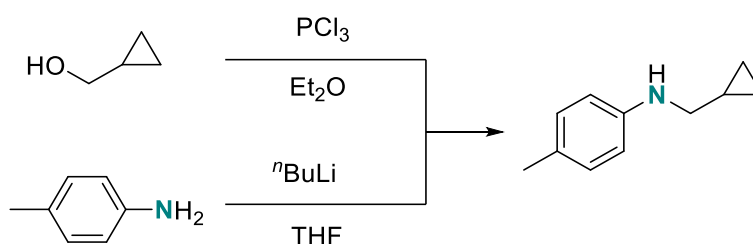
1-(^tButyl)imidazolidin-2-one (HL1)



HL1 was prepared following a modified literature procedure.¹¹ 2-Imidazolidone (1.7 g, 20 mmol) was slowly added to 5 ml ice-bath cooled concentrated sulfuric acid under vigorous stirring. The mixture was stirred for another 15 min, and ^tBuOH (3.0 g, 40 mmol) was added dropwise. The reaction was slowly warmed to room temperature and regularly checked by GC-MS until most 2-imidazolidone was consumed. The mixture was poured onto 100 g ice, neutralized using 1 M NaOH (aq.) and extracted using DCM (3 x 20 ml). The combined organic phases were washed with brine, dried over Na₂SO₄ and all solvent was removed in vacuo. The resulting solid was recrystallized from hexanes and sublimed under vacuum (1.2 g, 42%).

Cyclization and Radical Clock Substrates

N-(hex-5-en-1-yl)aniline and prop-1-en-2-ylcyclopropane were prepared following literature procedures.¹²⁻¹³



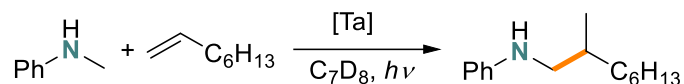
N-(cyclopropylmethyl)-4-methylaniline was prepared following a modified literature procedure. Cyclopropylmethanol (0.36 g, 5 mmol) was added to 10 ml Et₂O in a vial with a magnetic stir bar, and PCl₃ (0.34 g, 2.5 mmol) was added. The vial was capped and the mixture was stirred overnight. The top organic layer was taken out carefully using a Pasteur pipette without disturbing the bottom layer and passed through a CaCl₂ plug. The solution was used without further purification.

4-Methylaniline (0.85 g, 8 mmol) was charged into a N₂-filled Schlenk tube with stir bar, and 20 ml of dry THF was added. The Schlenk tube was cooled in a dry ice acetone bath and 1.6 M ⁿBuLi solution (4 ml, 6.4 mmol) was added. This mixture was stirred for another half an hour and after that, the Et₂O solution from the previous reaction was added dropwise. The mixture was slowly warmed to room temperature, quenched with saturated NH₄Cl (aq.), and extracted with Et₂O. The combined organic layers were dried in vacuo and the crude product was purified through column chromatography (SiO₂, 1:20 EtOAc:Hexanes) to give a colorless oil (0.36 g, 23%).

¹H NMR (C₆D₆, 300 MHz, 298K): δ = 7.00 (d, 2 H, J = 7.9 Hz), 6.44 (d, 2 H, J = 8.1 Hz), 3.26 (br. s, 1 H), 2.68 (t, 2 H, J = 6.2 Hz), 2.21 (s, 3 H), 0.86-0.69 (m, 1 H), 0.35-0.16 (m, 2 H), 0.06-0.13 (m, 2 H) ppm.

¹³C{¹H} NMR (C₆D₆, 75 MHz, 298K): δ = 146.91, 130.03, 126.12, 113.28, 49.21, 20.65, 11.21, 3.56 ppm.

S3. General Procedure for Photocatalytic Hydroaminoalkylation Using Tantalum Ureate Photo Catalyst



In a N₂-filled glove box Ta(CH₂SiMe₃)₃Cl₂ (**Ta1**, 5.1 mg, 0.01 mmol), **KL1** (1.8 mg, 0.01 mmol), *N*-methylaniline (10.7 mg, 0.1 mmol), 1-octene (11.2 mg, 0.1 mmol), 1,3,5-trimethoxybenzene (~3 mg, internal standard) were dissolved in 0.5 g Tol-*d*₈, and transferred to a J-Young NMR tube. The J-Young tube was capped and brought outside the glove box for a T₀ ¹H-NMR. After that, it was irradiated in front of a G4 tungsten-halogen lamp. The reaction was monitored by ¹H-NMR spectroscopy using 1,3,5-trimethoxybenzene as internal standard by integrating diagnostic signals, e.g. *ortho*-protons of the *N*-methylaniline vs. the signal of the internal standard at the start of the reaction and comparing this value with the signal of the *ortho*-protons of the amine product vs. the internal standard at various points as the reaction progressed.

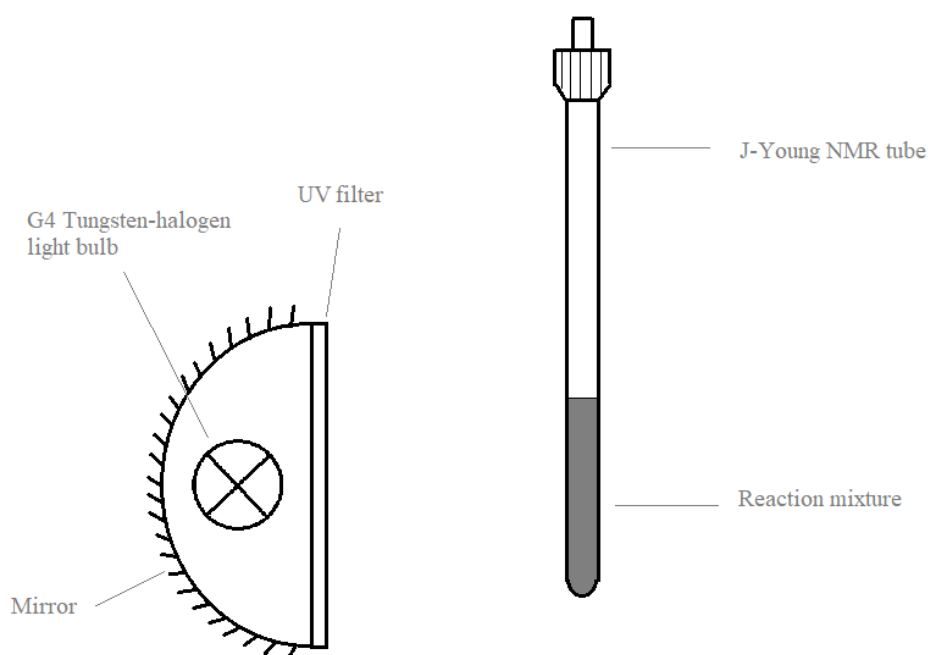
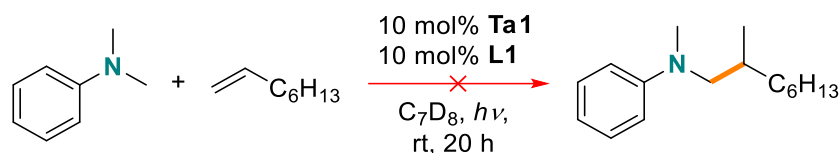


Figure S1. Photo reaction set up using a desk lamp

S4. Mechanistic Investigations

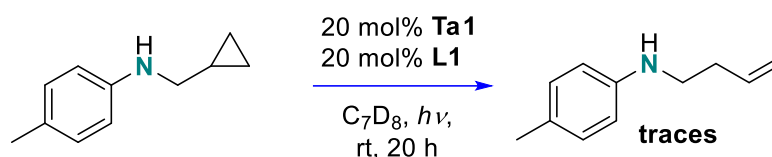
S4.1 Reaction with Tertiary Amines



Following the same procedure as for the general photocatalytic hydroaminoalkylation with *N,N*-dimethylaniline as amine substrate.

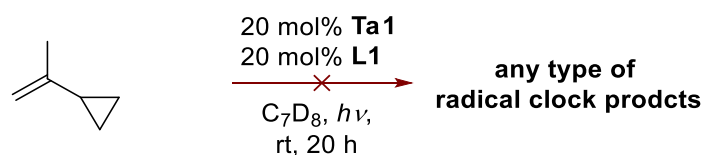
No consumption of *N,N*-dimethylaniline was observed by 1H -NMR spectroscopy monitoring and no product was detected in GC-MS.

S4.2 Amine Radical clock Experiment

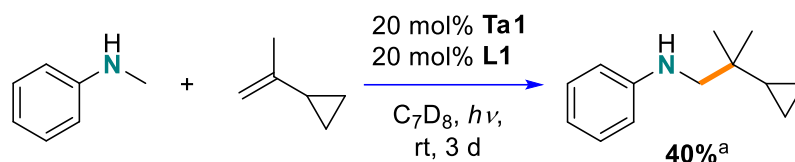


In a N_2 -filled glovebox *N*-(cyclopropylmethyl)-4-methylaniline (16.1 mg, 0.1 mmol), **Ta1** (10.2 mg, 0.02 mmol), **KL1** (3.6 mg, 0.02 mmol) and 1,3,5-trimethoxybenzene (~3 mg, internal standard) were dissolved in 0.5 g Tol- d_8 and transferred to a J-Young NMR tube. The J-Young tube was capped and brought outside the glove box for a T_0 1H -NMR spectrum. After that, it was irradiated in front of a G4 tungsten-halogen lamp for 20 h. Another 1H -NMR spectrum was taken. A new multiplet at approx. 5.1 ppm was found, which is close to the chemical shift of ring-opening products reported by the literature,¹⁴ suggesting possible amine radical formation (**Figure S88-90**).

S4.3 Alkene Radical Clock Experiment



In a N_2 -filled glovebox, prop-1-en-2-ylcyclopropane (8.2 mg, 0.1 mmol), **Ta1** (10.2 mg, 0.02 mmol), **KL1** (3.6 mg, 0.02 mmol) and 1,3,5-trimethoxybenzene (~3 mg, internal standard) were dissolved in 0.5 g Tol- d_8 and transferred to a J-Young NMR tube. The J-Young tube was capped and brought outside the glove box for a T_0 1H -NMR spectrum. After that, it was irradiated in front a G4 tungsten-halogen lamp for 20 h. Another 1H -NMR spectrum was taken and no new alkene signal could be identified, suggesting no ring opening occurred.



Following the same procedure as for the general photocatalytic hydroaminoalkylation. In a N₂-filled glove box, Ta(CH₂SiMe₃)₃Cl₂ (**Ta1**, 5.1 mg, 0.01 mmol), **KL1** (1.8 mg, 0.01 mmol), *N*-methylaniline (10.7 mg, 0.1 mmol), prop-1-en-2-ylcyclopropane (8.2 mg, 0.1 mmol), 1,3,5-trimethoxybenzene (~3 mg, internal standard) were dissolved in 0.5 g Tol-*d*₈ and transferred to a J-Young NMR tube. The J-Young tube was capped and brought outside the glove box for a T₀ ¹H-NMR spectrum. After that, it was irradiated in front of a G4 tungsten-halogen lamp for 3 d. Another ¹H-NMR spectrum was taken and the conversion of *N*-methylaniline was determined to be 40%. Only one hydroaminoalkylation regioisomer was formed (GC-MS).

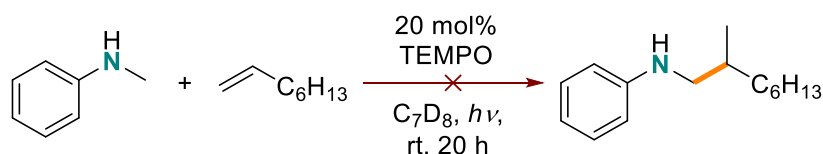
Due to signal overlap, *in situ* analysis of the product structure was challenging. Consequently, the J-Young NMR tube was opened and the reaction mixture was concentrated and the product was purified by column chromatography (SiO₂, 1:20 EtOAc:Hexanes) to give a colorless oil. Based on GC-MS and NMR analysis, it is a mixture of hydroaminoalkylation product (same as the product in reaction mixture) and co-eluting 1,3,5-trimethoxybenzene. Its structure was analyzed by NMR spectroscopy directly.

¹H NMR (CD₂Cl₂, 400 MHz, 298K): δ = 7.18-7.10 (m, 2 H), 6.75-6.62 (m, 3 H), 3.00 (s, 2 H), 0.83 (s, 6 H), 0.79-0.71 (m, 1 H), 0.38-0.30 (m, 2 H), 0.30-0.23 (m, 2 H) ppm

¹³C{¹H} NMR (CD₂Cl₂, 75 MHz, 298K): δ = 162.03, 129.50, 117.83, 113.66, 56.95, 33.71, 23.43, 19.75, 0.21. ppm.

signals at 93.16 and 55.68 ppm are from 1,3,5-trimethoxybenzene.

S4.4 TEMPO Initiation Experiment



In a N₂-filled glove box, *N*-methylaniline (10.7 mg, 0.1 mmol), 1-octene (11.2 mg, 0.1 mmol), 1,3,5-trimethoxybenzene (~3 mg, internal standard) and TEMPO (3.1 mg, 0.02 mmol) were dissolved in Tol-*d*₈ and transferred to a J-Young NMR tube. The J-Young tube was capped and brought outside the glove box for a T₀ ¹H-NMR spectrum. After that, it was irradiated in front of a G4 tungsten-halogen lamp for 20 h. Another ¹H-NMR spectrum was taken and no hydroaminoalkylation product formation was observed. GC-MS analysis confirmed these results.

S4.5 Kinetic Isotope Effect

KIE experiments were performed according to literature.⁷ In a N₂-filled glove box, Ta(CH₂SiMe₃)₃Cl₂ (**Ta1**, 20.4 mg, 0.04 mmol), **KL1** (7.2 mg, 0.04 mmol), 1-octene (44.8 mg, 0.4 mmol) and 1,3,5-trimethoxybenzene (~12 mg, internal standard) were dissolved in 4.0 g Tol-*d*₈ and separated to 4 identical portions. PhNHCH₃ (10.7 mg, 0.1 mmol), PhNDCH₃ (10.8 mg, 0.1 mmol), PhNHCD₃ (11.0 mg, 0.1 mmol) or PhNDCD₃ (11.1 m, 0.1 mmol) were added to one of the portions. Then each portion was divided into two portions (duplicates) and transferred to two J-Young NMR tubes.

The in total eight J-Young NMR tubes were capped and brought outside the glove box for T₀ ¹H-NMR spectra. After that, they were irradiated in front of a G4 tungsten-halogen lamp and every hour a ¹H-NMR spectrum was collected using 1,3,5-trimethoxybenzene as internal standard by integrating the signals of the *ortho*-protons of the *N*-methylanilines vs. the signal of the internal standard at the start of the reaction and comparing this value with the signal of the *ortho*-protons of the amine product vs. the internal standard at various points as the reaction progressed.

The average yields and errors of each duplicated experiments were calculated and plotted vs. the time. Initiation periods >1 h were observed in all cases. Thus, the initial rates of the reactions were calculated from the slope of the linear fitting between 2 to 6 h. The initiation periods of the reactions were calculated from the intercept of the linear fitting between 2 to 6 h. The calculated initial rates and initiation periods are listed in **Table S1**.

Table S1. Initial rate and induction period of reaction between PhNHCH₃ (with different degree of deuteration) and 1-octene.

Amine	Initial Rate (×10⁻⁶ mol/h)	Induction Period (h)
PhNHCH ₃	1.42±0.06	1.45
PhNHCD ₃	1.07±0.02	1.48
PhNDCH ₃	0.87±0.05	2.09
PhNDCD ₃	0.49±0.04	1.56

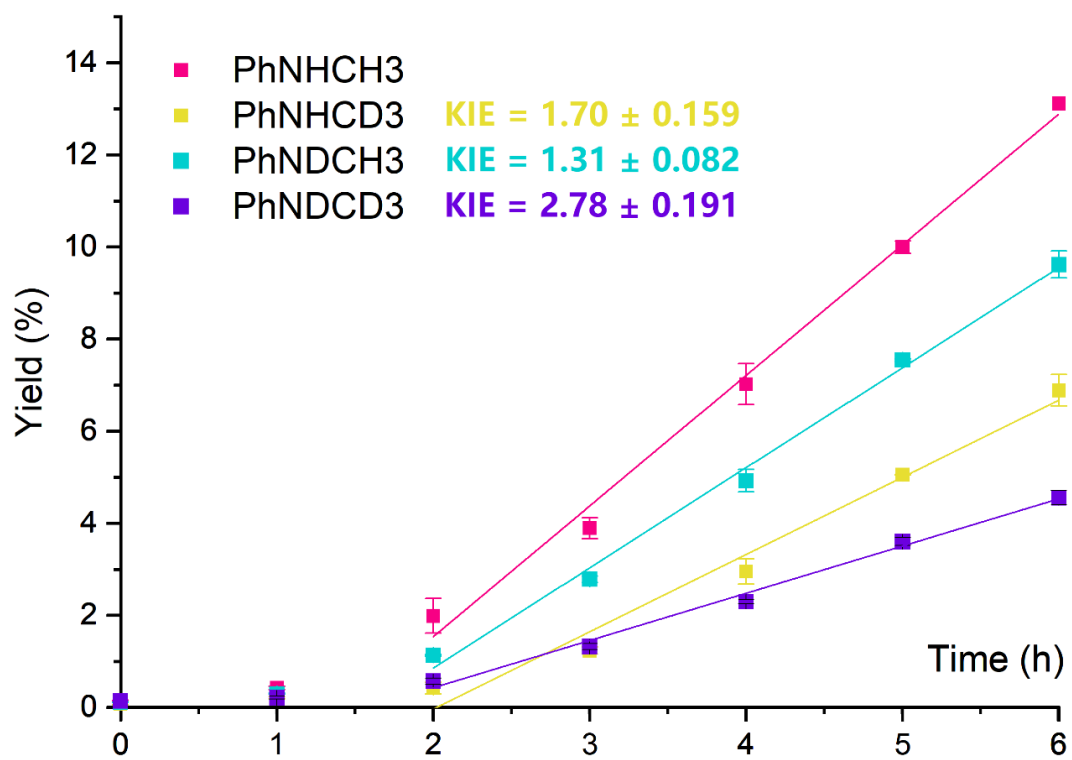


Figure S2. First order kinetic plot for the photocatalyzed hydroaminoalkylation with PhNHCH₃ (pink), PhNHCD₃ (yellow), PhNDCH₃ (blue), PhND₃CD₃ (purple).

S5. DFT Studies and Discussion

According to the regioselectivity for the product, the radical clock experiments and the kinetic isotope experiments, tantalum amido radicals are key intermediates for this type of hydroaminoalkylation and concerted addition of an excited state tantalum amido diradical **B** to an alkene **C** is a key step in the catalytic cycle (**Scheme 6**). To access the diradical, a photonic excitation of tantalum aziridine **A** is proposed, which emphasizes the important role of the saturated cyclic ureate ligand for the photo catalytic reactivity.

To investigate the difference in photo catalytic reactivity of saturated cyclic ureate coordinated tantalum complex (**TaL1**) and other *N,O*-chelated tantalum complexes (**TaL2-TaL5**), DFT calculations were performed. Tantalum pyridonate complex **TaL4**, which has no photo catalytic reactivity, was chosen as a comparison to **TaL1** due to its relatively simple structure.

The ground state geometry of tantalum aziridine **A** and the excited state geometry of tantalum amido diradical **B** were optimized for both **TaL1** and **TaL4**. In both cases, the Ta–C distance increases after excitation, suggesting weakening of the Ta–C bond. However, in **TaL1** the bond extends by 0.102 Å (2.134 to 2.236 Å), which is more significant than in **TaL4** (0.071 Å, 2.148 to 2.219 Å). Consequently, the photonic excitation induced weakening of the Ta–C bond is more efficient with **L1** as ligand compared to **L4**.

The excitation of **TaL1** and **TaL4** to the corresponding excited states **TaL1*** and **TaL4*** was analyzed. The transition of **TaL1**→**TaL1*** is a typical ligand to metal charge transfer, where the electrons from the amido ligand flow to the tantalum metal center (**Figure S3** top). However, in the case of **TaL4**→**TaL4***, the transition consists not only charge transfer from amido ligand to Ta metal center, but also to the pyridonate ligand (**Figure S3** bottom). Furthermore, the distance between the centroids of electron and hole in **TaL1*** is 3.043 Å, while being 3.730 Å in **TaL4***, which also suggest a longer charge transfer distance to the ligand. Thus, the pyridonate ligand with conjugated moiety hosts the excited radical and stabilizes the system, which leads to stronger (thus less active) Ta–C bond.

An even more important feature of the excited state could be generated by mapping the single occupied natural orbitals of the excited states at CI level. (**Figure S4, S5**) The two single occupied natural orbitals of **TaL1** only distribute on the tantalum amido moiety but not the cyclic ureate ligand (**Figure S4**, Isovalue = 0.035), while in the case of **TaL4** both single occupied natural orbitals extend all the way to the pyridonate ligand (**Figure S5**). Thus, in the case of **TaL4** the conjugated pyridonate ligand acts as a “electron sink” and helps to stabilize the system by extending the conjugation. Consequently, the unpaired electrons are no longer restricted to the tantalum amido moiety.

Conclusively, the saturated cyclic ureate ligand of **TaL1** with no conjugated moiety helps to localize the unpaired electrons in the excited state diradical within the tantalum amido moiety and facilitates the concerted addition to the alkene. The conjugated moieties in other ligands (**L2-L5**) provide delocalized conjugated systems, in which the unpaired electrons can move freely. This leads to poor orbital overlapping with the alkene and disfavors a concerted addition.

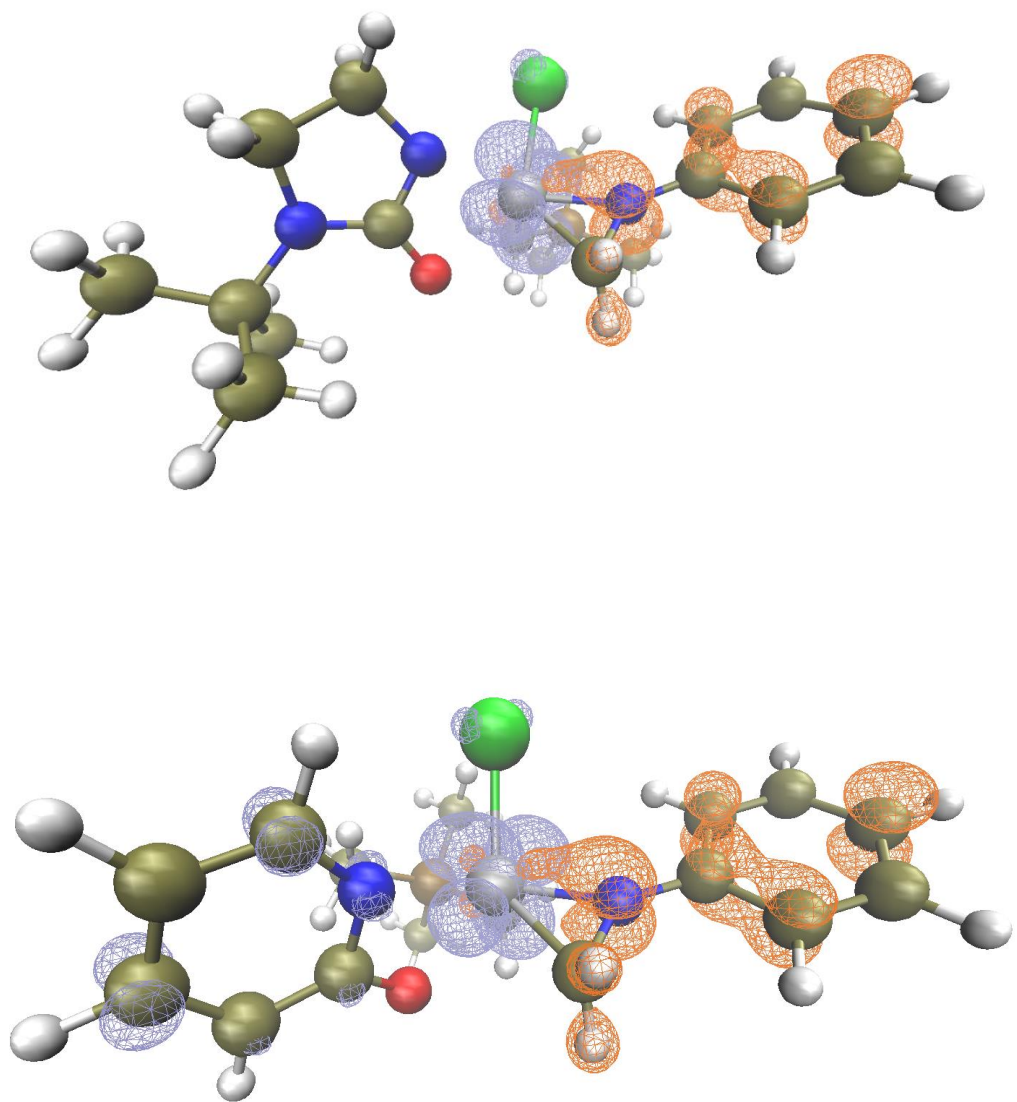


Figure S3. Electron analysis of **TaL1*** and **TaL4***. Orange mesh indicates holes after excitation, and ice-blue mesh indicates electrons after excitation. (Opt: M06L-D3/Def2SVP, TD: M06L-D3/Def2TZVPP, both with SMD (toluene) solvent model, Isovalue=0.005)

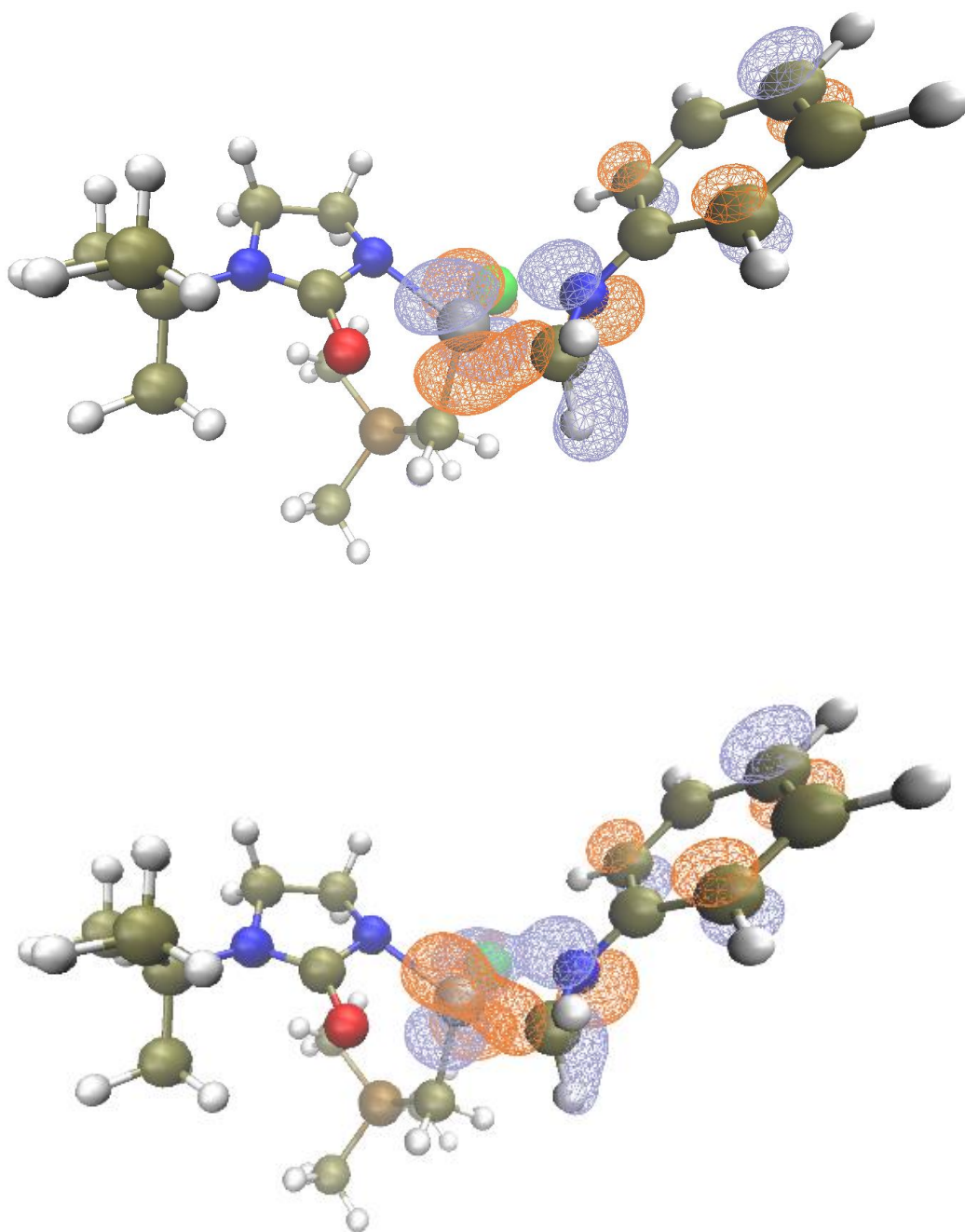


Figure S4. Single occupied molecular orbitals of **TaL1*** diradical. (Opt: M06L-D3/Def2SVP, TD: M06L-D3/Def2TZVPP, both with SMD (toluene) solvent model, Isovalue=0.005)

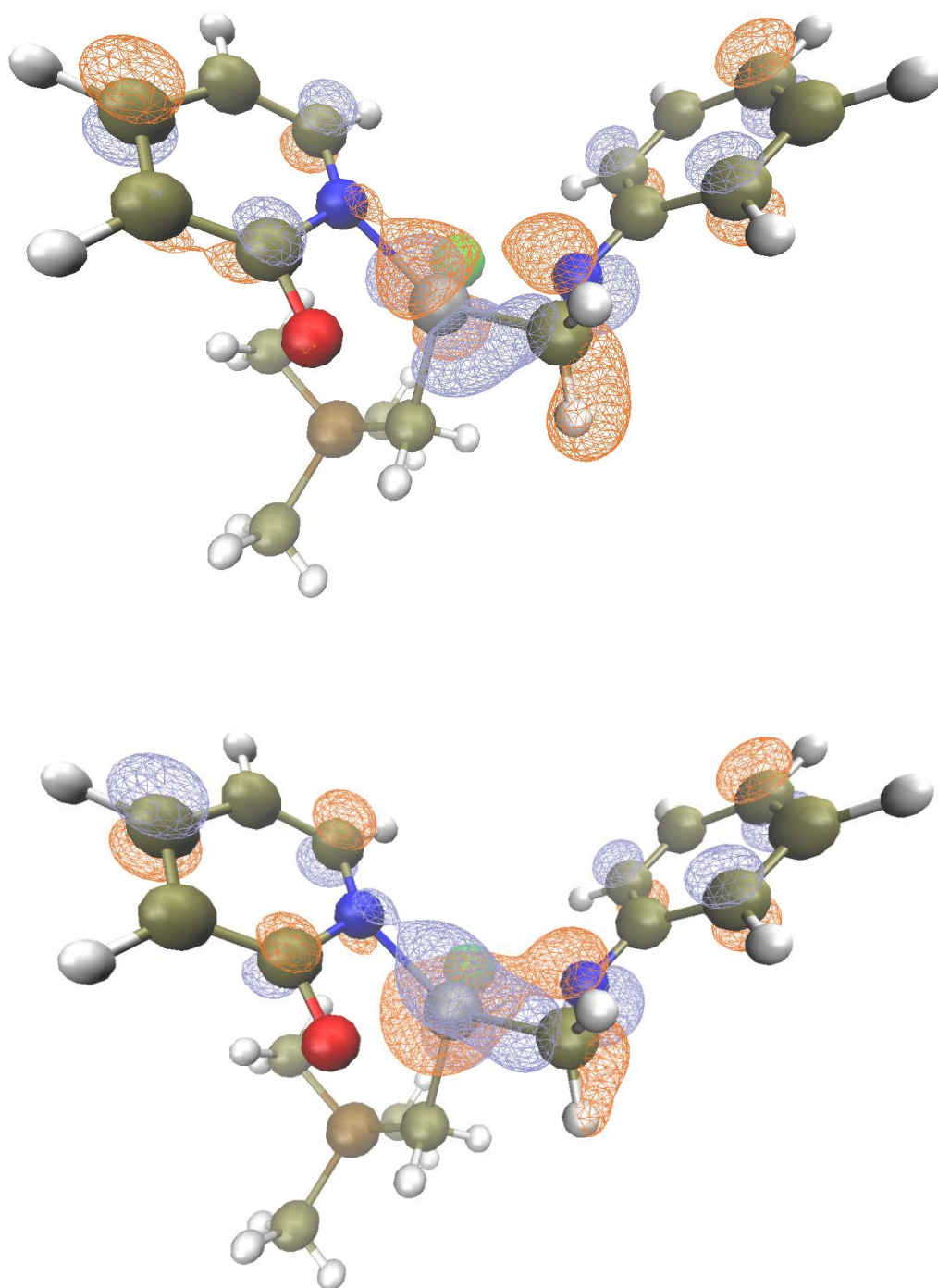


Figure S5. Single occupied molecular orbitals of **TaL4*** diradical. (Opt: M06L-D3/Def2SVP, TD: M06L-D3/Def2TZVPP, both with SMD (toluene) solvent model, Isovalue=0.005)

S6. Photophysical Results

Because of the use of a G4 tungsten-halogen light bulb with a UV filter as the light source for our photocatalytic reaction, we assumed that the photo catalyst harvests the visible and NIR light, especially in the red to near IR region where the energy output peaks with a tungsten-halogen light bulb. To proof this assumption photophysical experiments were conducted.

The UV-Vis spectra of **TaL1** pre-catalyst, substrate mixture, reaction mixture at T0 and reaction mixture after irradiating for 1 h were collected (**Figure S6**). Surprisingly, no absorption peak but only some tailing could be identified in the range of > 400 nm. This suggests there is no major species in the reaction mixture harvesting light > 400 nm.

It was then proposed that the photo catalyst utilizes the trace amount of UV light for the reaction to turn-over. However, removing the UV filter in front of the tungsten-halogen light lead to poorer reactivity and using a direct UV lamp (365 nm or 254 nm) gave no reactivity at all.

Finally, we decided to measure the relative reactivity at different wavelengths. We prepared reaction samples according to the general procedure (see **S3**). Instead of a tungsten-halogen lamp that emits a continuous spectrum, we applied a series of narrow band filters to a Xenon lamp to access light at different wavelengths. The reactivities were calculated via NMR yields, corrected by dividing by ($T_{Max} * \Delta\lambda(1/2)$). There results were listed in **Table S2** and plotted vs. the wavelength (**Figure S6**).

Surprisingly, the reactivity peaks at 440 nm and decreases at both shorter wavelength (380 nm) and longer wavelength (500 nm). Consequently, the photo active species should absorb 440 nm light extensively. However, there is no absorption peak at approx. 440 nm in the UV-Vis spectra of the reaction mixture before and after irradiation. We hypothesize that either the concentration of photo active species is very low or the species is so short-living that it cannot be detected using a common UV-Vis spectrometer.

The absorption wavelength of **TaL1** in toluene was simulated using TD-DFT (**Figure S7**). Interestingly, although there is no major absorption in the region > 360 nm, the second transition has an excitation energy of 2.66 eV, corresponding to absorption at 466 nm. This is close the experimentally observed reactivity maxima. The oscillator strength is only 0.0036, making it an inefficient transition. This may explain the observed slow reaction at ~440 nm.

Table S2. Filter parameters and wavelength-dependent reactivity

Entry	λ_{Max} (nm)	T_{Max} (%)	$\Delta\lambda(1/2)$ (nm)	Raw yields (%)	Corrected yields (%)
1	382	34	15	13.8	27.1
2	399	31	10	20.0	64.5
3	420.5	45	12	26.5	49.1
4	442	35	8	23.6	84.3
5	458.5	44	9	28.9	73.0
6	480	43.5	8	6.9	19.8
7	500.5	40	8	4.8	15.0
8	518.5	37.5	5.5	3.0	14.5

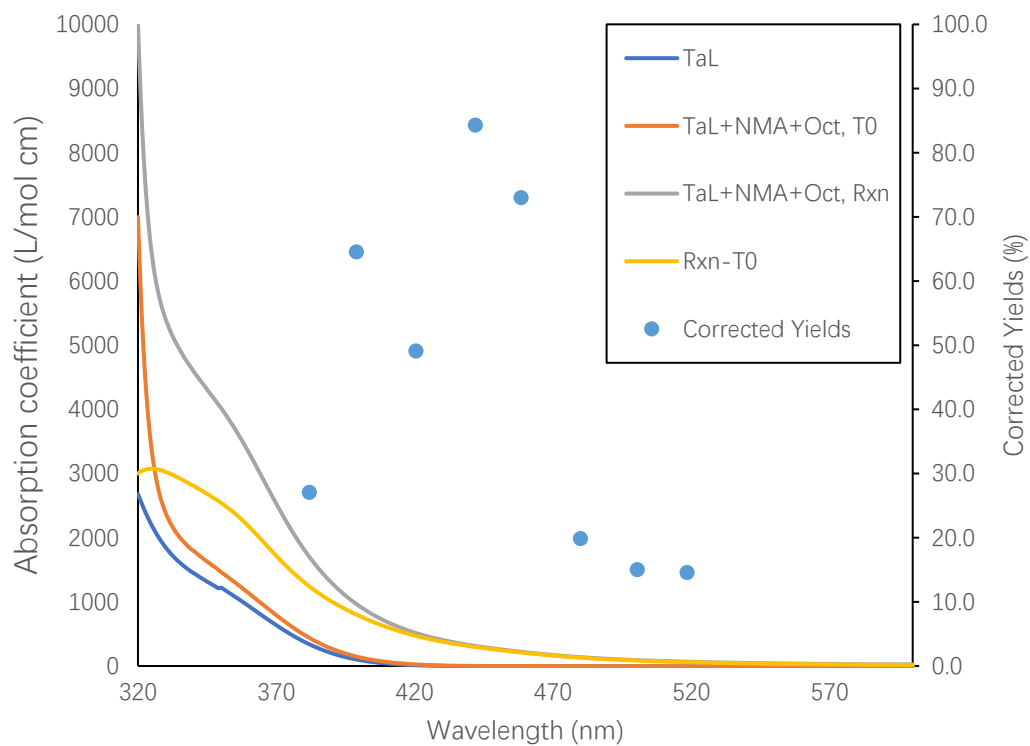


Figure S6. Absorption spectra of **TaL1** pre-catalyst (blue line), reaction mixture at T_0 (orange line) and after 1 h irradiation (grey line). Difference between before and after irradiation is plotted as yellow line. Purple dots represent relative yields under different wavelength irradiation.

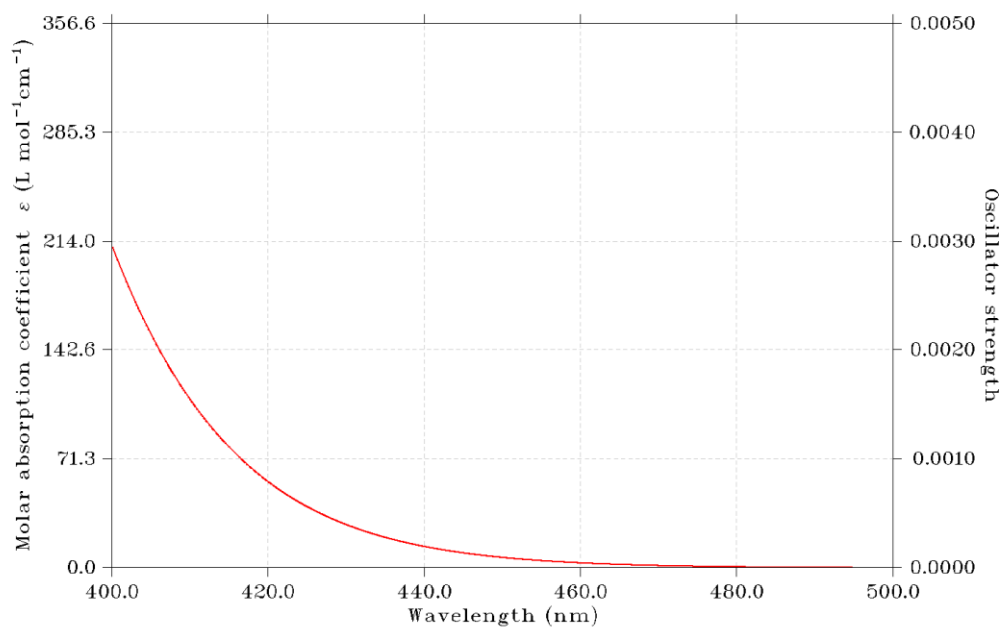
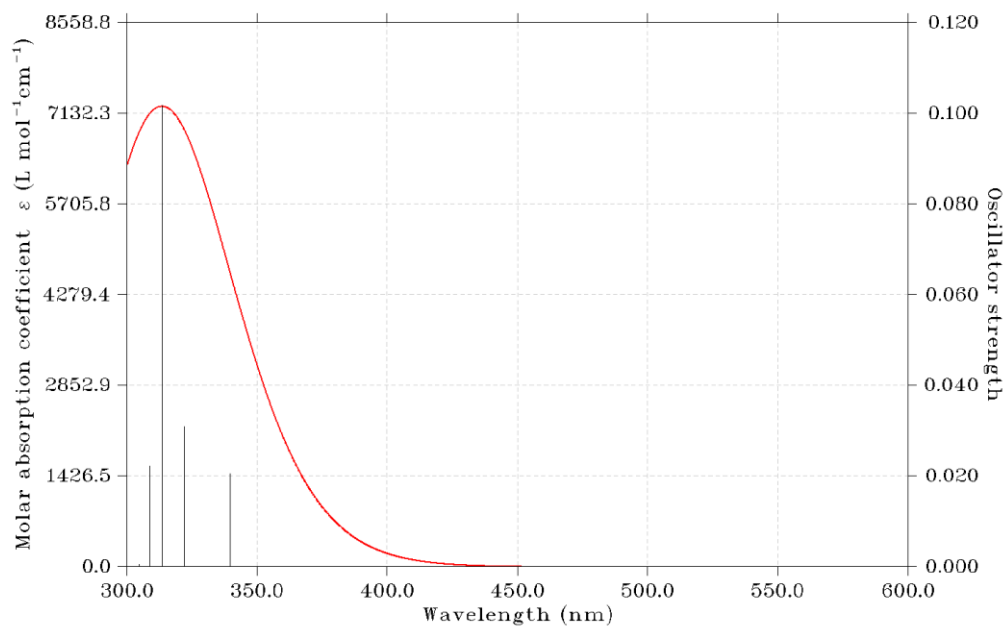


Figure S7.1. Simulated UV-Vis absorption spectrum of **TaL1** pre-catalyst in toluene. (Opt: M06L-D3/Def2SVP, TD: M06L-D3/Def2TZVPP, both with SMD (toluene) solvent model)

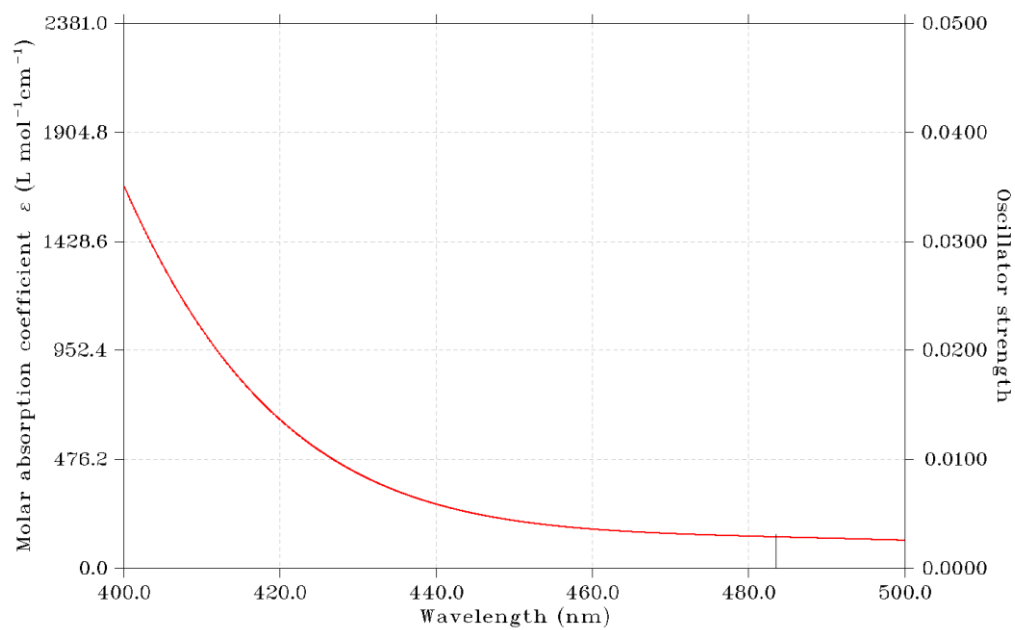
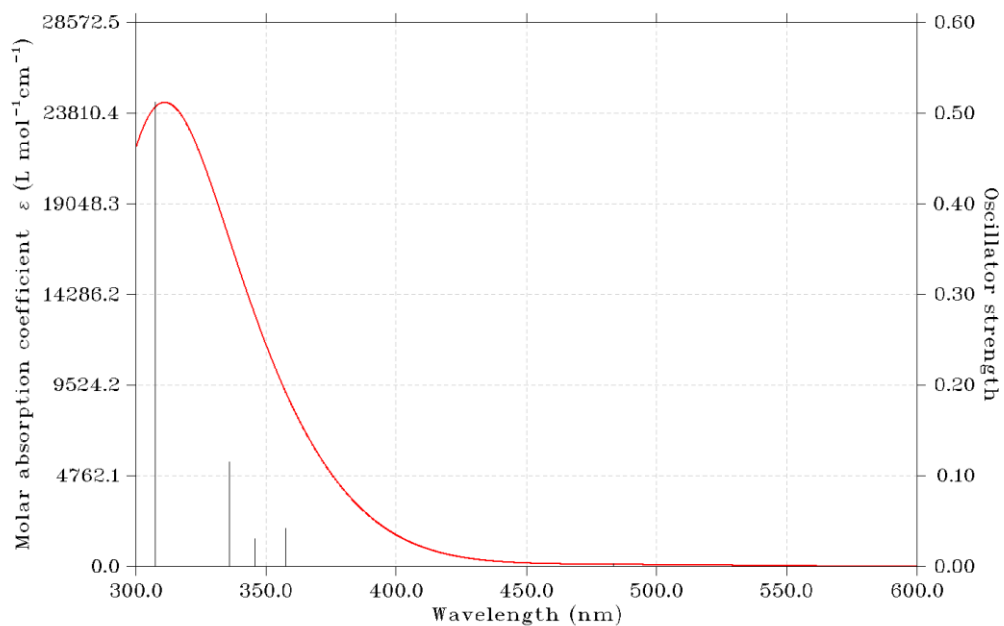


Figure S7.2. Simulated UV-Vis absorption spectrum of **TaL1** tantalaziridine intermedia in toluene. (Opt: M06L-D3/Def2SVP, TD: M06L-D3/Def2TZVPP, both with SMD (toluene) solvent model)

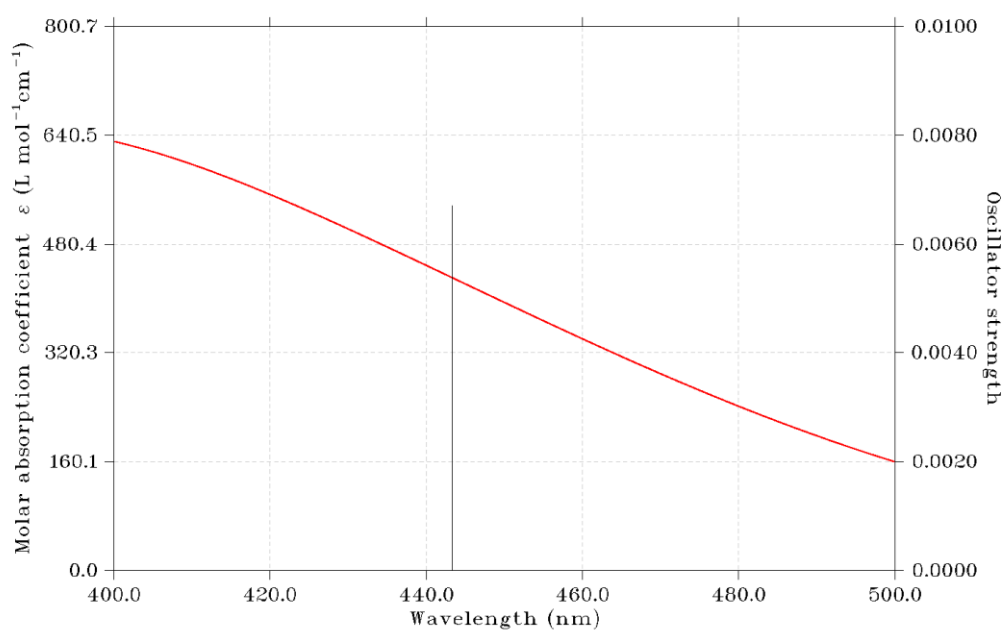
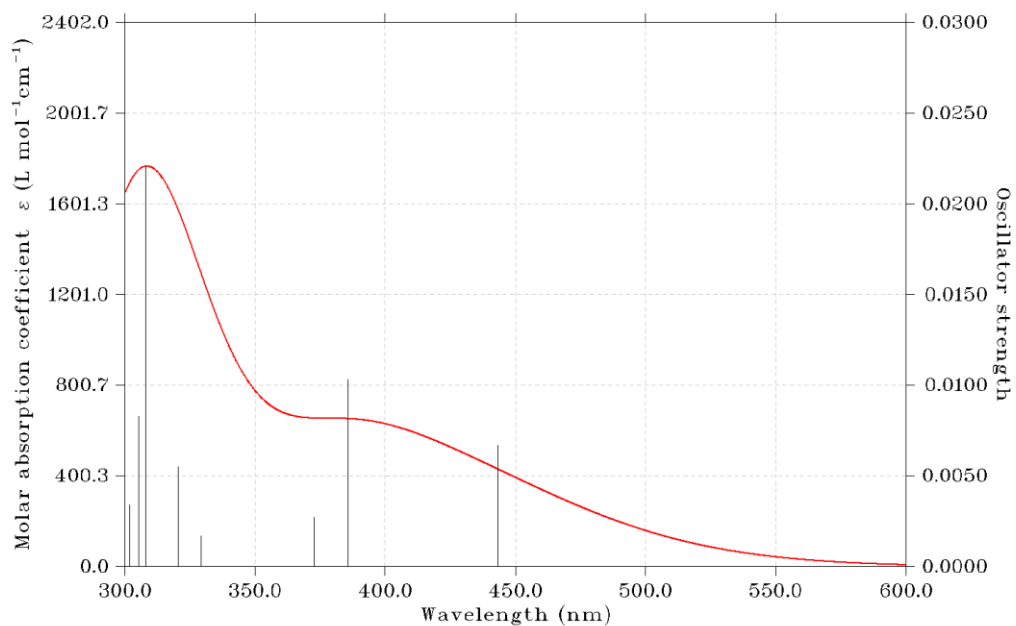


Figure S7.3. Simulated UV-Vis absorption spectrum of **TaL1** pre-catalyst in toluene. (Opt: M06L-D3/Def2SVP, TD: M06L-D3/Def2TZVPP, both with SMD (toluene) solvent model)

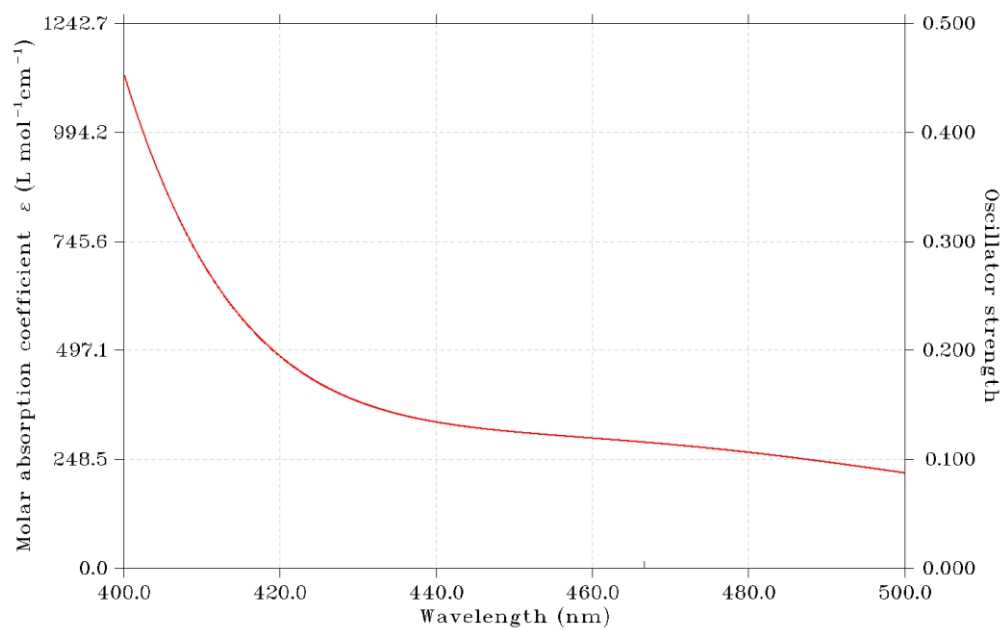
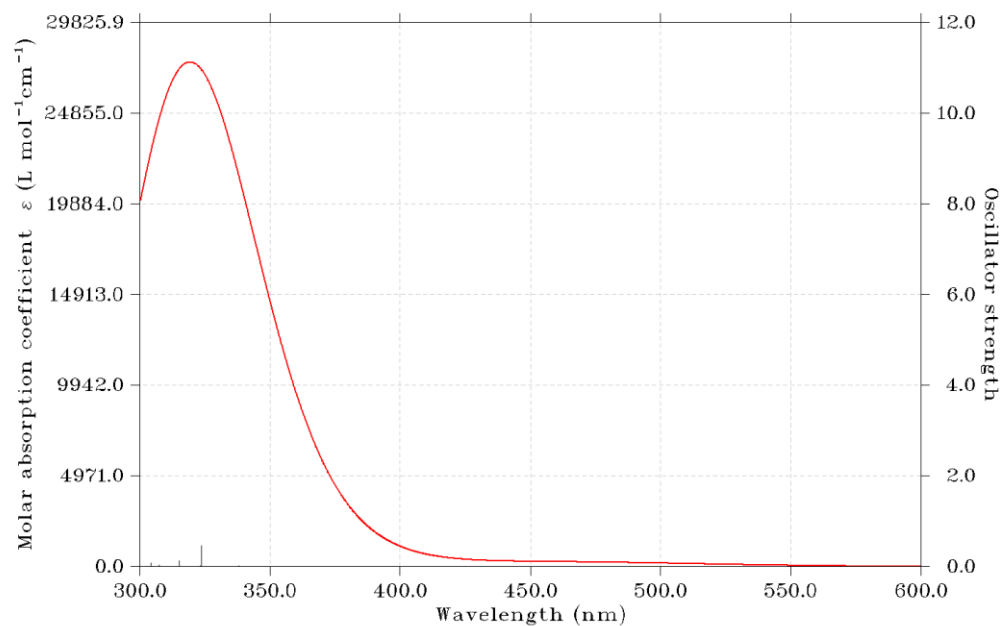
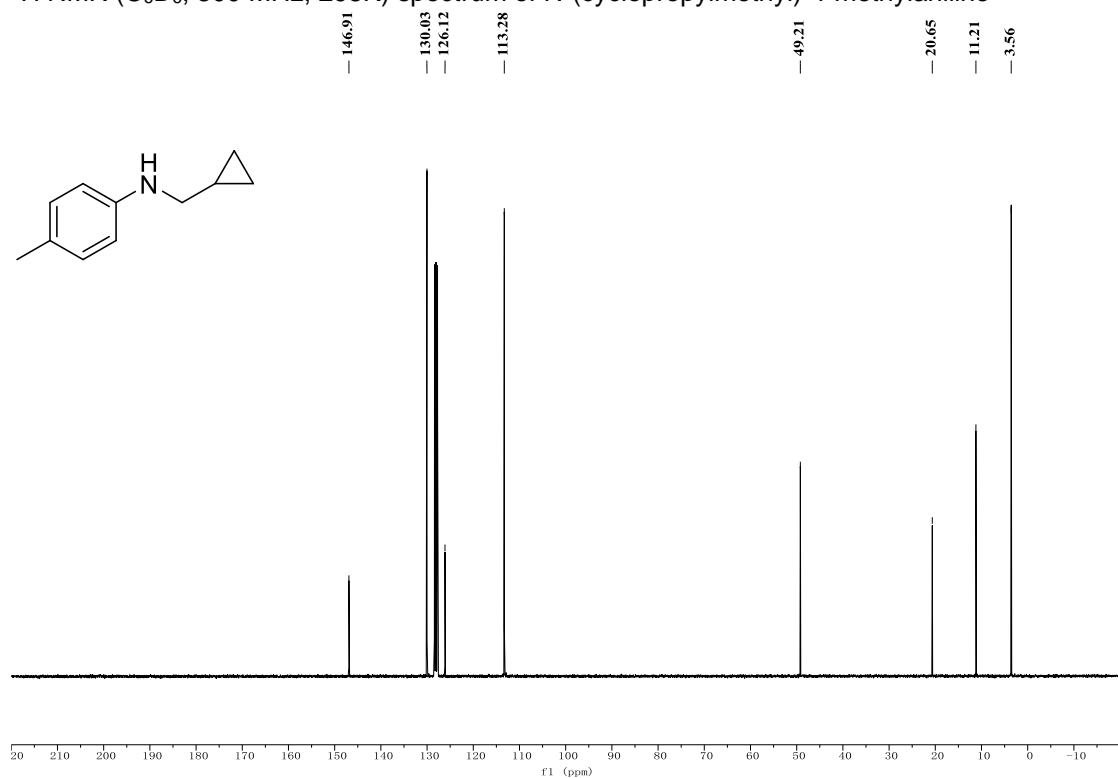
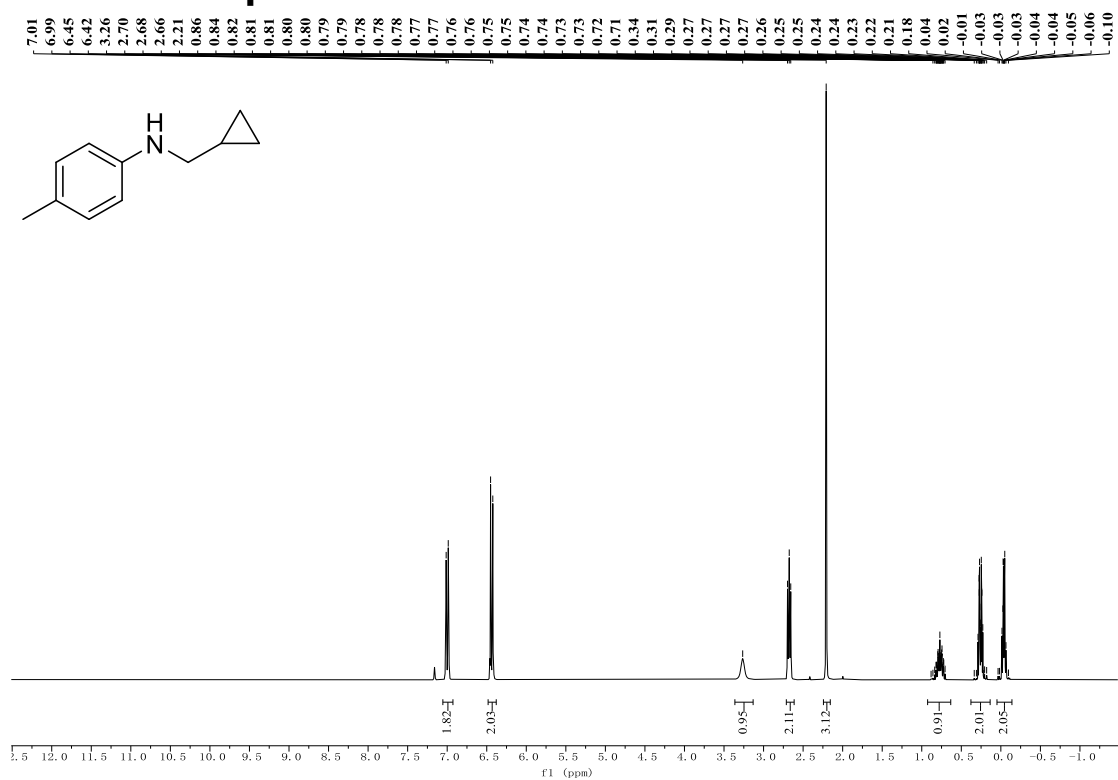


Figure S7.4. Simulated UV-Vis absorption spectrum of **TaL1** tantalaziridine intermedia in toluene. (Opt: M06L-D3/Def2SVP, TD: M06L-D3/Def2TZVPP, both with SMD (toluene) solvent model)

S7. NMR Spectra



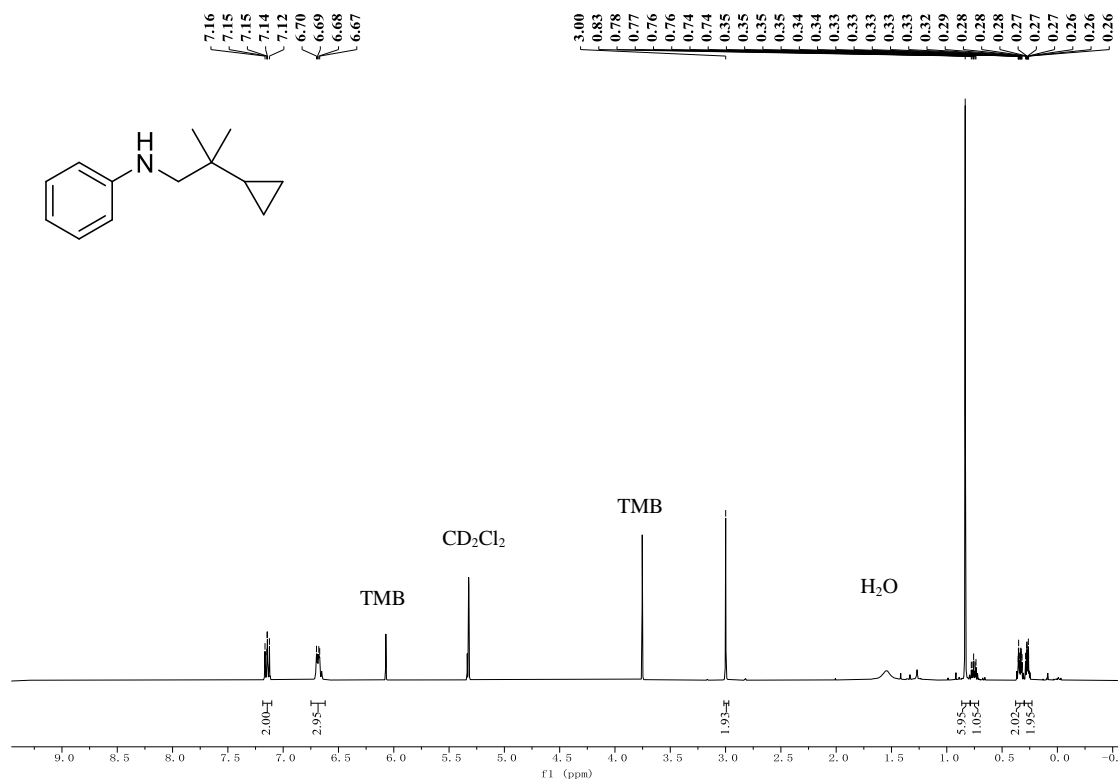


Figure S10

¹H NMR (CD₂Cl₂, 400 MHz, 298K) spectrum of N-(2-cyclopropyl-2-methylpropyl)aniline. Peaks at 6.07 and 3.75 ppm are from TMB internal standard

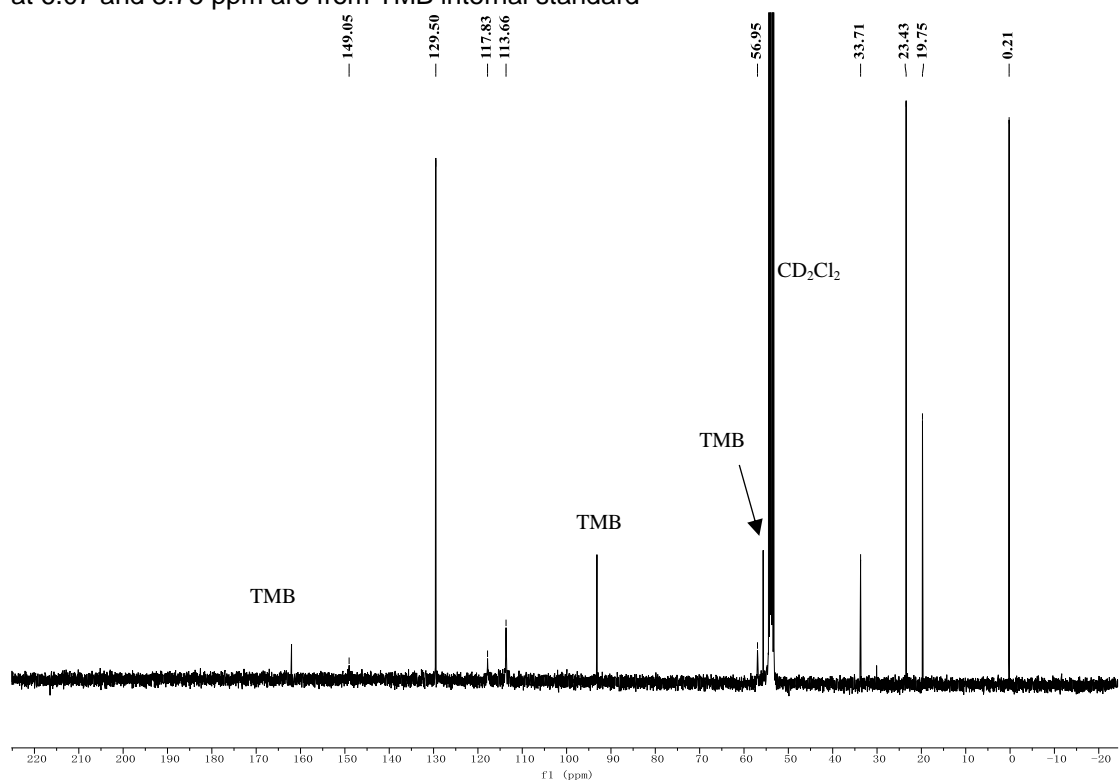


Figure S11

¹³C{¹H} NMR (CD₂Cl₂, 400 MHz, 298K): Peaks at 162.03, 93.16 and 55.68 ppm are from TMB internal standard.

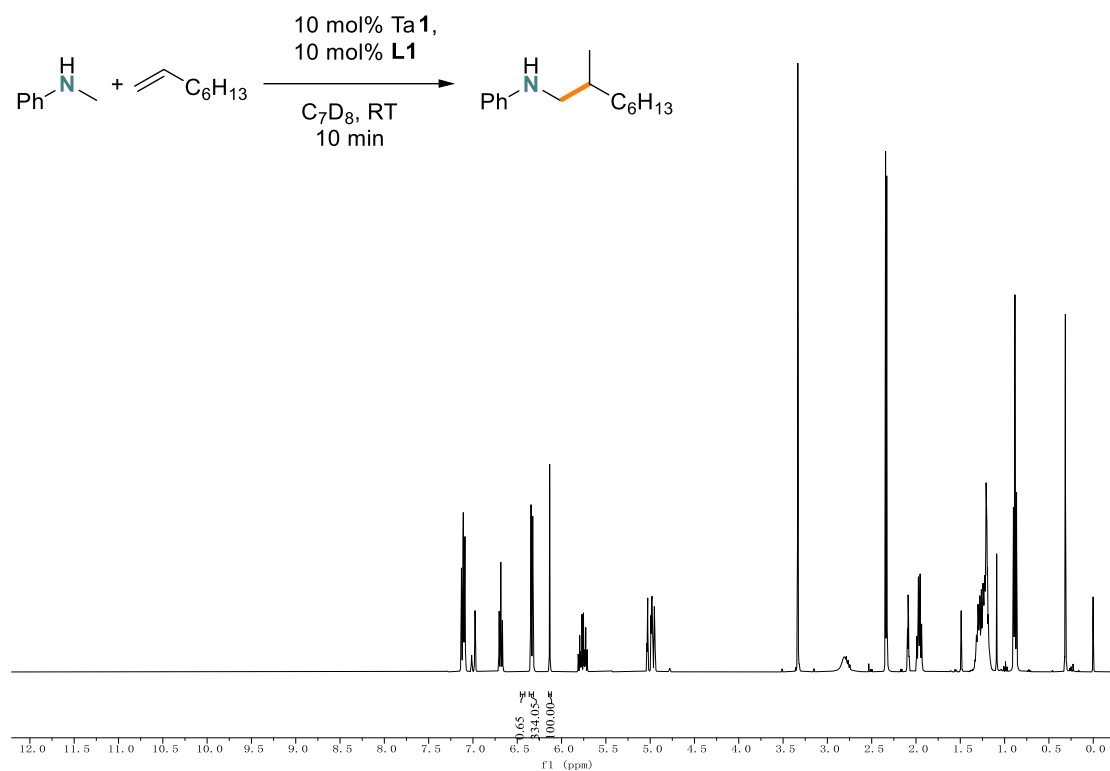


Figure S12

^1H NMR spectrum of reaction between 1-octene and N-methylaniline with 10 mol% TaL1 after 10 min in C_7D_8 at RT

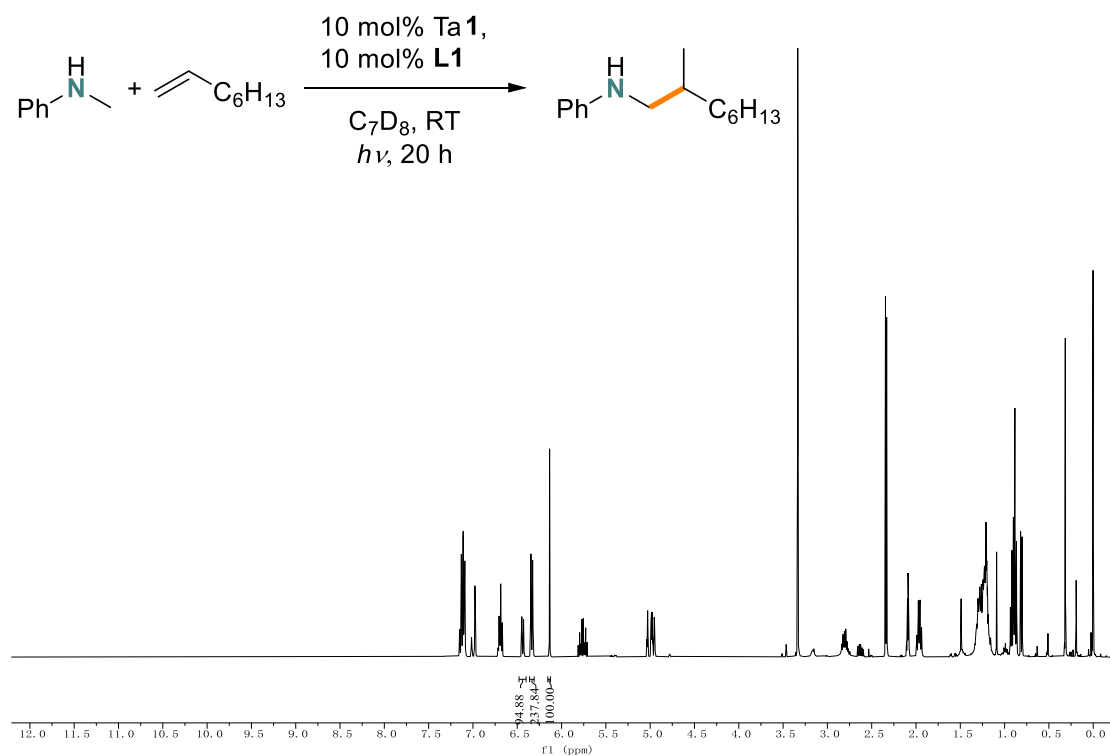


Figure S13

^1H NMR spectrum of reaction between 1-octene and N-methylaniline with 10 mol% TaL1 after 20 h irradiation in C_7D_8 at RT

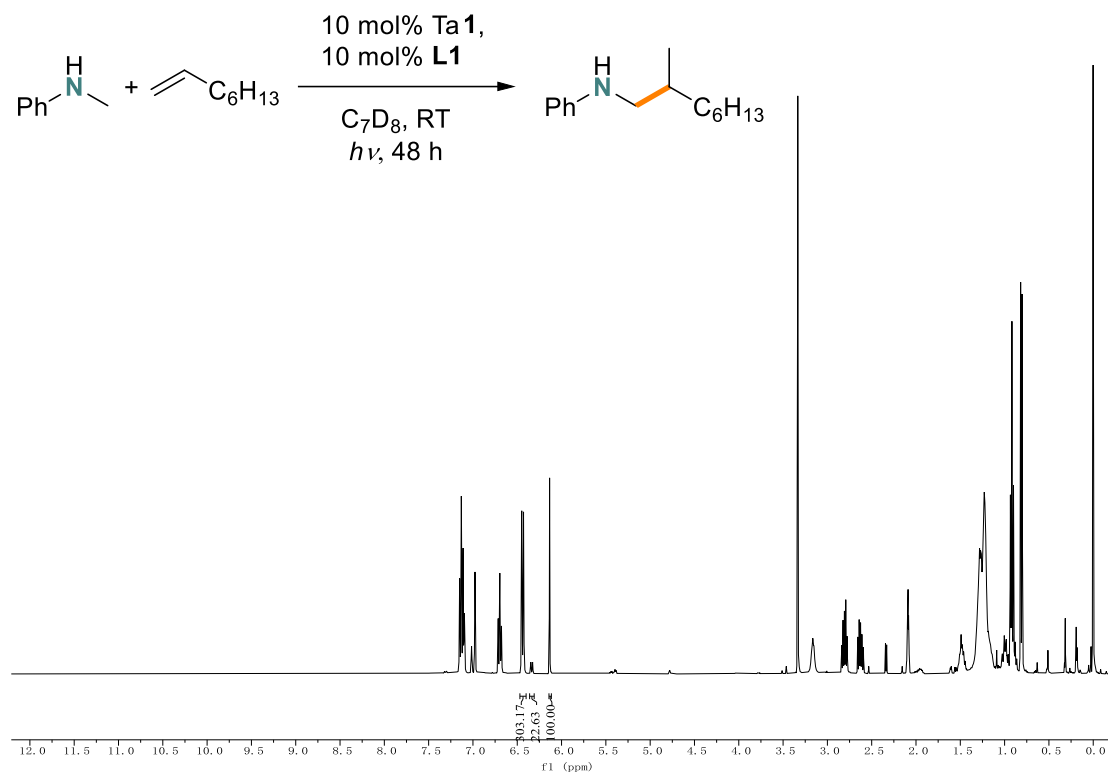


Figure S14

^1H NMR spectrum of reaction between 1-octene and N-methylaniline with 10 mol% TaL1 after 48 h under irradiation in C_7D_8 at RT

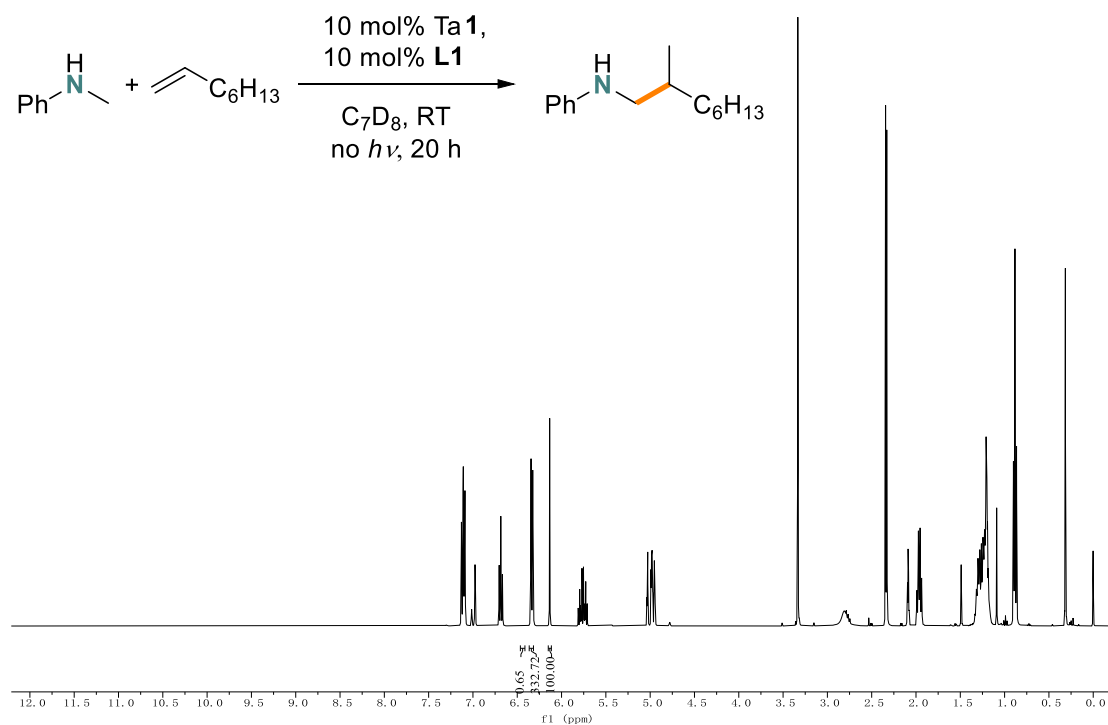


Figure S15

^1H NMR spectrum of reaction between 1-octene and N-methylaniline with 10 mol% TaL1 after 20 h without irradiation (foiled) in C_7D_8 at RT

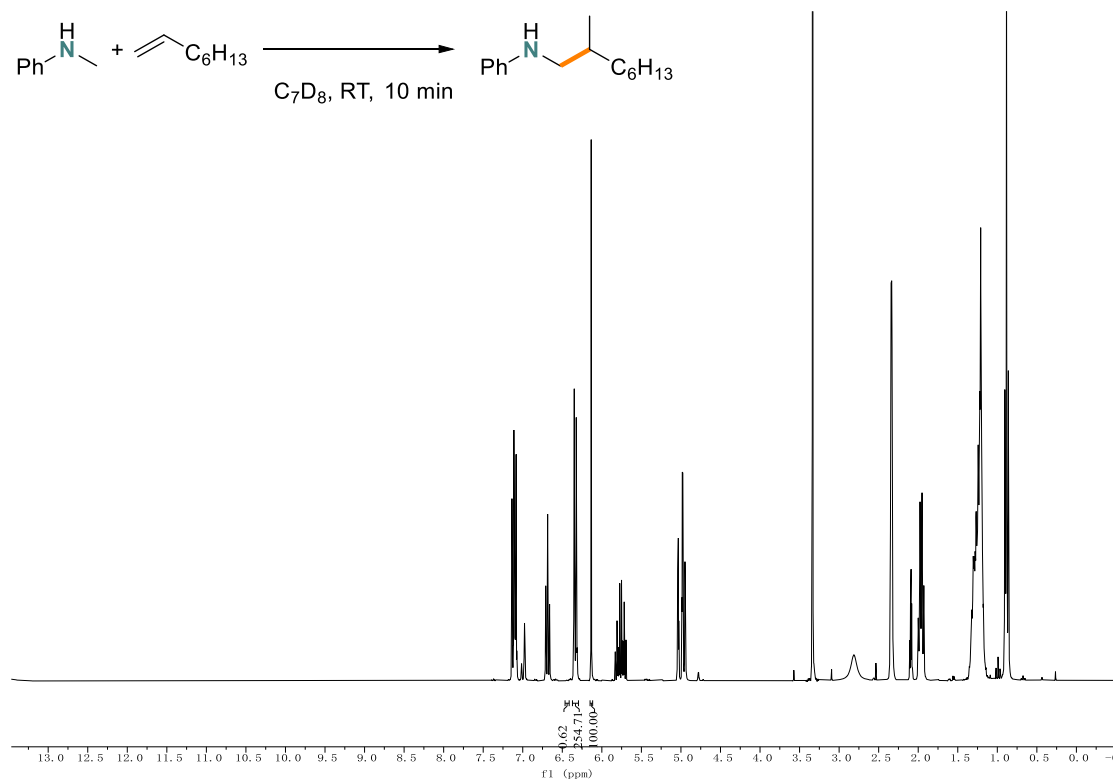


Figure S16

^1H NMR spectrum of reaction between 1-octene and N-methylaniline without TaL1 after 10 min in C_7D_8 at RT

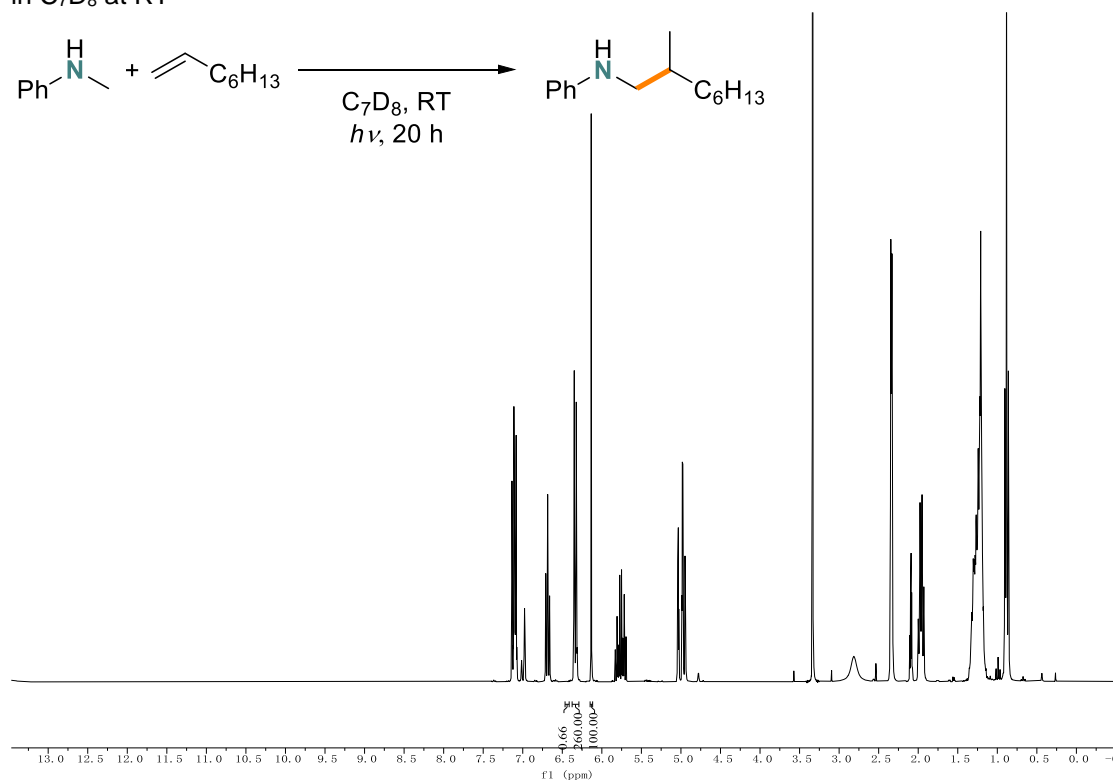


Figure S17

^1H NMR spectrum of reaction between 1-octene and N-methylaniline without TaL1 after 20 h under irradiation in C_7D_8 at RT

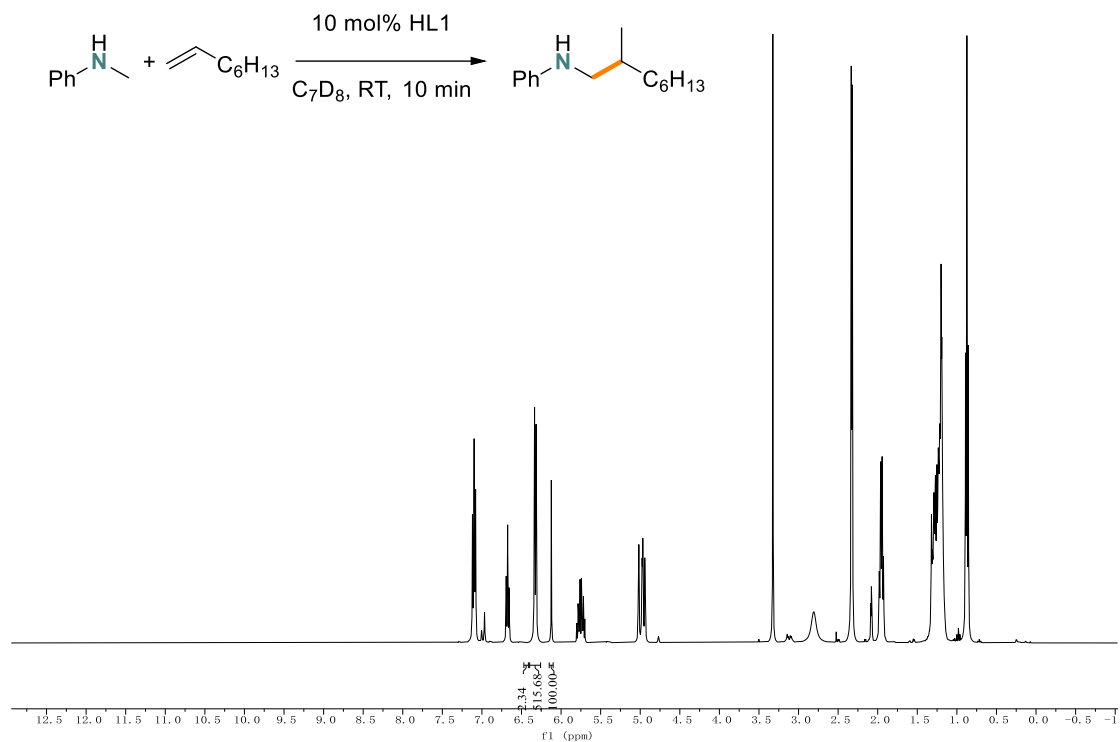


Figure S18

^1H NMR spectrum of reaction between 1-octene and N-methylaniline with 10 mol% HL1 after 10 min in C_7D_8 at RT

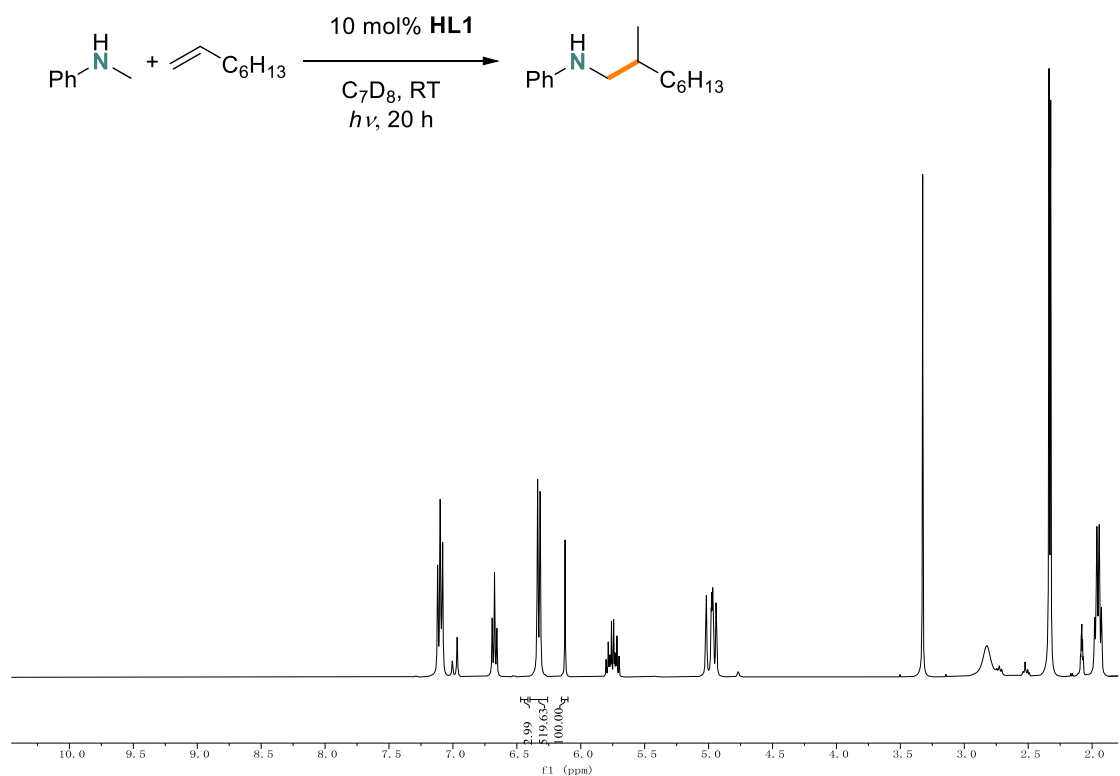


Figure S19

^1H NMR spectrum of reaction between 1-octene and N-methylaniline with 10 mol% HL1 after 20 h irradiation in C_7D_8 at RT

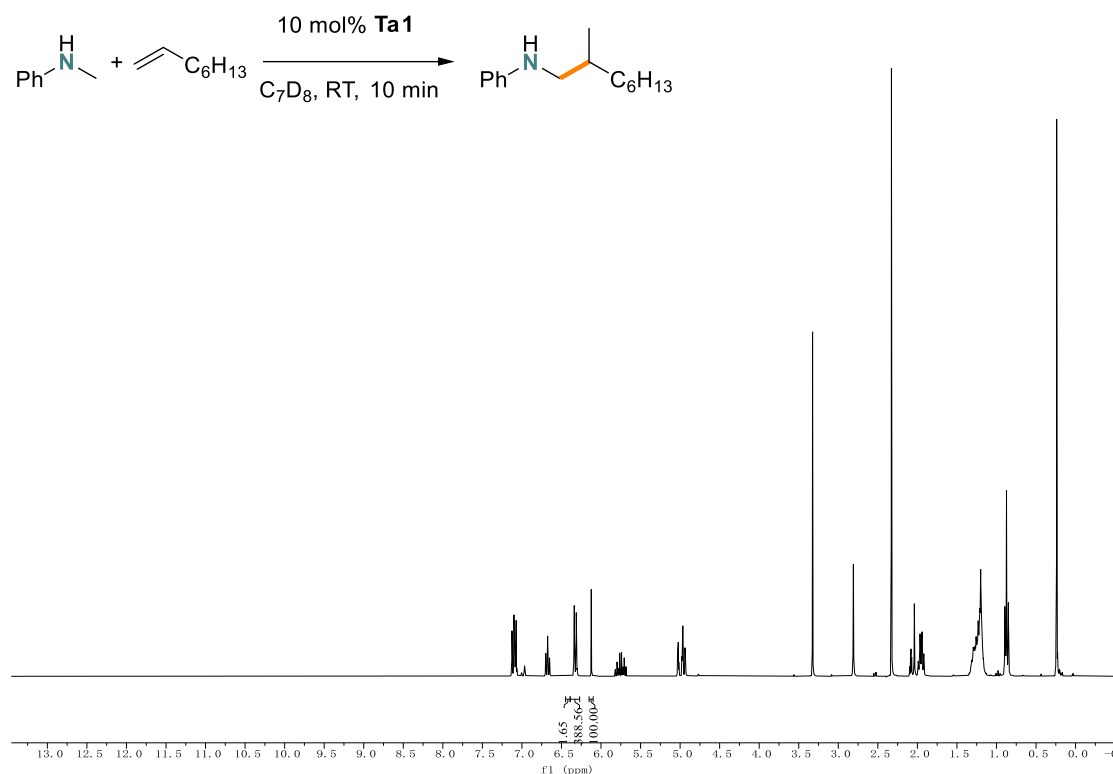


Figure S20

^1H NMR spectrum of reaction between 1-octene and N-methylaniline with 10 mol% Ta(CH₂SiMe₃)₃Cl₂ after 10 min in C₇D₈ at RT

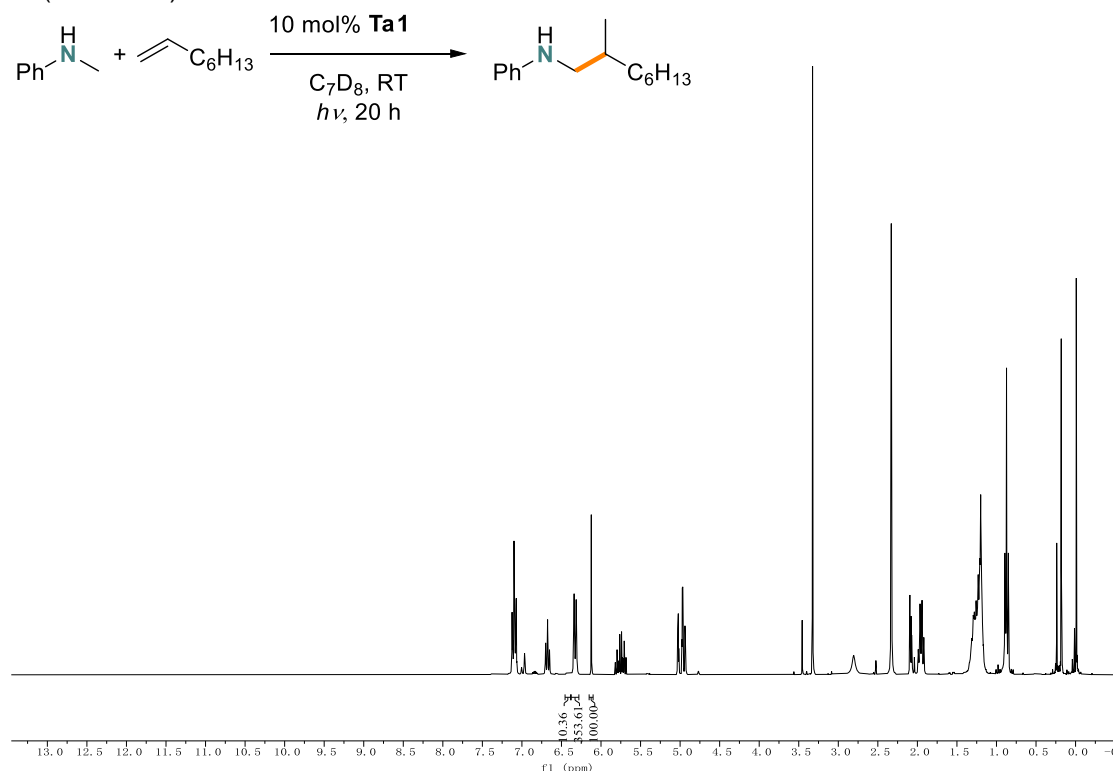


Figure S21

^1H NMR spectrum of reaction between 1-octene and N-methylaniline with 10 mol% Ta(CH₂SiMe₃)₃Cl₂ after 20 h irradiation in C₇D₈ at RT

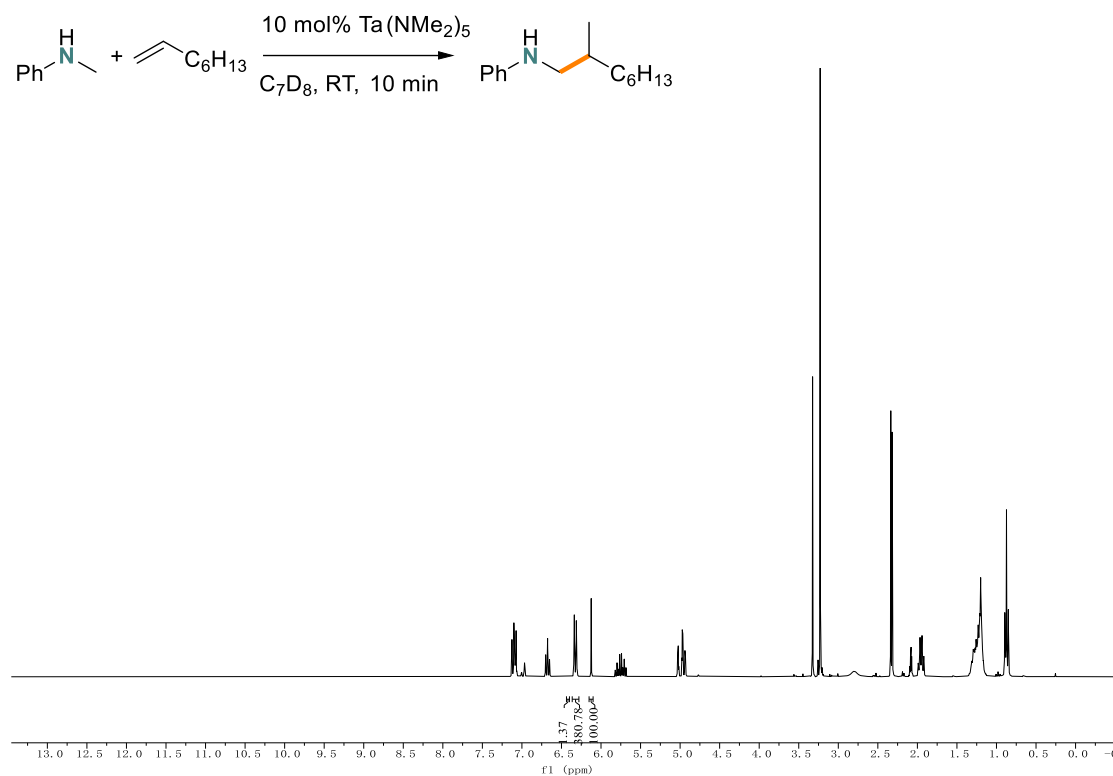


Figure S22

^1H NMR spectrum of reaction between 1-octene and N-methylaniline with 10 mol% $\text{Ta}(\text{NMe}_2)_5$ after 10 min in C_7D_8 at RT

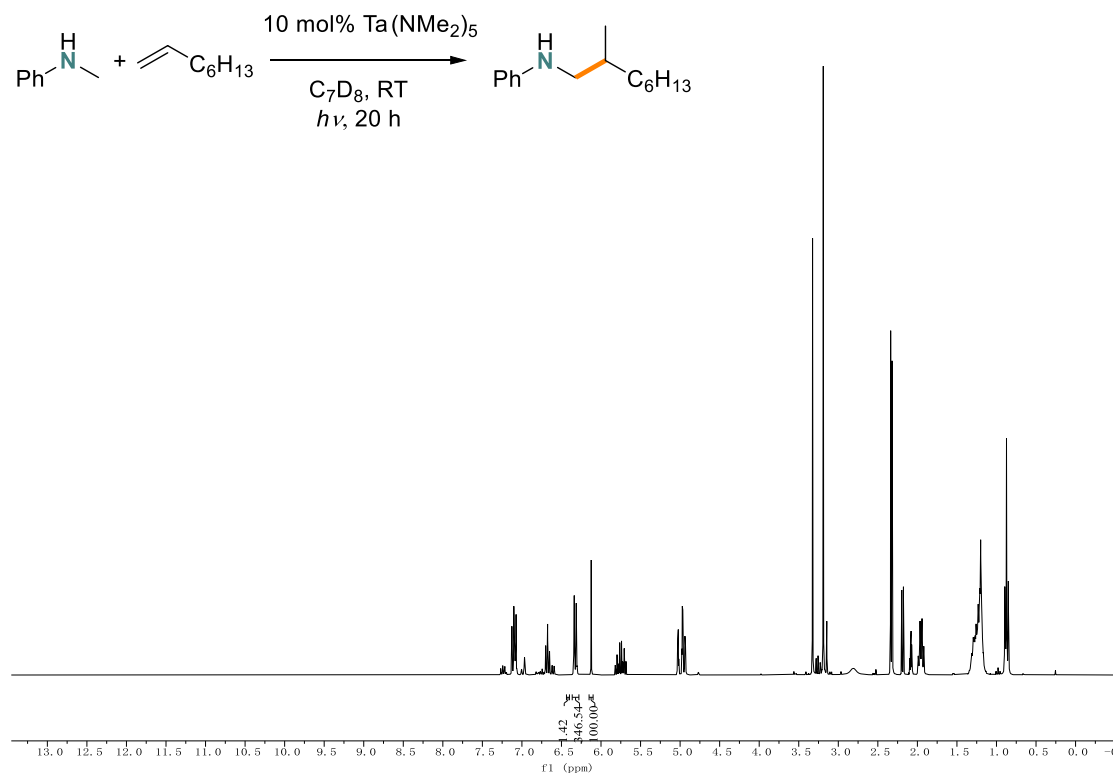


Figure S23

^1H NMR spectrum of reaction between 1-octene and N-methylaniline with 10 mol% $\text{Ta}(\text{NMe}_2)_5$ after 20 h irradiation in C_7D_8 at RT

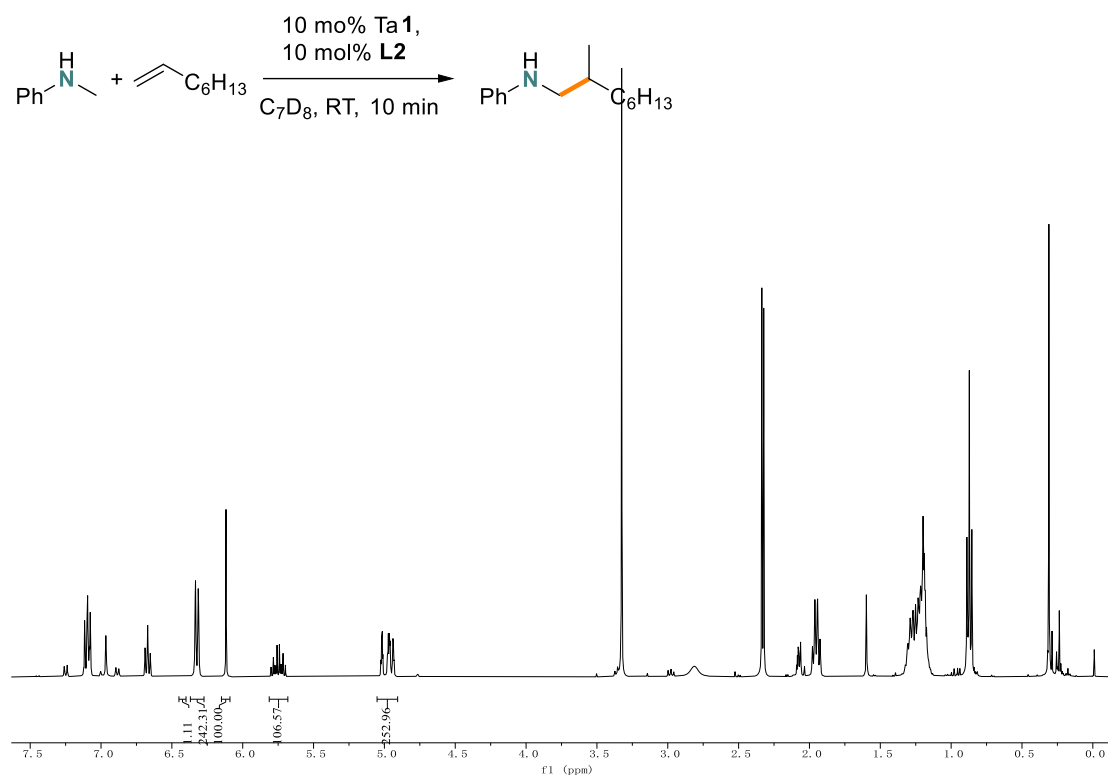


Figure S24

^1H NMR spectrum of reaction between 1-octene and N-methylaniline with 10 mol% TaL2 after 10 min in C_7D_8 at RT

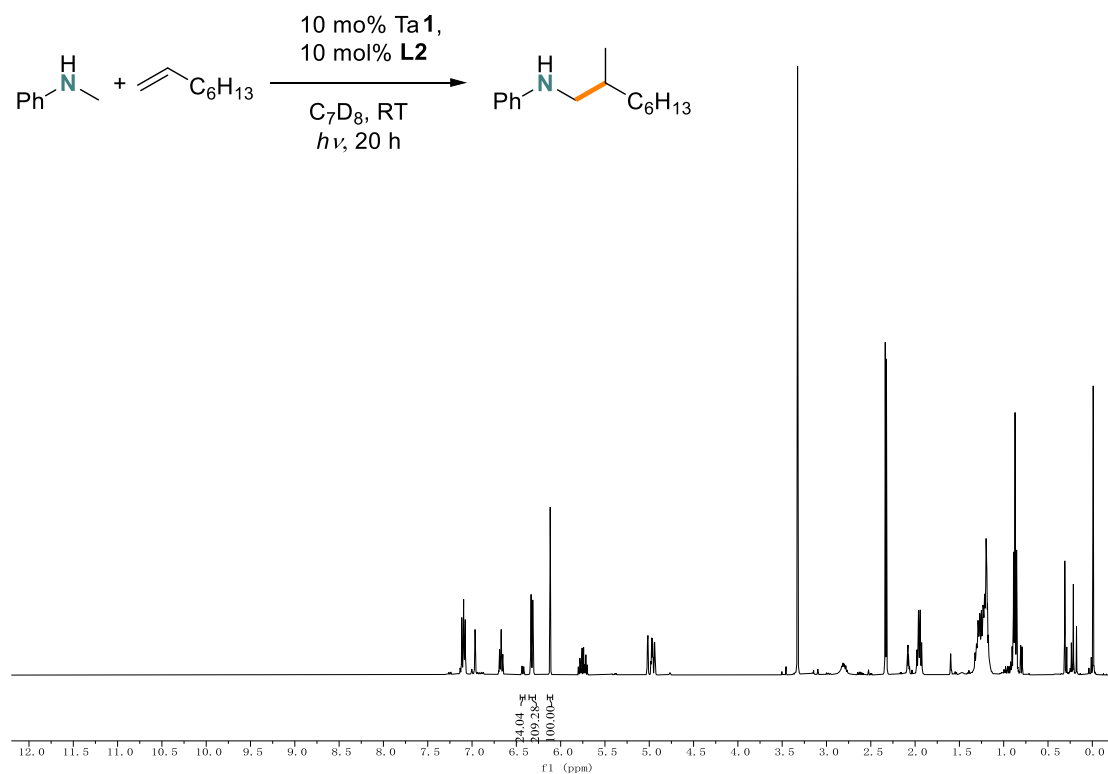


Figure S25

^1H NMR spectrum of reaction between 1-octene and N-methylaniline with 10 mol% TaL3 after 20 h irradiation in C_7D_8 at RT

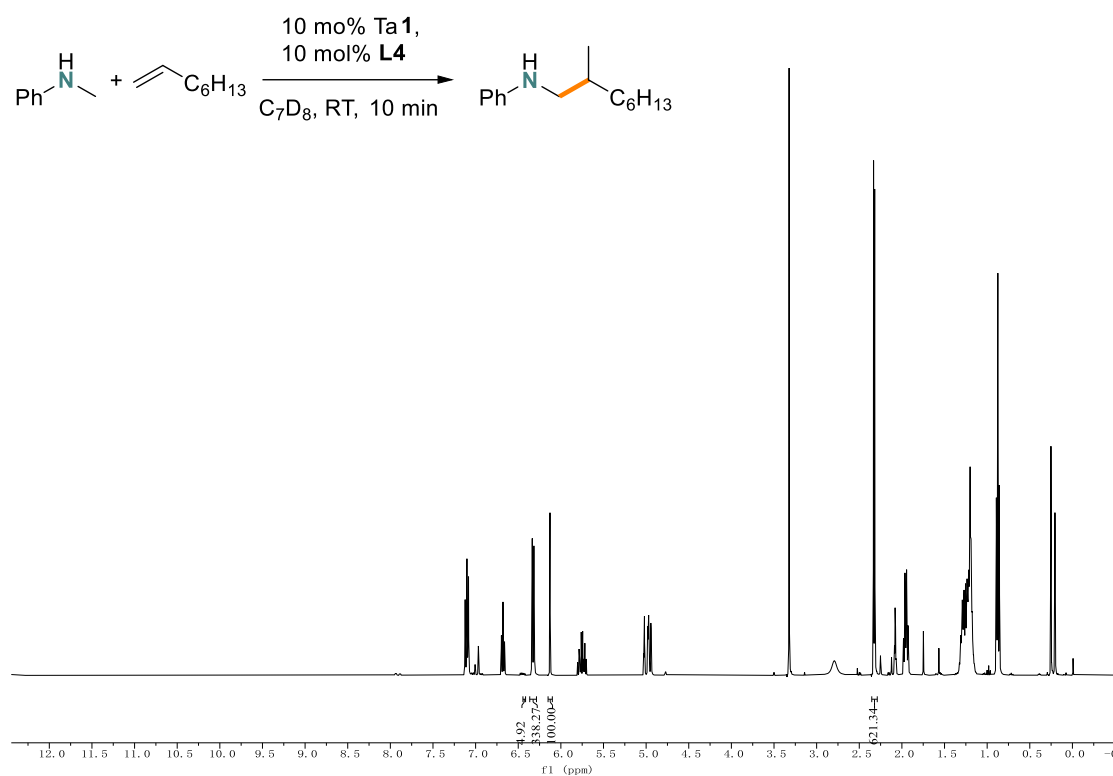


Figure S28

^1H NMR spectrum of reaction between 1-octene and N-methylaniline with 10 mol% TaL4 after 10 min in C_7D_8 at RT

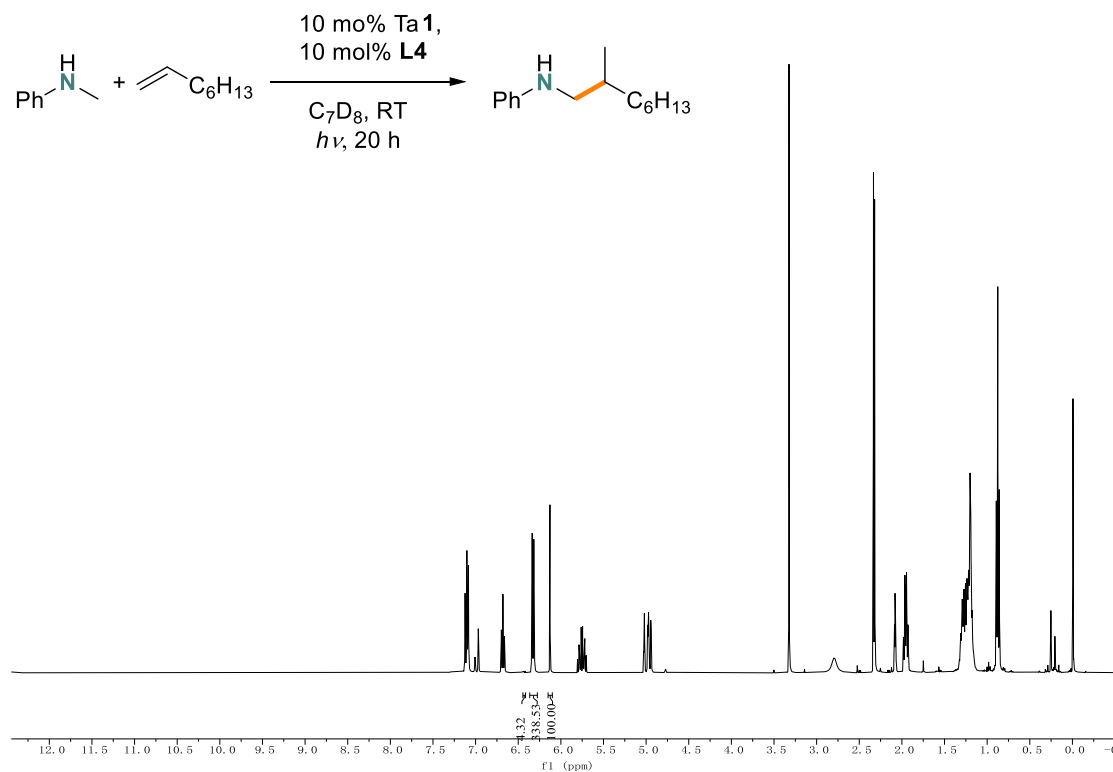


Figure S29

^1H NMR spectrum of reaction between 1-octene and N-methylaniline with 10 mol% TaL4 after 20 h irradiation in C_7D_8 at RT

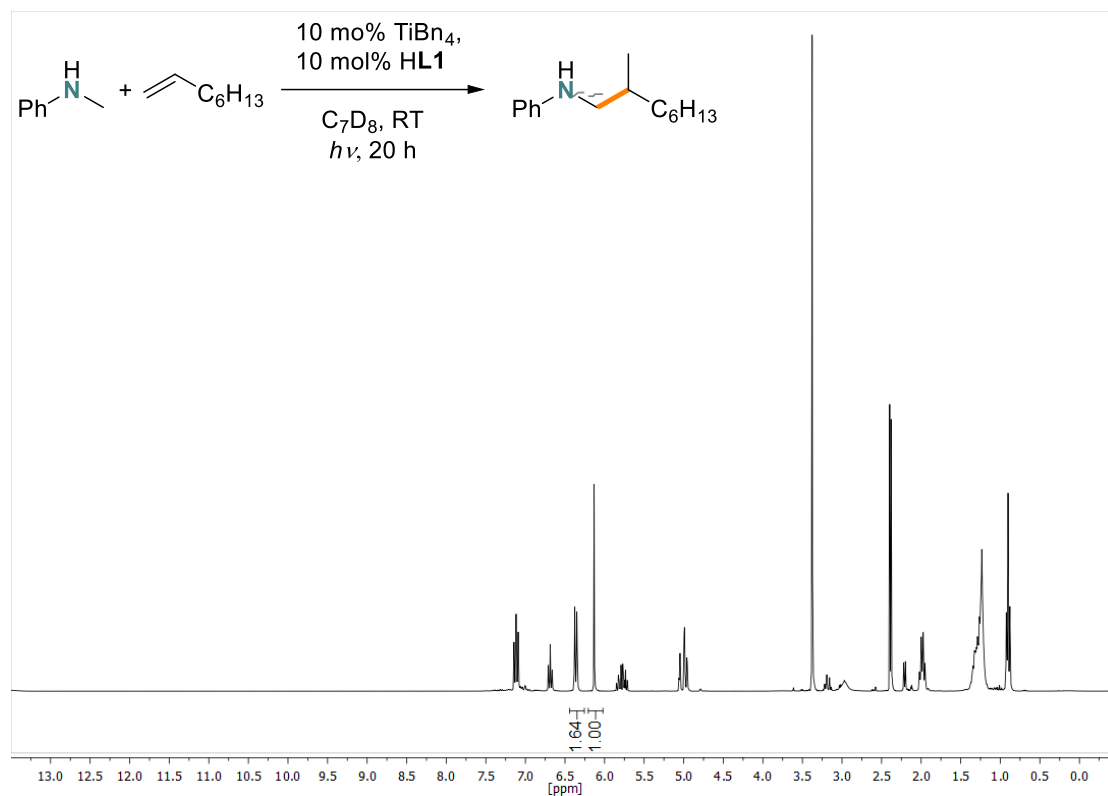


Figure S32

^1H NMR spectrum of reaction between 1-octene and N-methylaniline with 10 mol% TiBn_4 + **HL1** after 20 h irradiation in C_7D_8 at RT

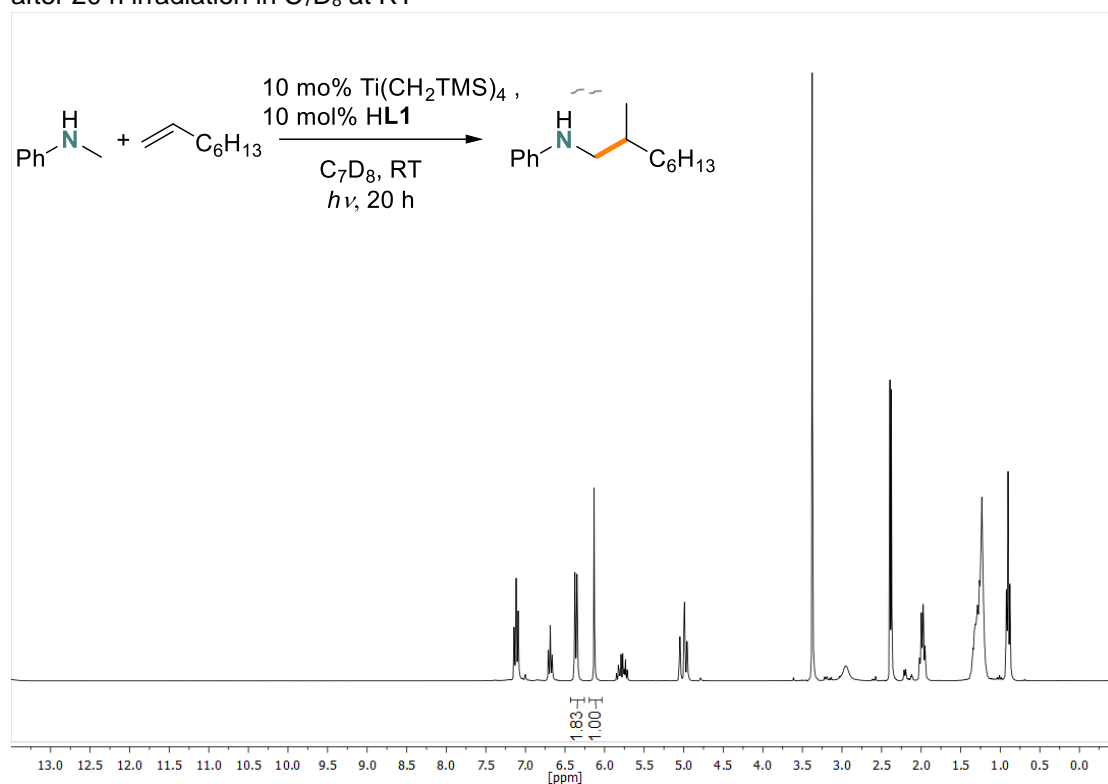


Figure S33

^1H NMR spectrum of reaction between 1-octene and N-methylaniline with 10 mol% $\text{Ti}(\text{CH}_2\text{TMS})_4$ + **HL1** after 20 h irradiation in C_7D_8 at RT

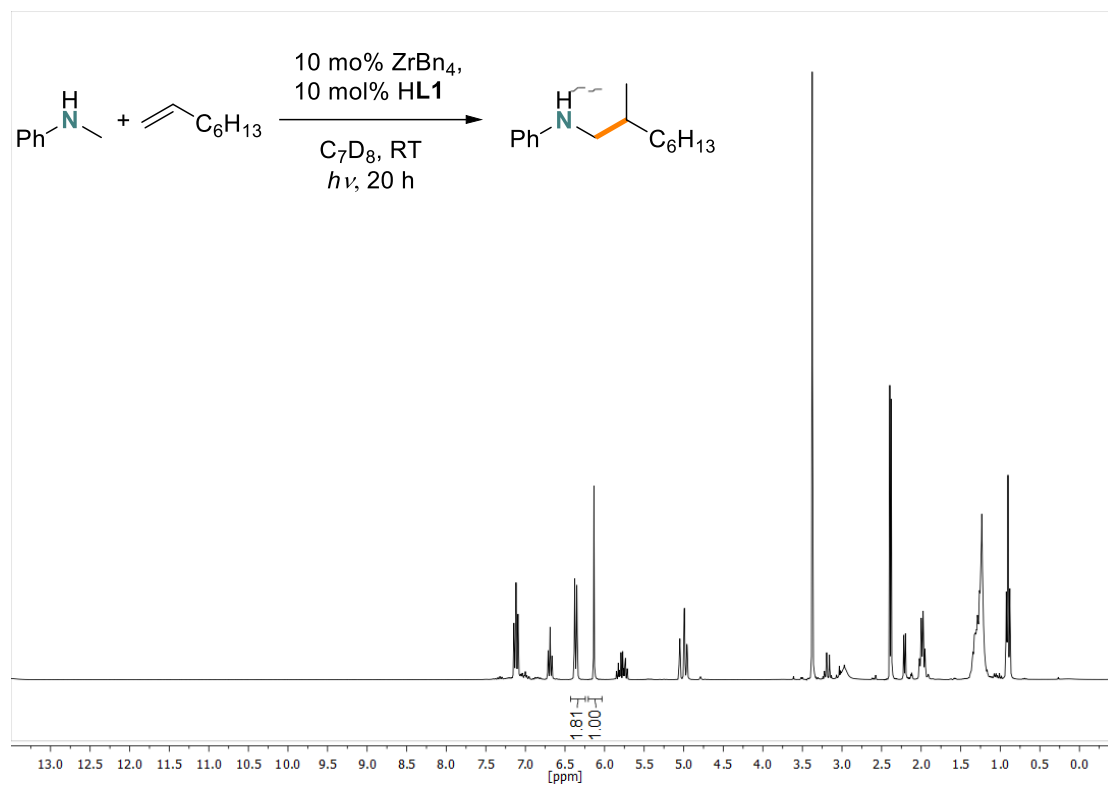


Figure S34

^1H NMR spectrum of reaction between 1-octene and N-methylaniline with 10 mol% ZrBn₄ + HL1 after 20 h irradiation in C₇D₈ at RT

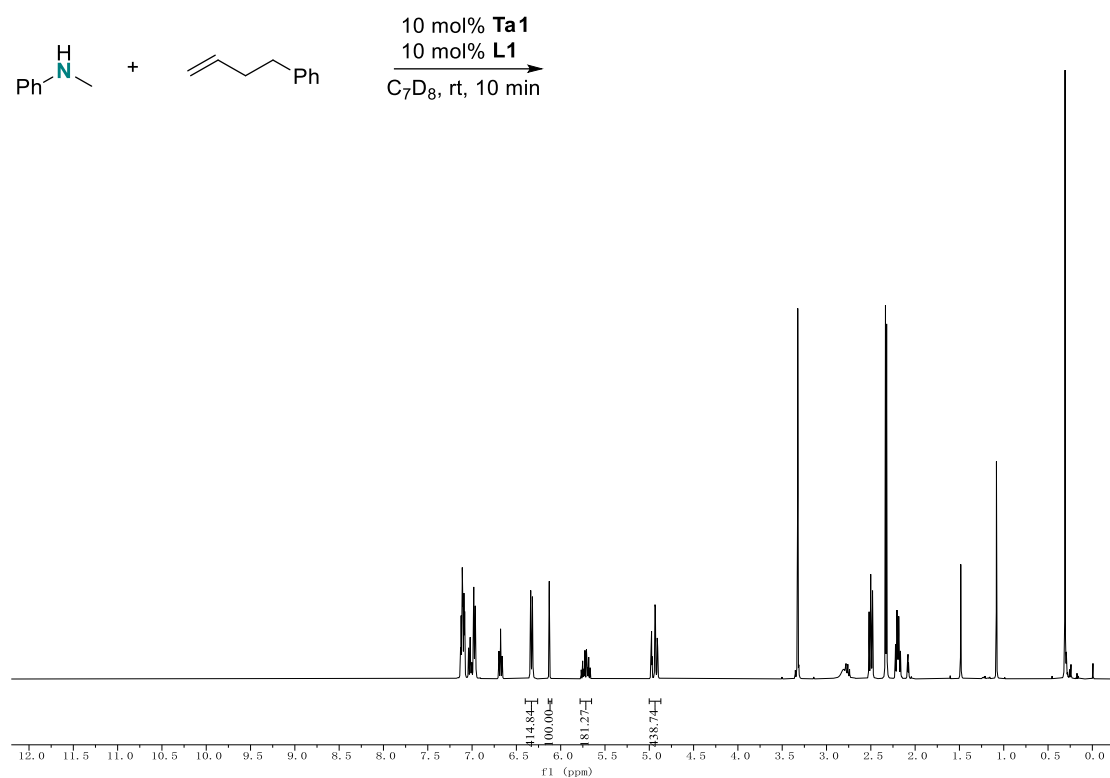


Figure S35

^1H NMR spectrum of reaction between but-3-en-1-ylbenzene and N-methylaniline with 10 mol% TaL1 after 10 min in C_7D_8 at RT

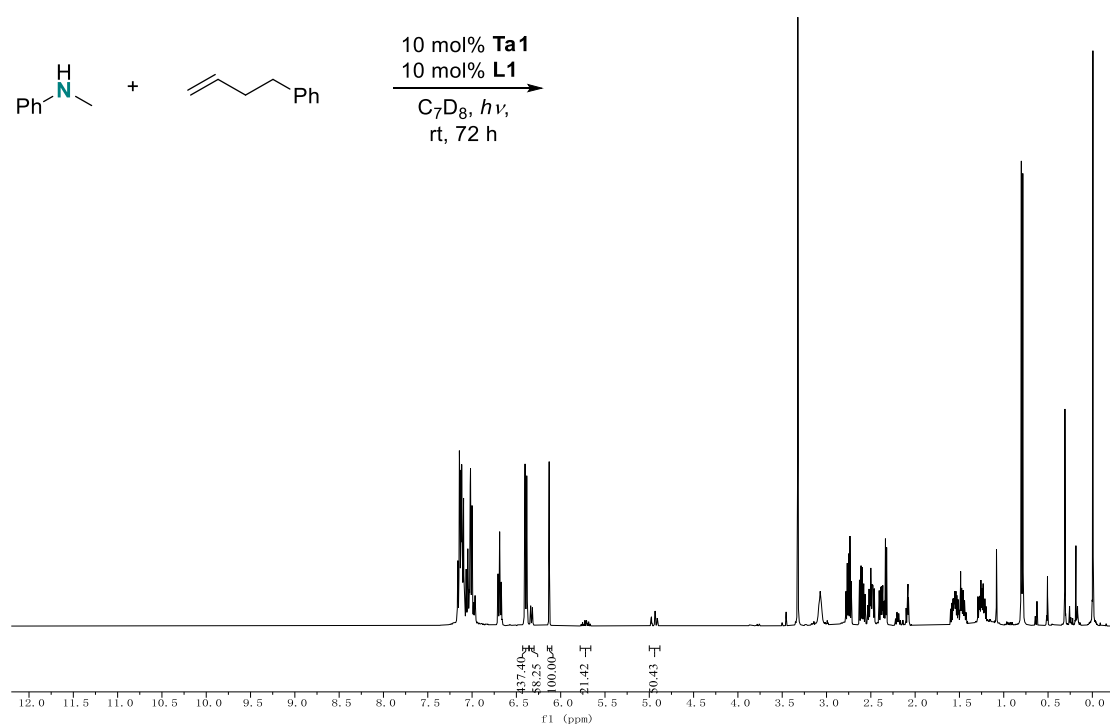


Figure S36

^1H NMR spectrum of reaction between but-3-en-1-ylbenzene and N-methylaniline with 10 mol% TaL1 after 72 h irradiation in C_7D_8 at RT

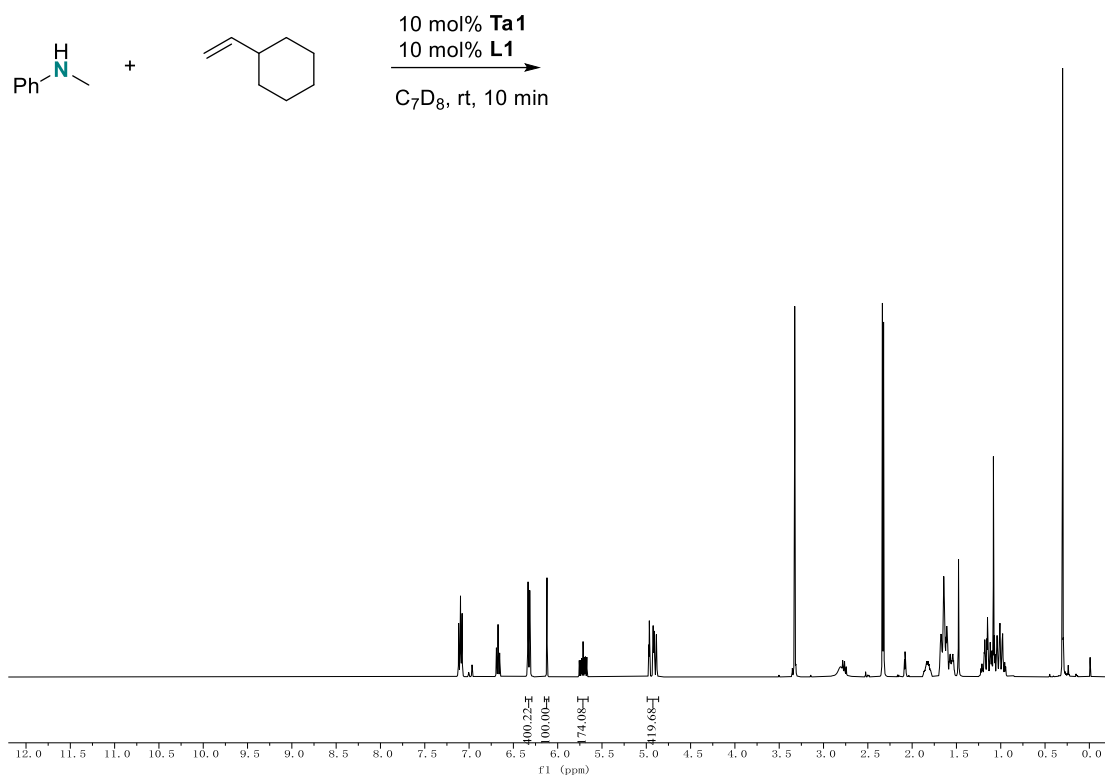


Figure S37

^1H NMR spectrum of reaction between vinylcyclohexane and N-methylaniline with 10 mol% TaL1 after 10 min in C_7D_8 at RT

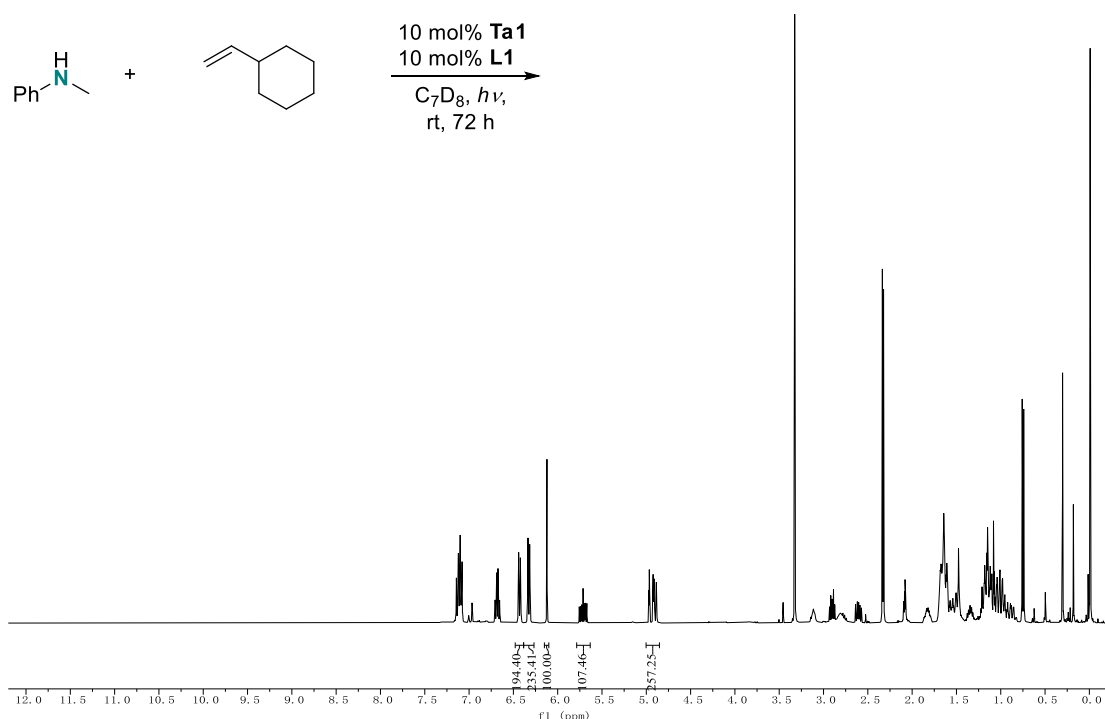


Figure S38

^1H NMR spectrum of reaction between vinylcyclohexane and N-methylaniline with 10 mol% TaL1 after 72 h irradiation in C_7D_8 at RT

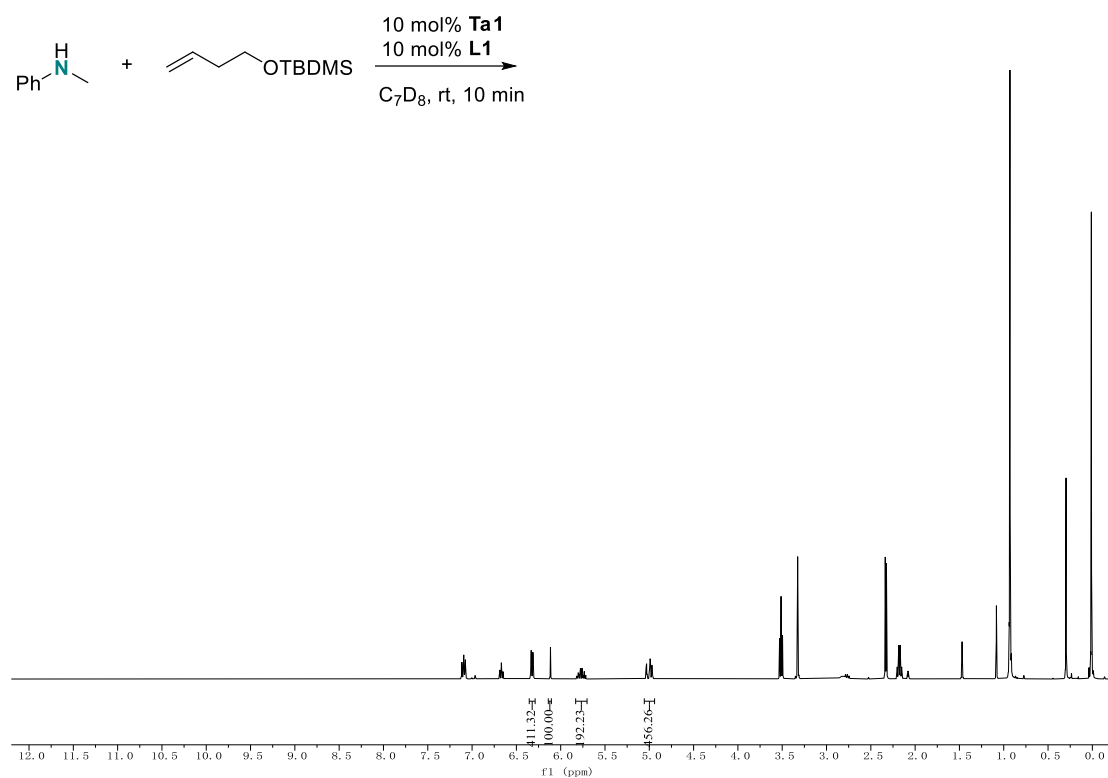


Figure S39

^1H NMR spectrum of reaction between (but-3-en-1-yloxy)(tert-butyl)dimethylsilane and N-methylaniline with 10 mol% TaL1 after 10 min in C_7D_8 at RT

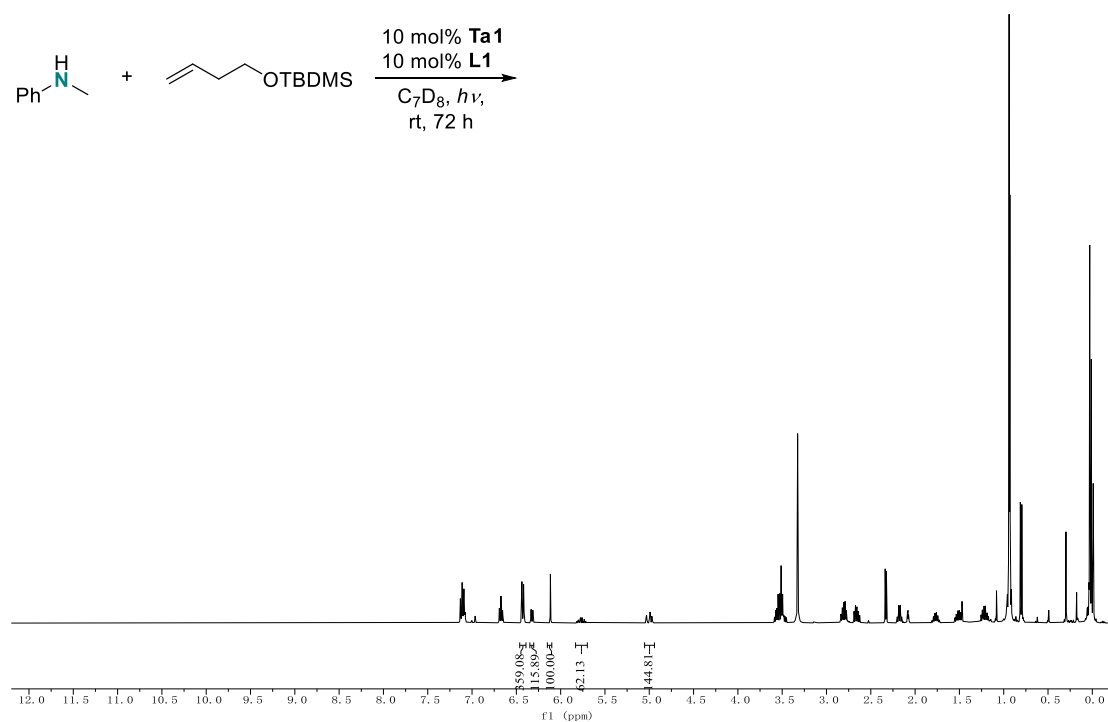


Figure S40

^1H NMR spectrum of reaction between (but-3-en-1-yloxy)(tert-butyl)dimethylsilane and N-methylaniline with 10 mol% TaL1 after 72 h irradiation in C_7D_8 at RT

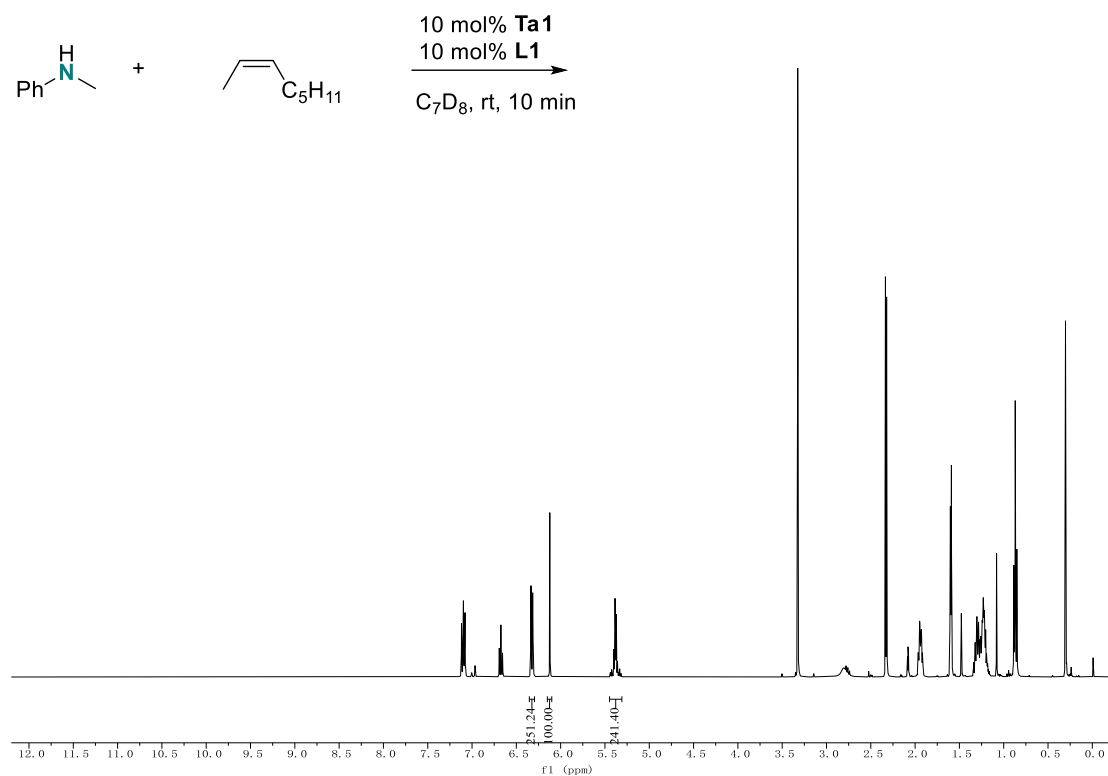


Figure S41

^1H NMR spectrum of reaction between 2-octene and N-methylaniline with 10 mol% TaL1 after 10 min in C_7D_8 at RT

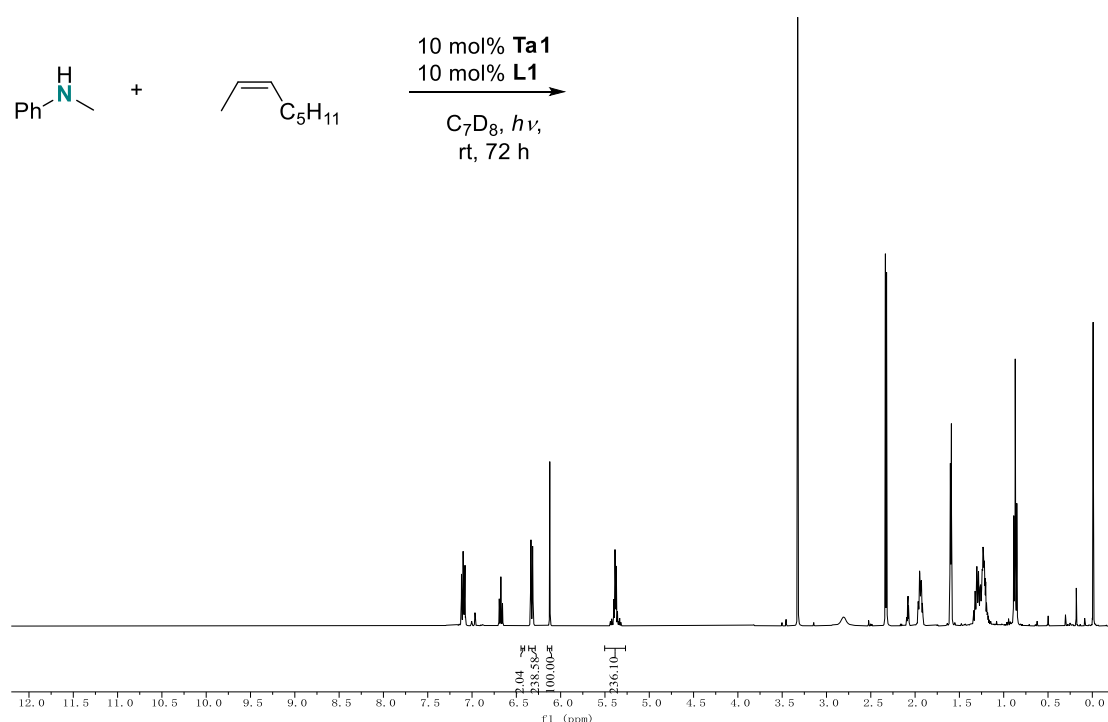


Figure S42

^1H NMR spectrum of reaction between 2-octene and N-methylaniline with 10 mol% TaL1 after 72 h irradiation in C_7D_8 at RT

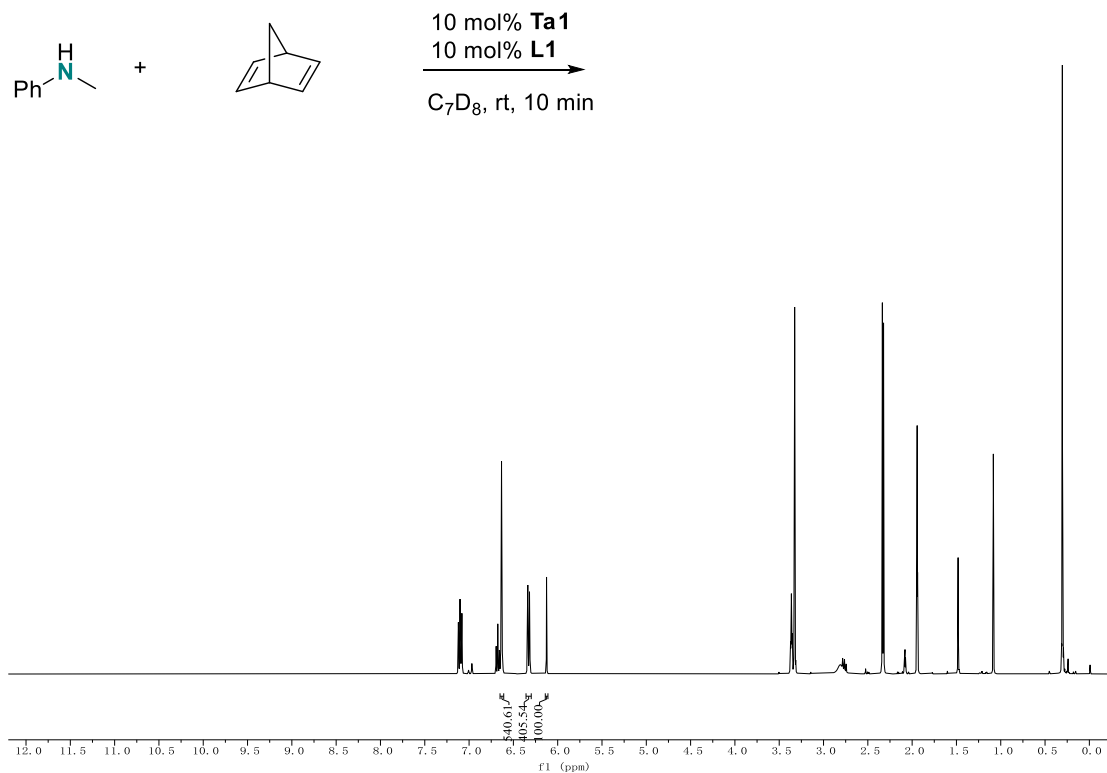


Figure S43

^1H NMR spectrum of reaction between norbornadiene and N-methylaniline with 10 mol% TaL1 after 10 min in C_7D_8 at RT

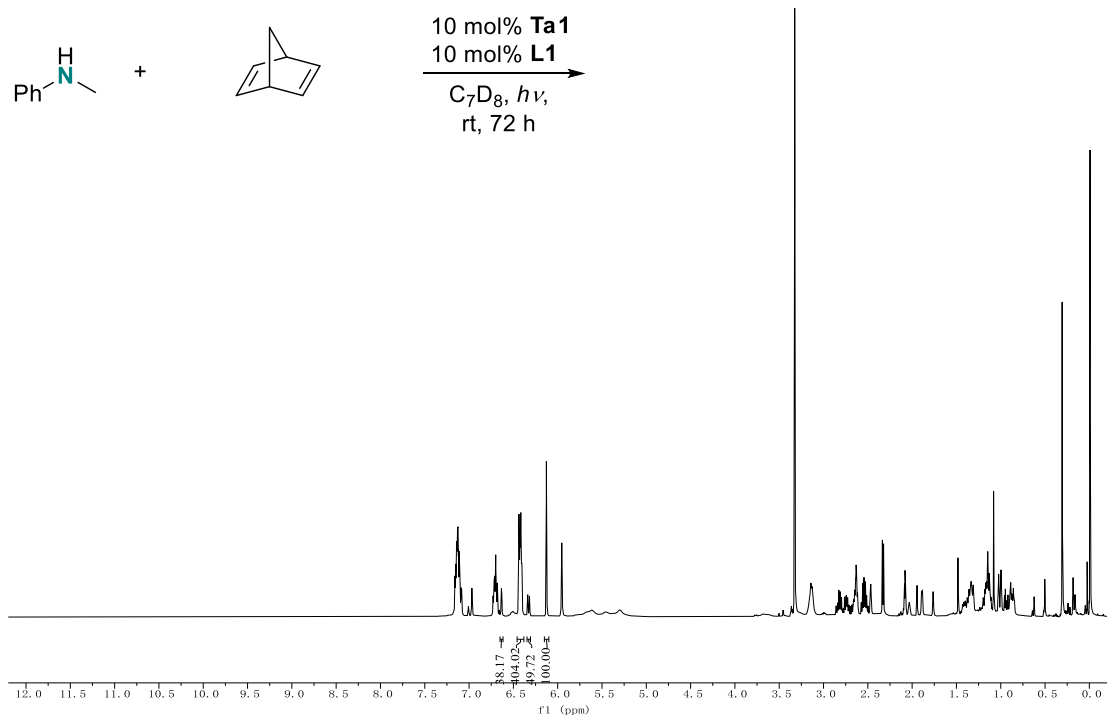


Figure S44

^1H NMR spectrum of reaction between norbornadiene and N-methylaniline with 10 mol% TaL1 after 72 h irradiation in C_7D_8 at RT

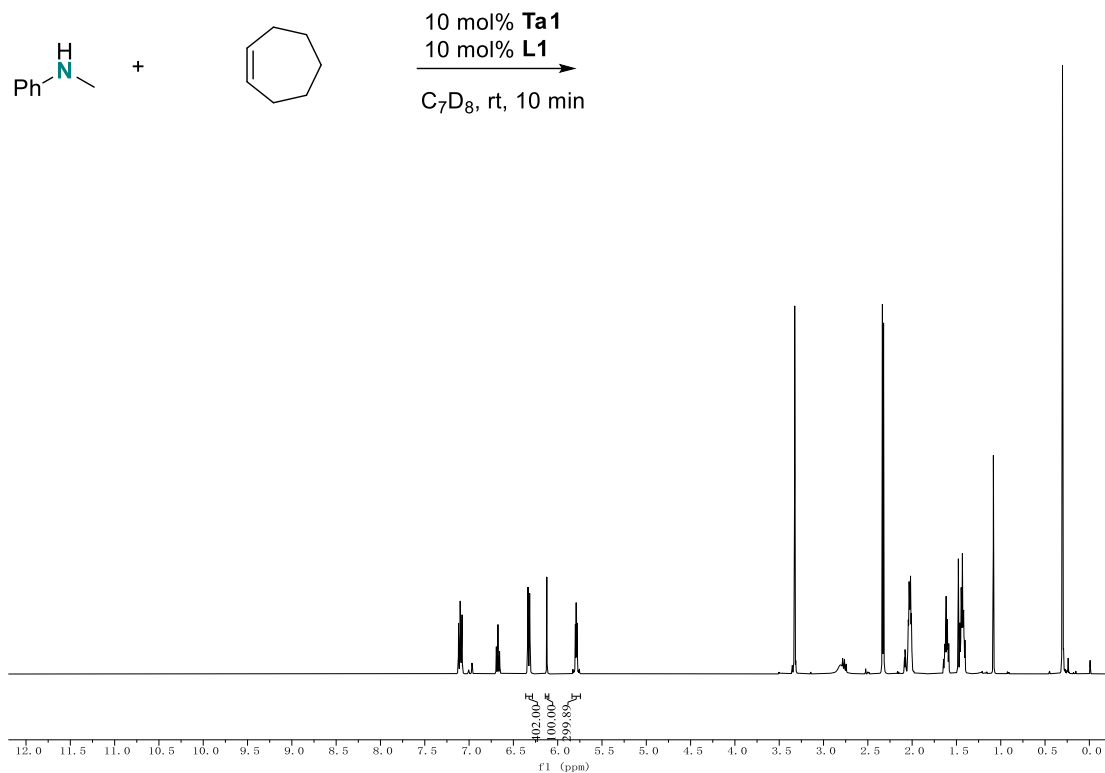


Figure S45

^1H NMR spectrum of reaction between cycloheptene and N-methylaniline with 10 mol% TaL1 after 10 min in C_7D_8 at RT

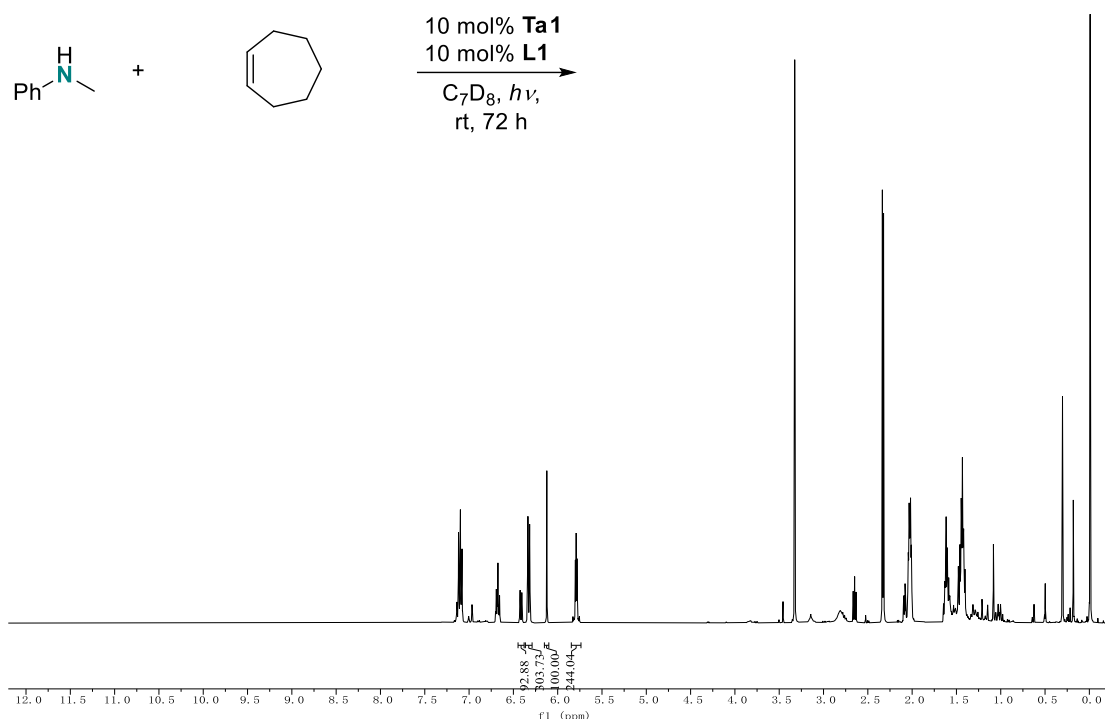


Figure S46

^1H NMR spectrum of reaction between cycloheptene and N-methylaniline with 10 mol% TaL1 after 72 h irradiation in C_7D_8 at RT

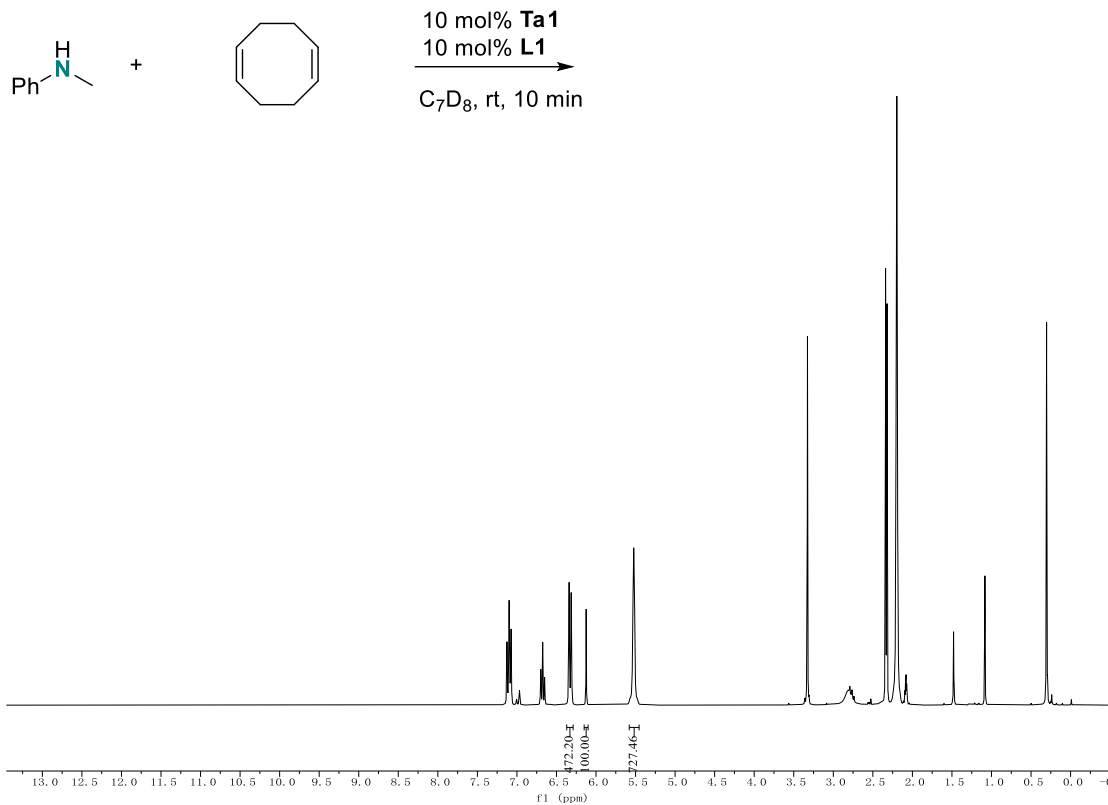


Figure S47

^1H NMR spectrum of reaction between 1,5-cyclooctadiene and N-methylaniline with 10 mol% TaL1 after 10 min in C_7D_8 at RT

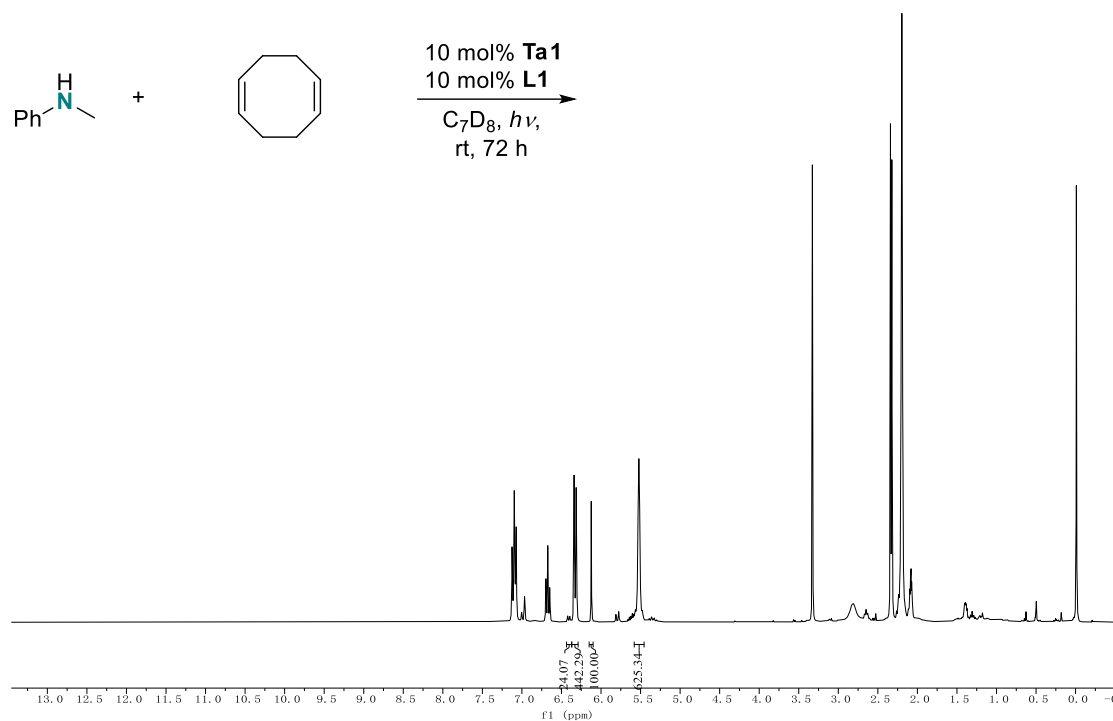


Figure S48

^1H NMR spectrum of reaction between 1,5-cyclooctadiene and N-methylaniline with 10 mol% TaL1 after 72 h irradiation in C_7D_8 at RT

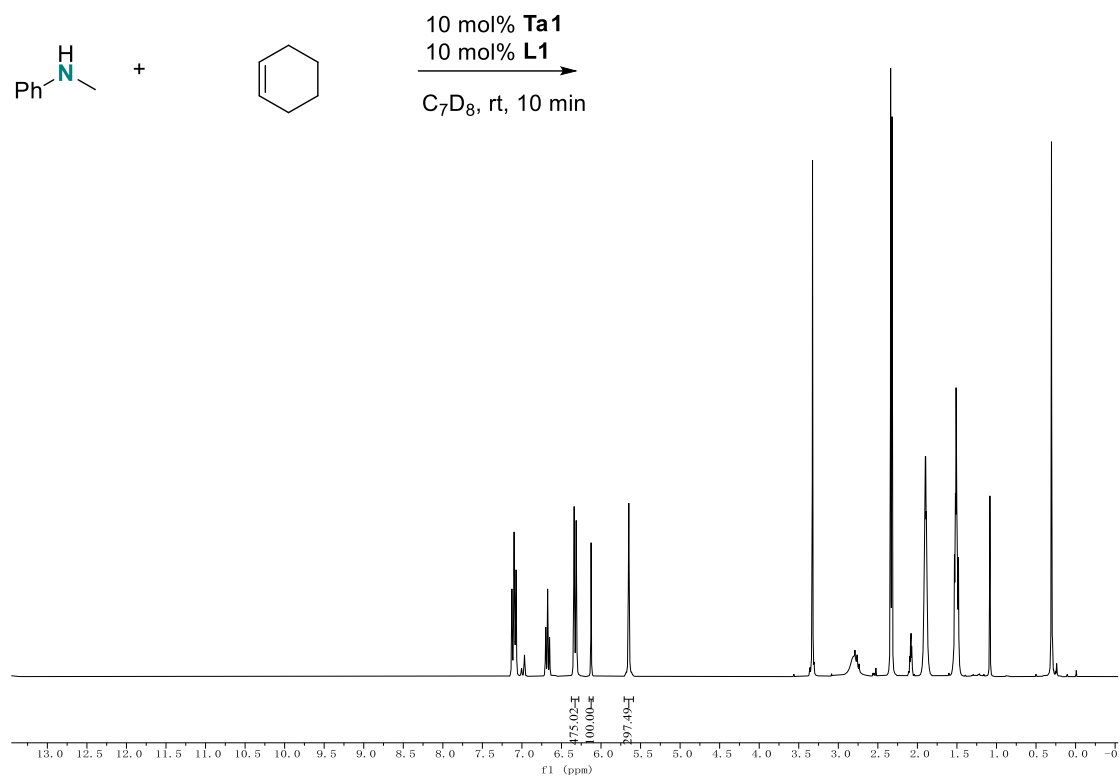


Figure S49

^1H NMR spectrum of reaction between cyclohexene and N-methylaniline with 10 mol% TaL1 after 10 min in C_7D_8 at RT

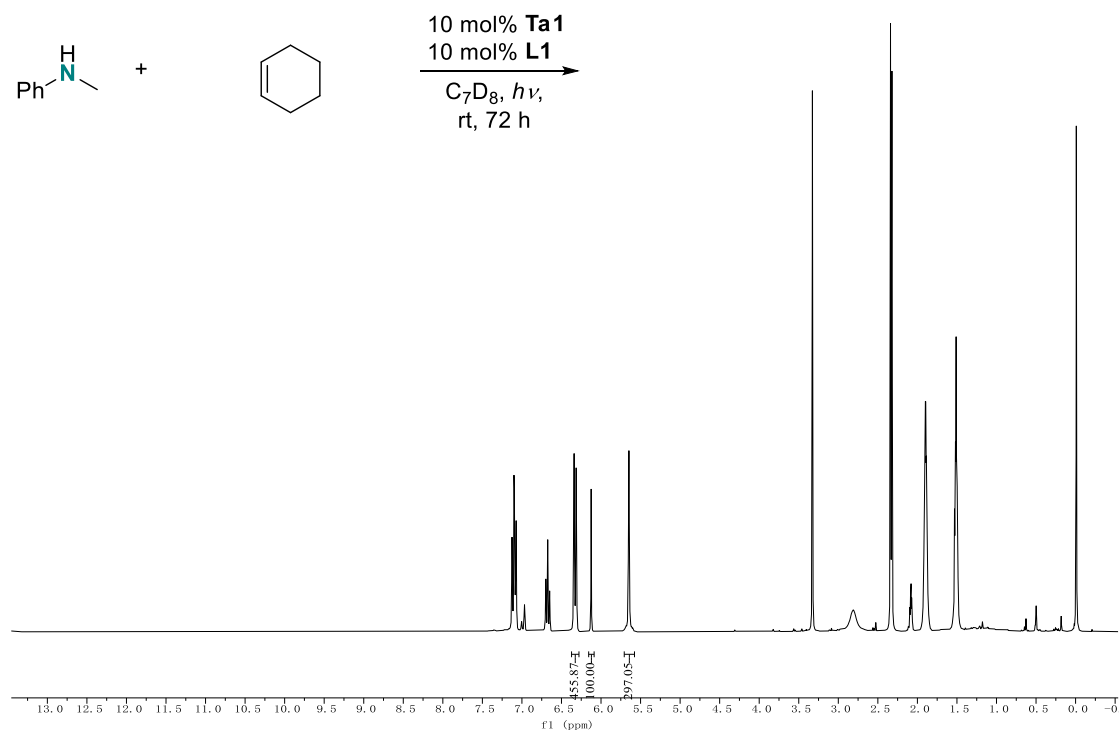


Figure S50

^1H NMR spectrum of reaction between cyclohexene and N-methylaniline with 10 mol% TaL1 after 72 h irradiation in C_7D_8 at RT

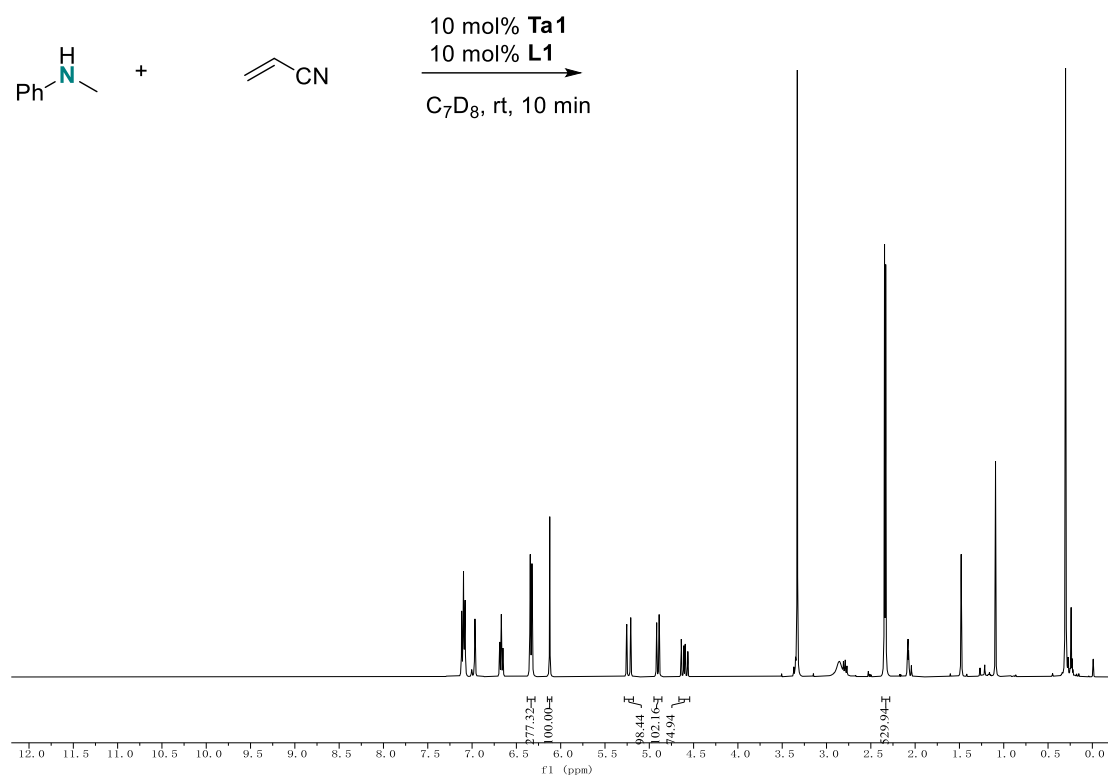


Figure S53

^1H NMR spectrum of reaction between acrylonitrile and N-methylaniline with 10 mol% TaL1 after 10 min in C_7D_8 at RT

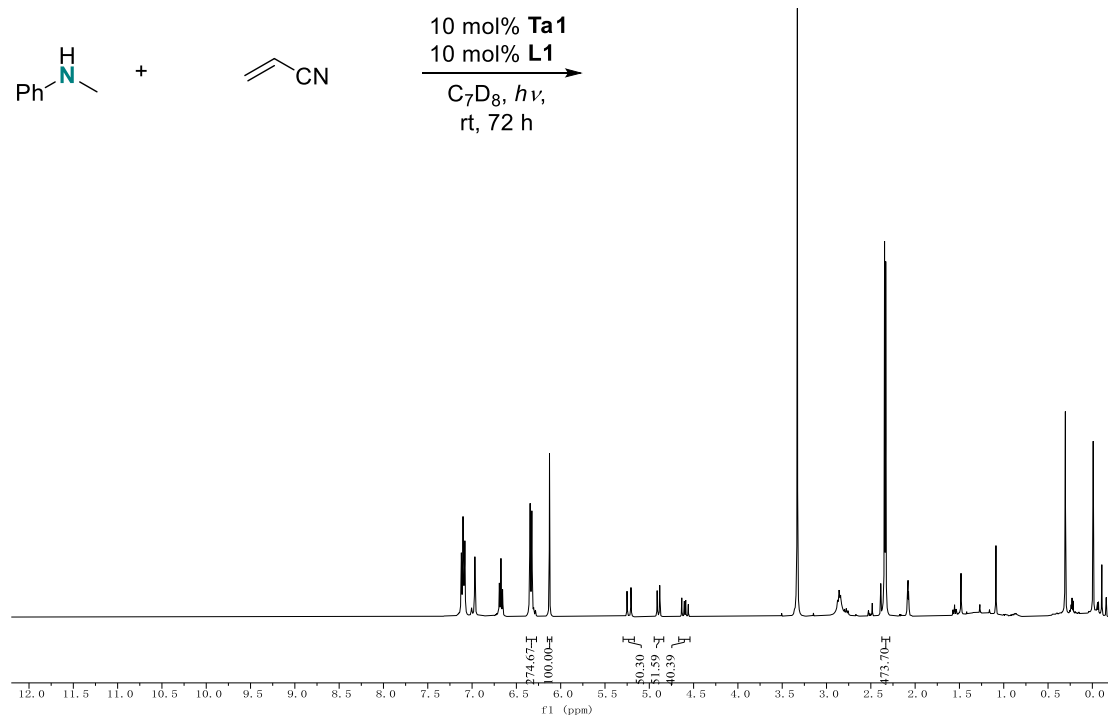


Figure S54

^1H NMR spectrum of reaction between acrylonitrile and N-methylaniline with 10 mol% TaL1 after 72 h irradiation in C_7D_8 at RT

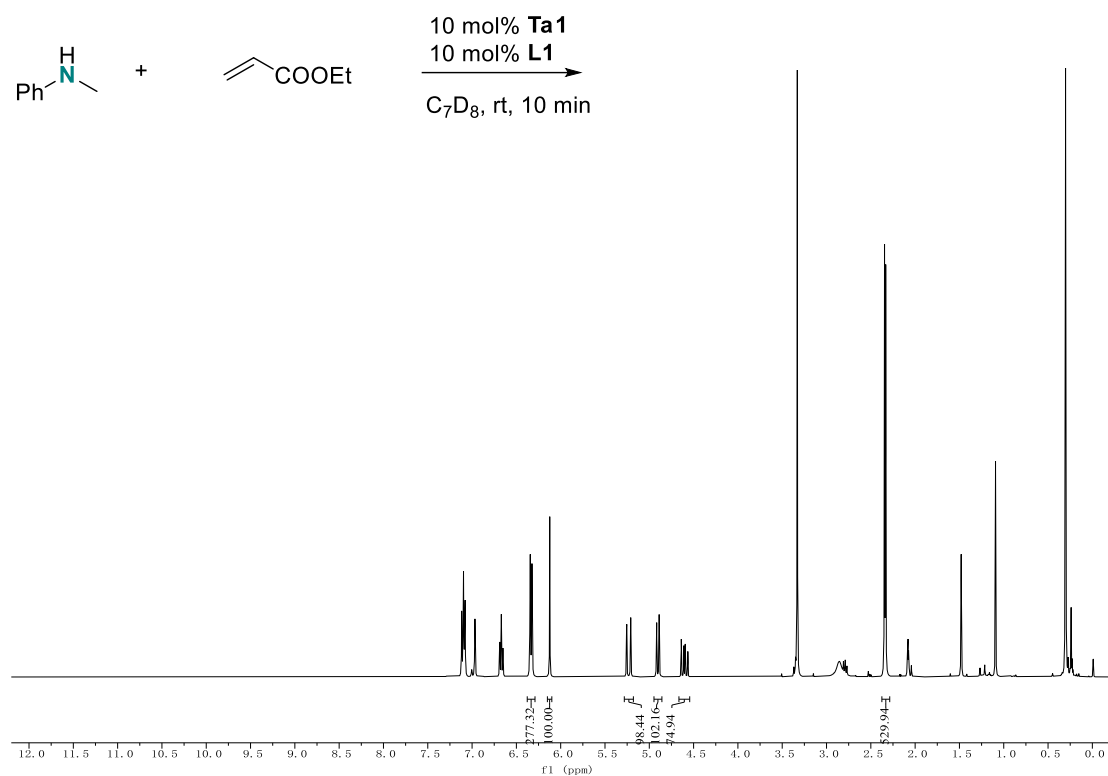


Figure S55

^1H NMR spectrum of reaction between ethylacrylate and N-methylaniline with 10 mol% TaL1 after 10 min in C_7D_8 at RT

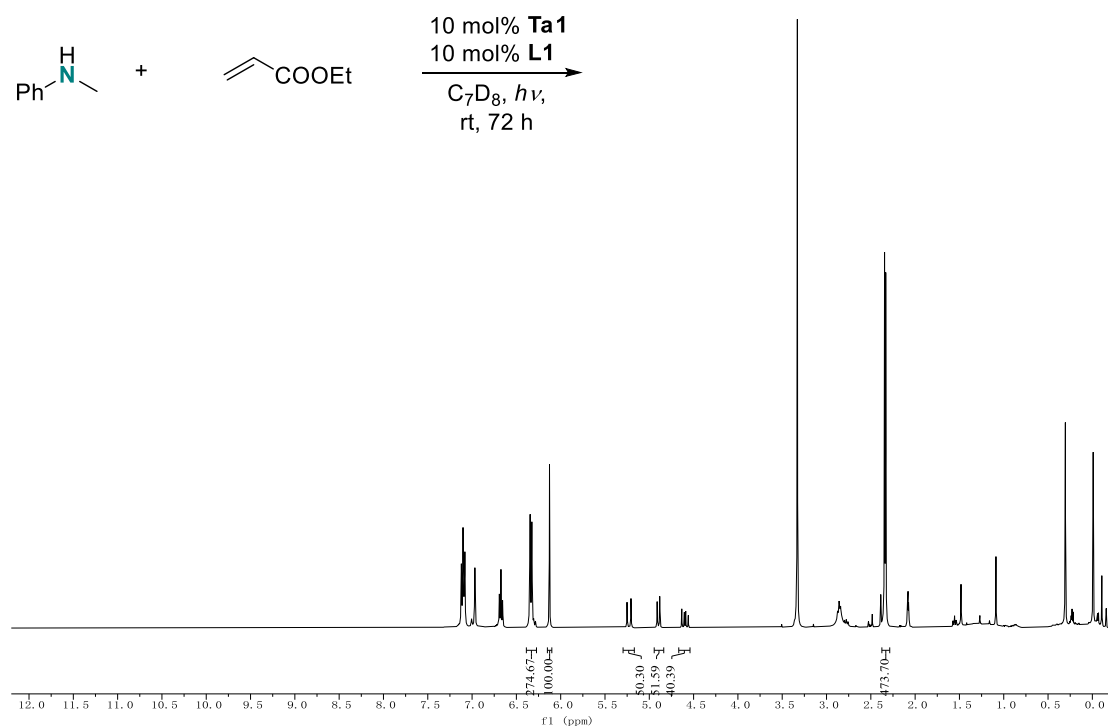


Figure S56

^1H NMR spectrum of reaction between ethylacrylate and N-methylaniline with 10 mol% TaL1 after 72 h irradiation in C_7D_8 at RT

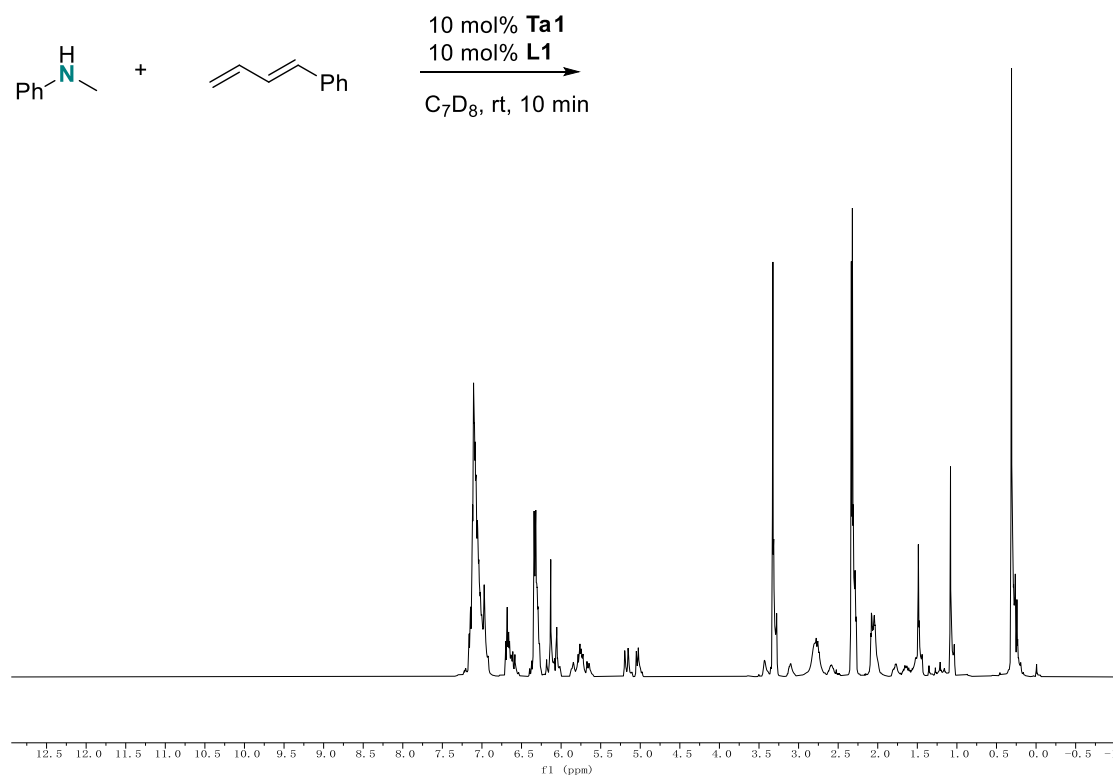


Figure S57

^1H NMR spectrum of reaction between 1-phenylbutadiene and N-methylaniline with 10 mol% TaL1 after 10 min in C_7D_8 at RT

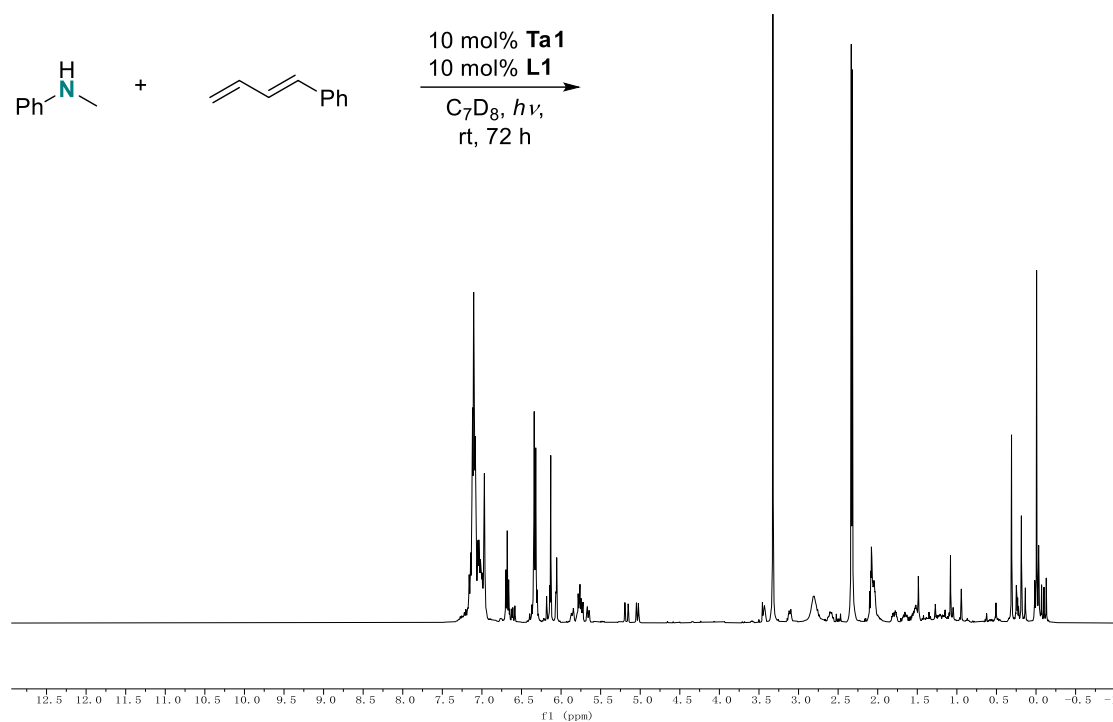


Figure S58

^1H NMR spectrum of reaction between 1-phenylbutadiene and N-methylaniline with 10 mol% TaL1 after 72 h irradiation in C_7D_8 at RT

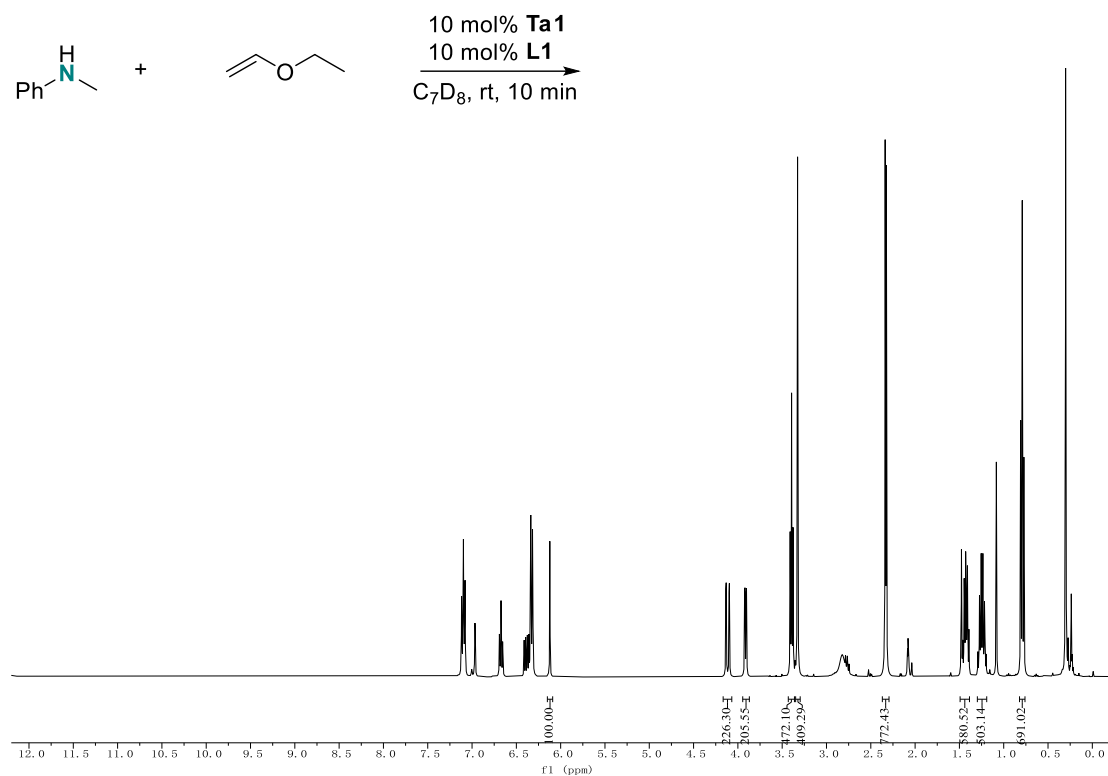


Figure S59

^1H NMR spectrum of reaction between ethyl vinyl ether and N-methylaniline with 10 mol% TaL1 after 10 min in C_7D_8 at RT

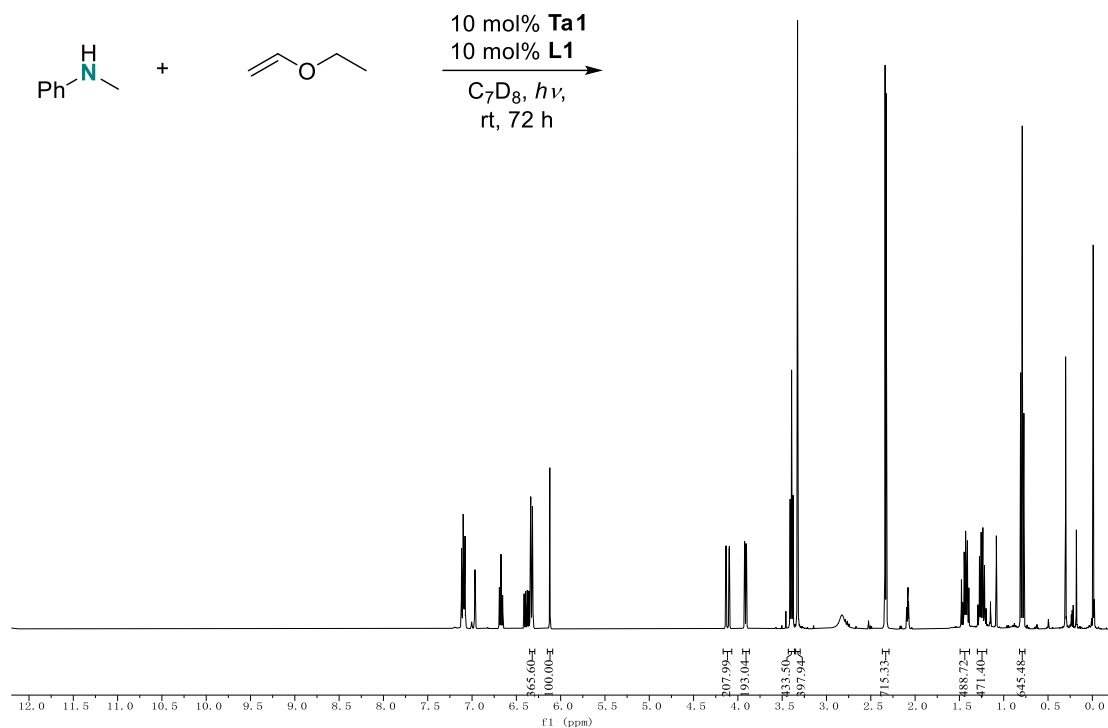


Figure S60

^1H NMR spectrum of reaction between ethyl vinyl ether and N-methylaniline with 10 mol% TaL1 after 72 h irradiation in C_7D_8 at RT

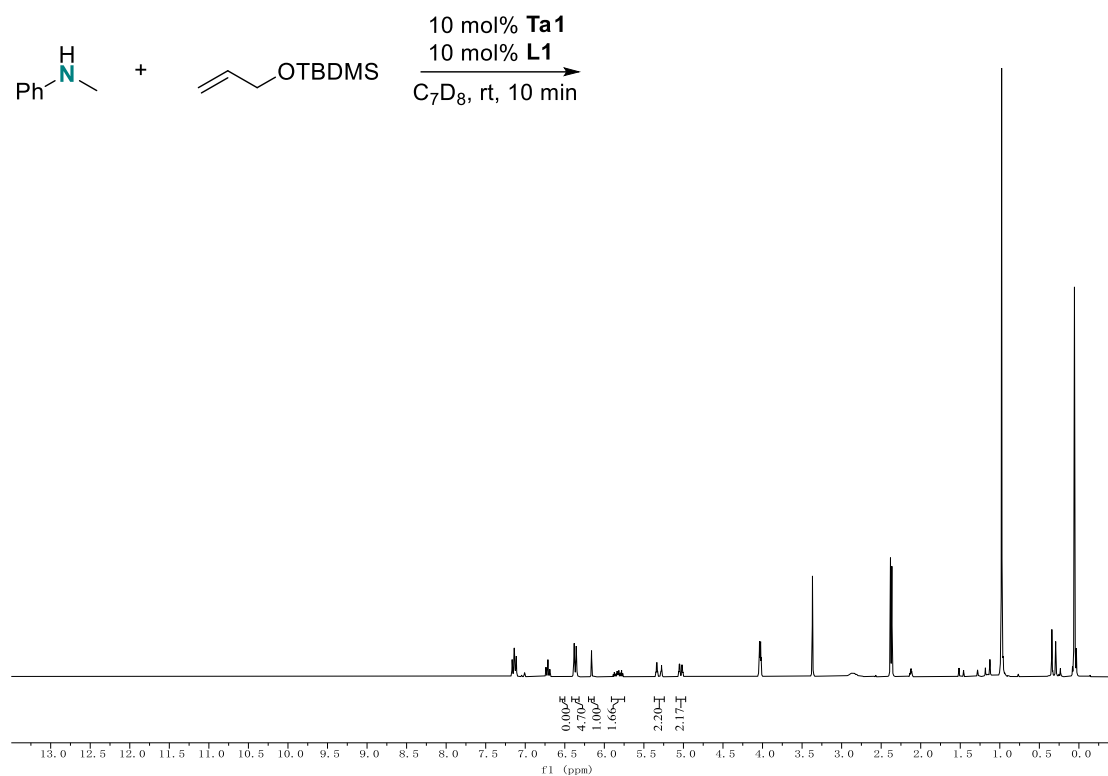


Figure S61

^1H NMR spectrum of reaction between (allyloxy)(tert-butyl)dimethylsilane and N-methylaniline with 10 mol% TaL1 after 10 min in C_7D_8 at RT

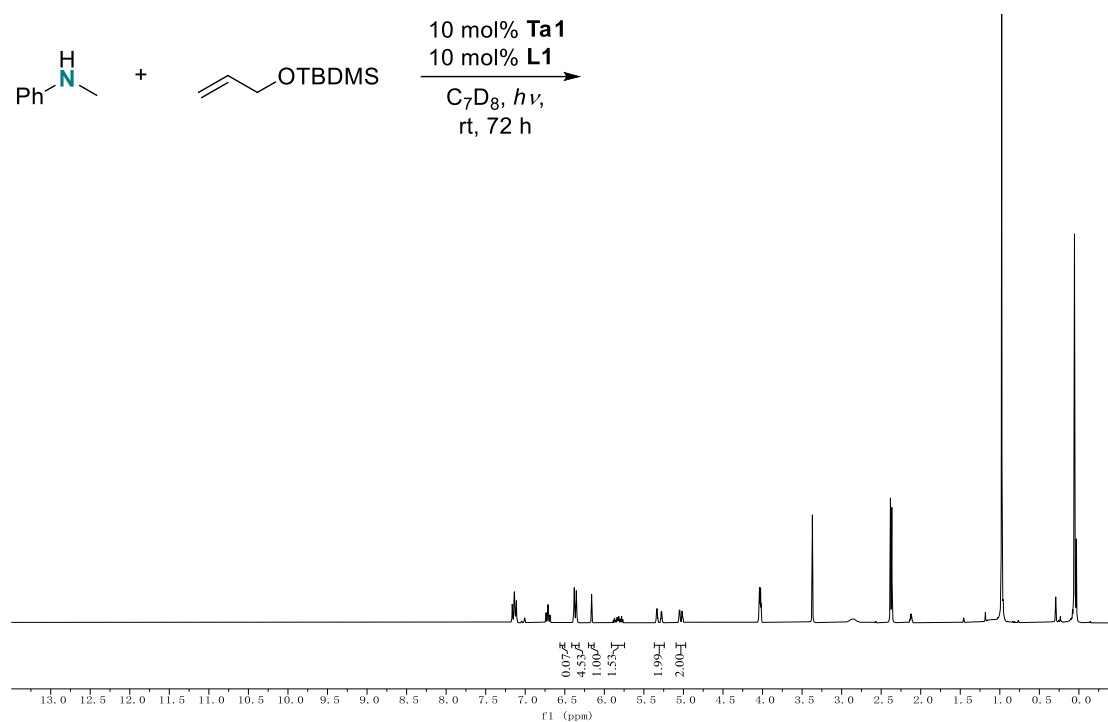


Figure S62

^1H NMR spectrum of reaction between (allyloxy)(tert-butyl)dimethylsilane and N-methylaniline with 10 mol% TaL1 after 72 h irradiation in C_7D_8 at RT

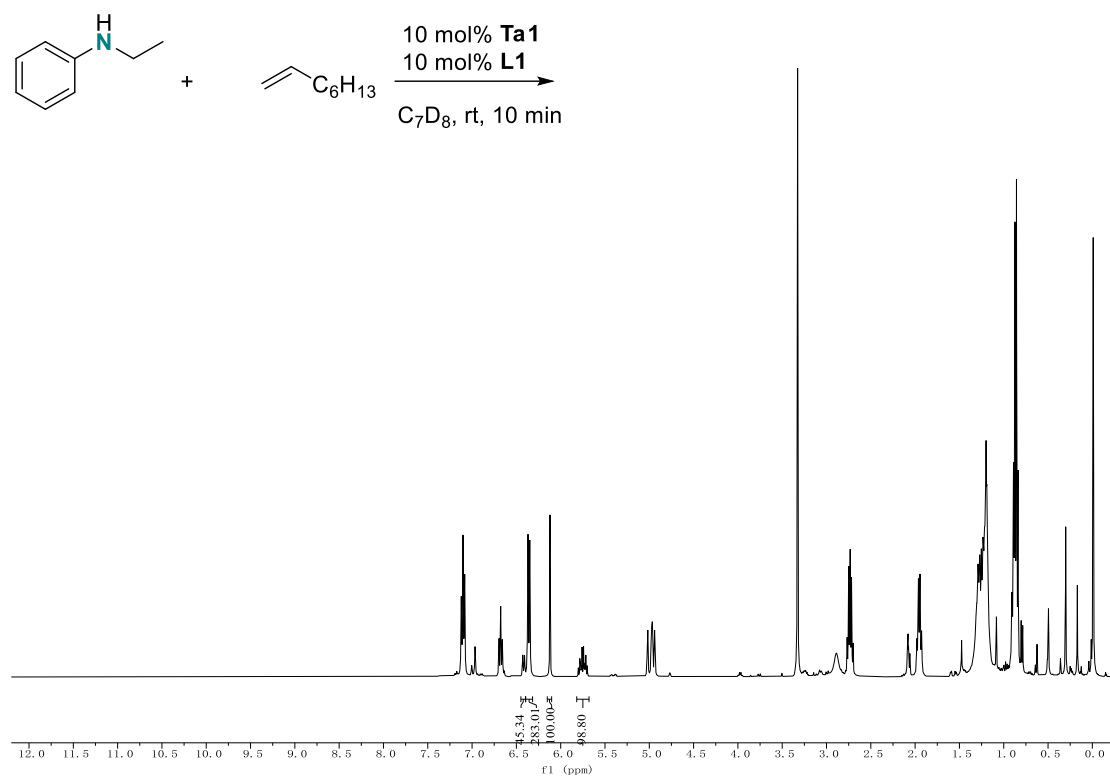


Figure S67

^1H NMR spectrum of reaction between 1-octene and N-ethylaniline with 10 mol% TaL1 after 10 min in C_7D_8 at RT

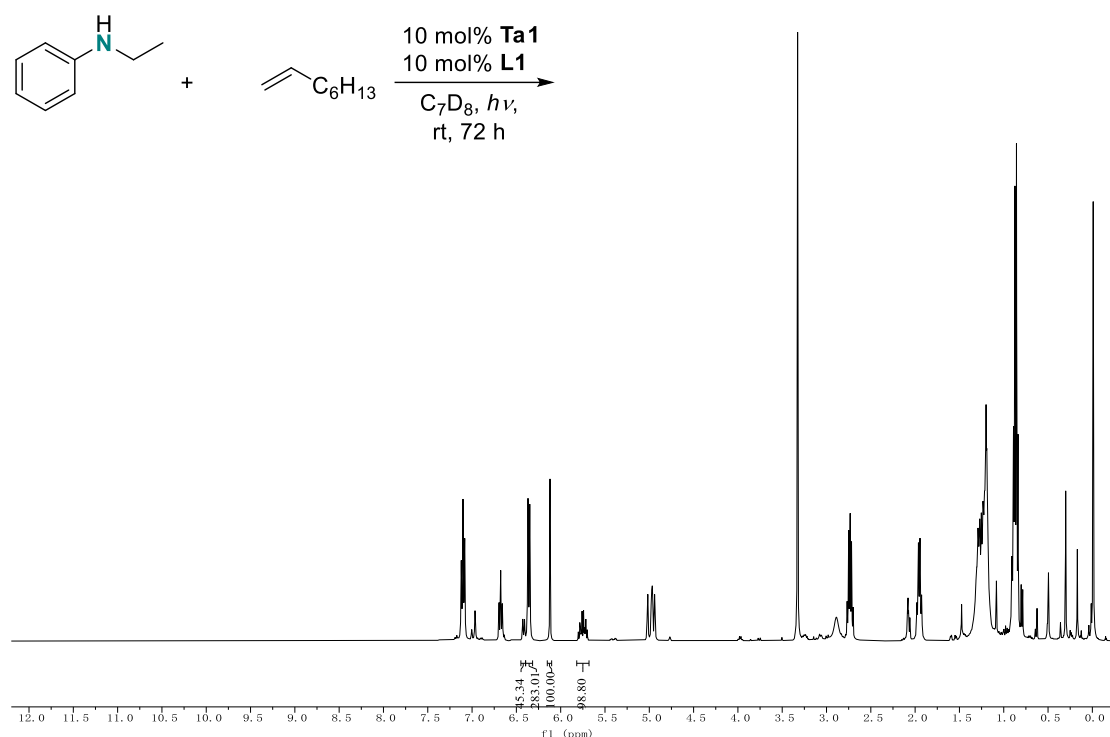


Figure S68

^1H NMR spectrum of reaction between 1-octene and N-ethylaniline with 10 mol% TaL1 after 72 h $h\nu$ irradiation in C_7D_8 at RT

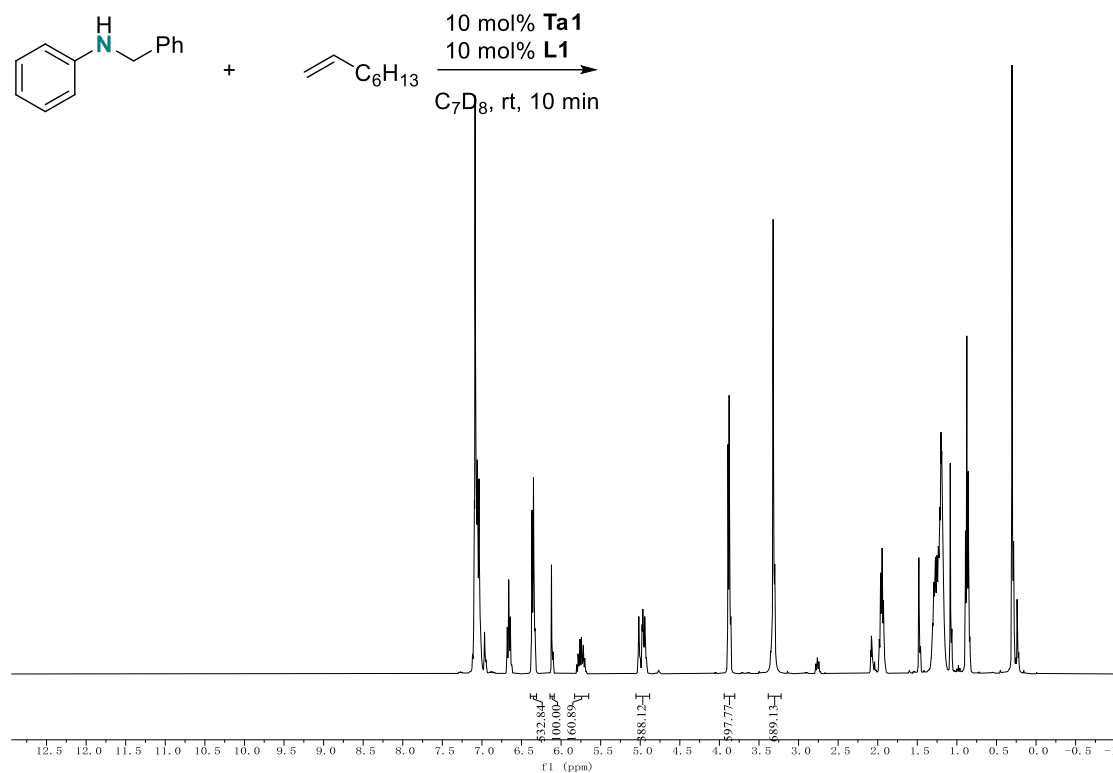


Figure S69

^1H NMR spectrum of reaction between 1-octene and N-benzylaniline with 10 mol% TaL1 after 10 min in C_7D_8 at RT

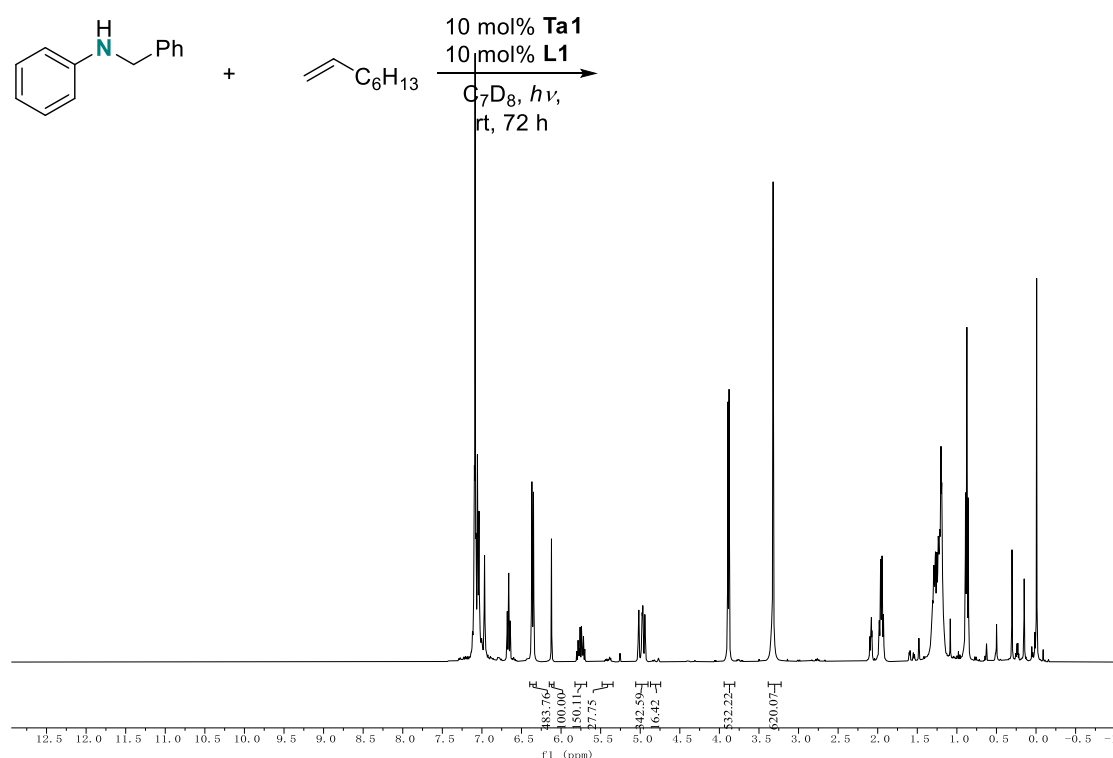


Figure S70

^1H NMR spectrum of reaction between 1-octene and N-benzylaniline with 10 mol% TaL1 after 72 h irradiation in C_7D_8 at RT

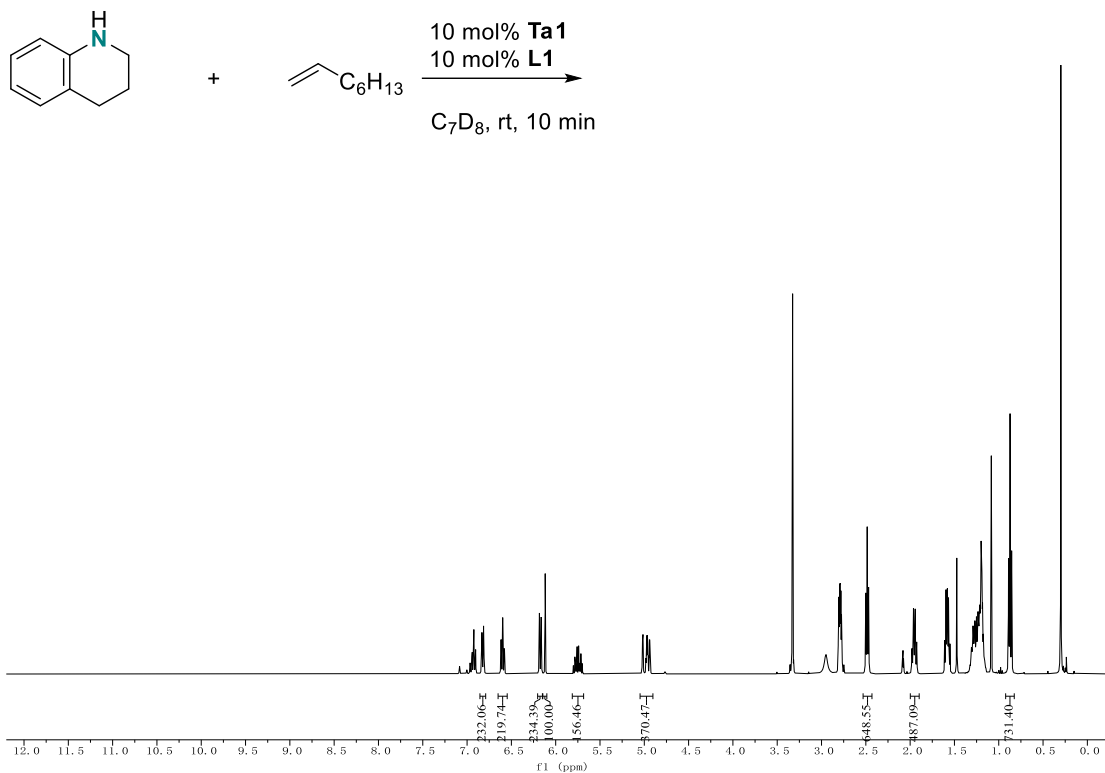


Figure S71

^1H NMR spectrum of reaction between 1-octene and 1,2,3,4-tetrahydroquinoline with 10 mol% TaL1 after 10 min in C_7D_8 at RT

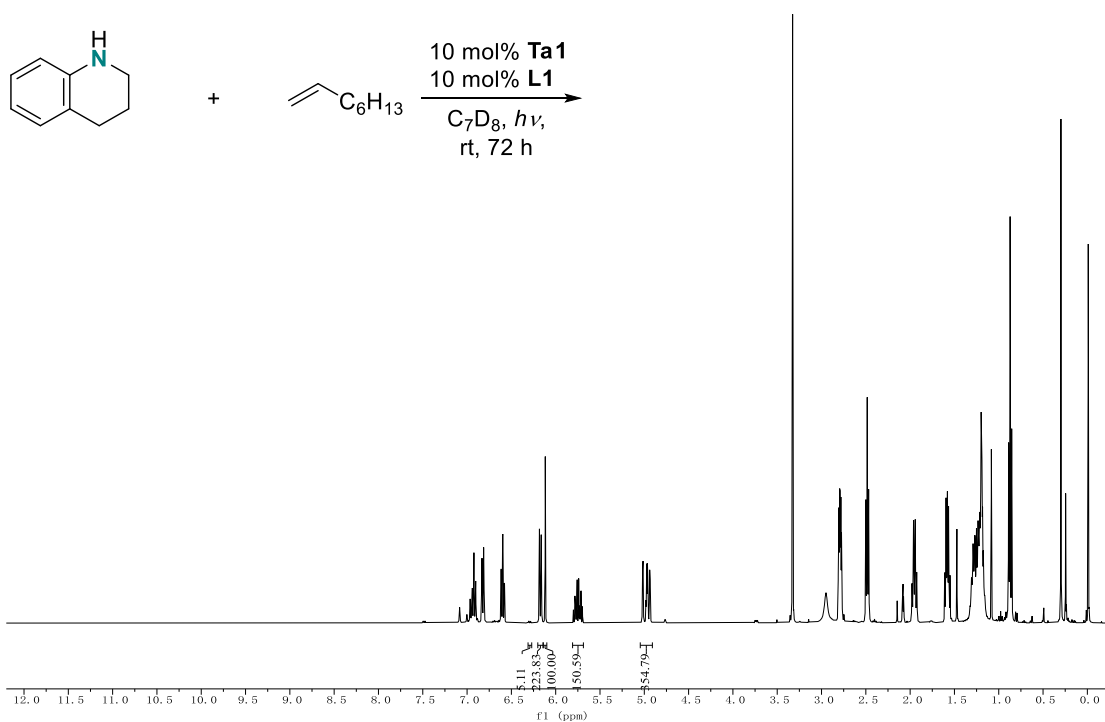


Figure S72

^1H NMR spectrum of reaction between 1-octene and 1,2,3,4-tetrahydroquinoline with 10 mol% TaL1 after 72 h irradiation in C_7D_8 at RT

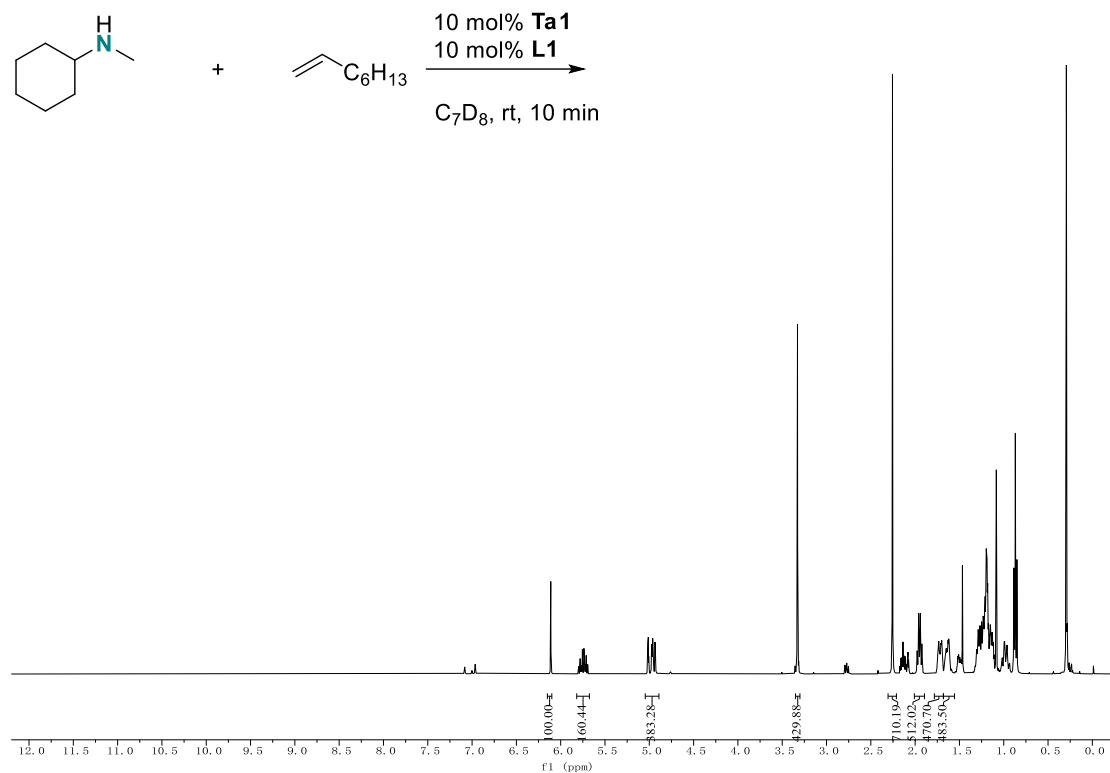


Figure S73

^1H NMR spectrum of reaction between 1-octene and N-methylcyclohexanamine with 10 mol% TaL1 after 10 min in C_7D_8 at RT

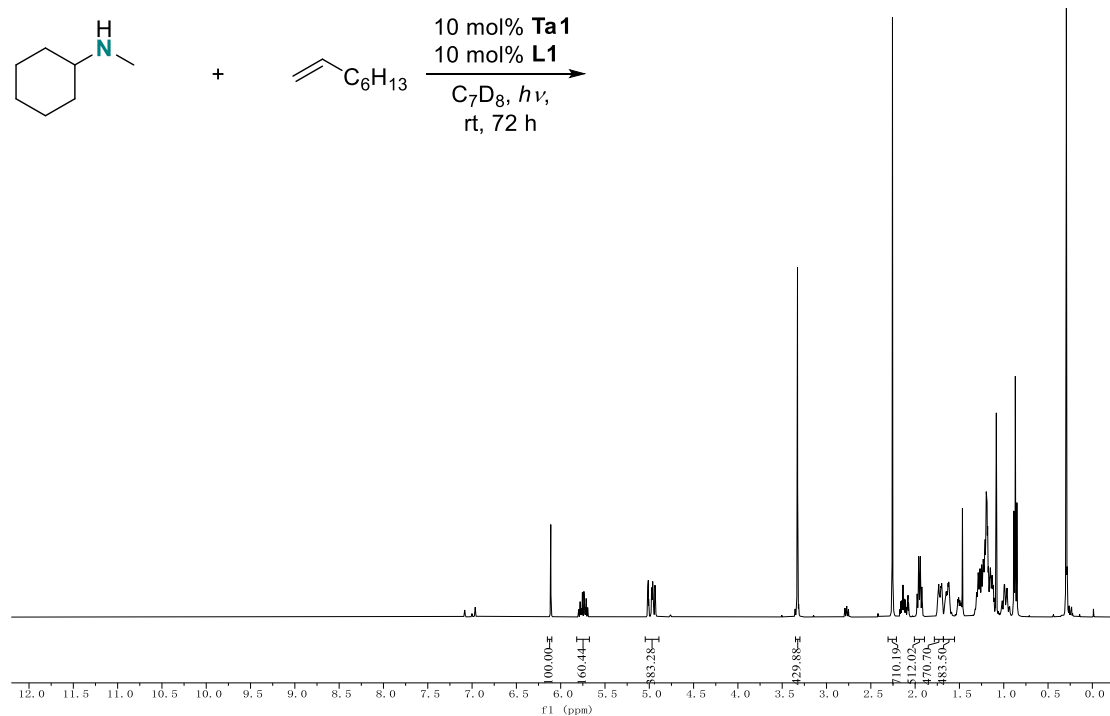


Figure S74

^1H NMR spectrum of reaction between 1-octene and N-methylcyclohexanamine with 10 mol% TaL1 after 72 h irradiation in C_7D_8 at RT

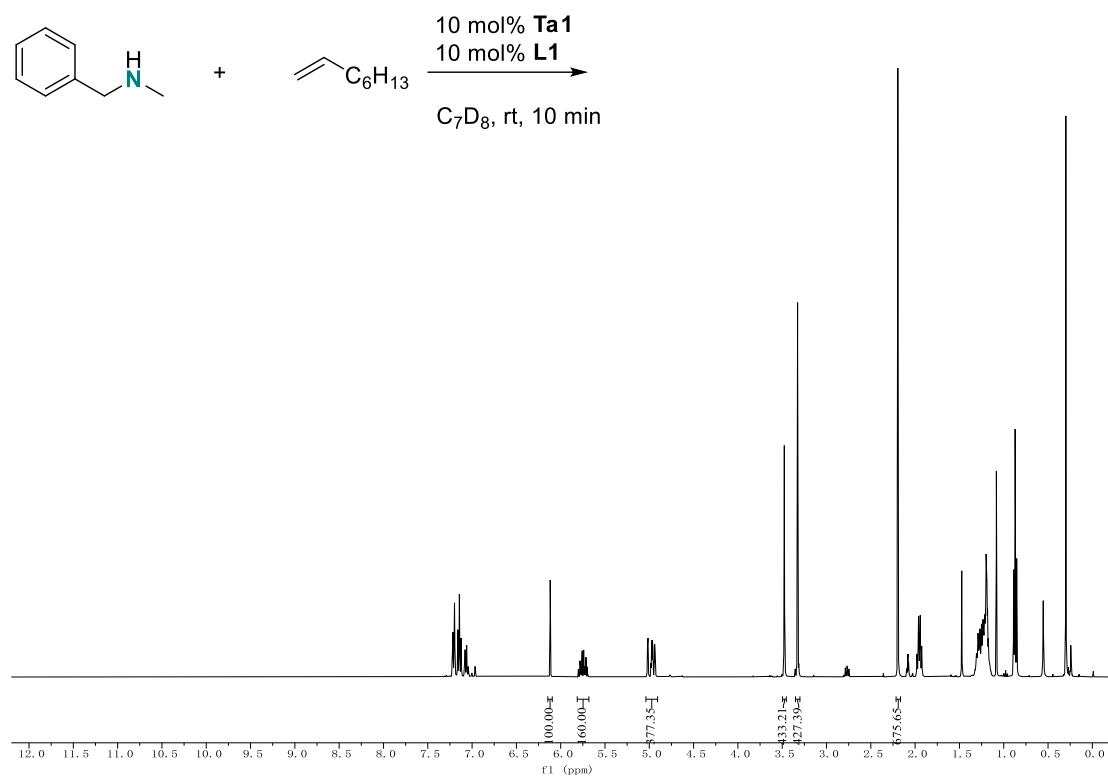


Figure S75

^1H NMR spectrum of reaction between 1-octene and N-methylbenzylamine with 10 mol% TaL1 after 10 min in C_7D_8 at RT

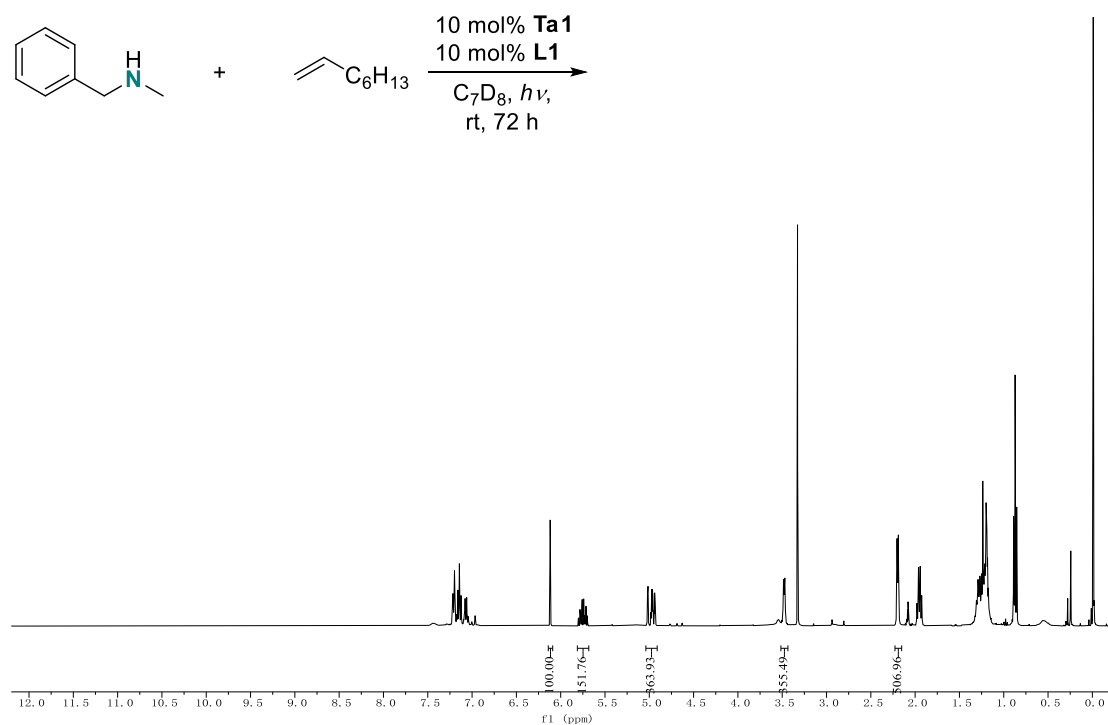


Figure S76

^1H NMR spectrum of reaction between 1-octene and N-methylbenzylamine with 10 mol% TaL1 after 72 h irradiation in C_7D_8 at RT

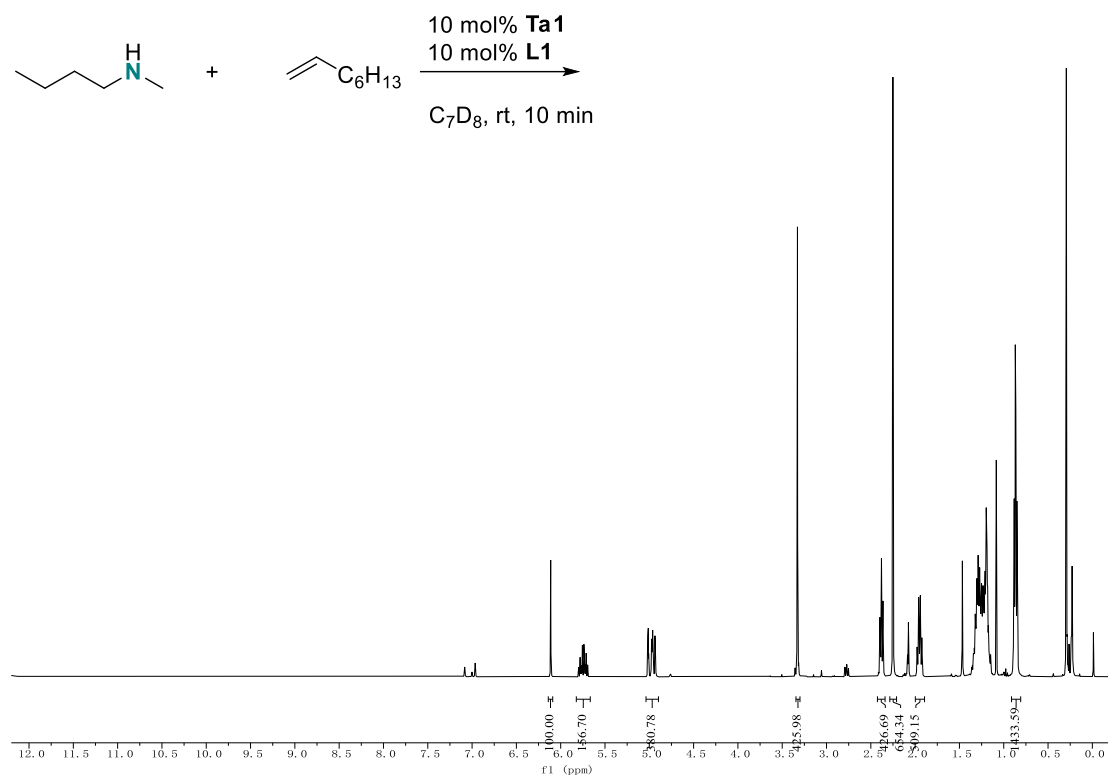


Figure S77

^1H NMR spectrum of reaction between 1-octene and N-methylbutylamine with 10 mol% TaL1 after 10 min in C_7D_8 at RT

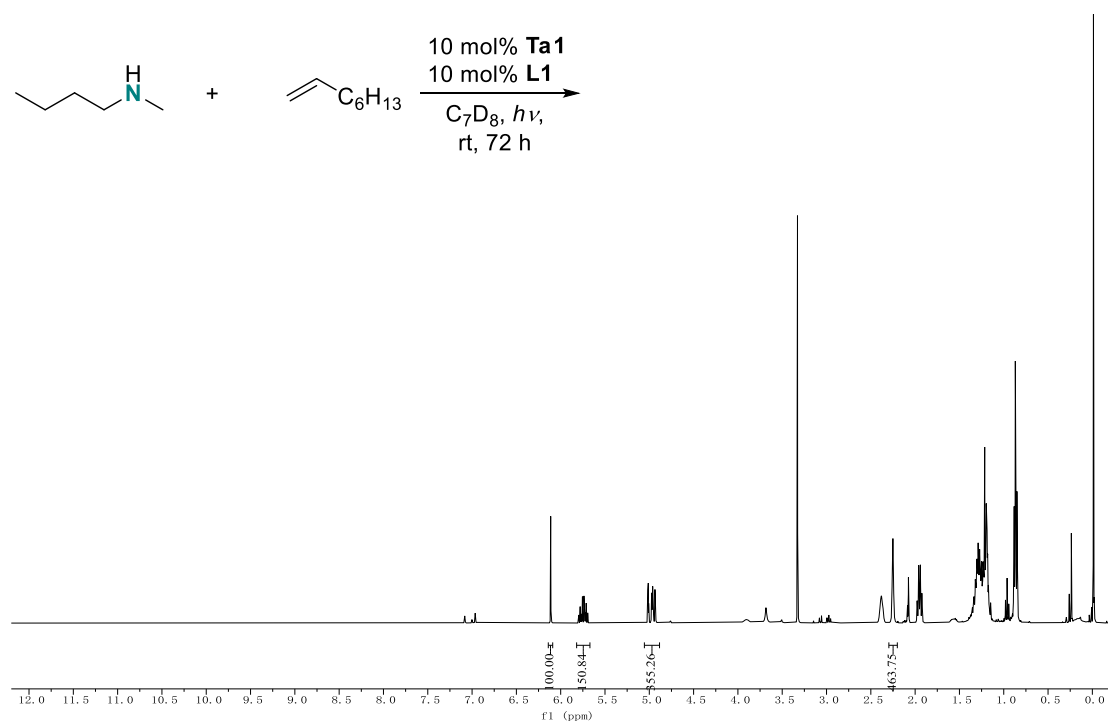


Figure S78

^1H NMR spectrum of reaction between 1-octene and N-methylbutylamine with 10 mol% TaL1 after 72 h irradiation in C_7D_8 at RT

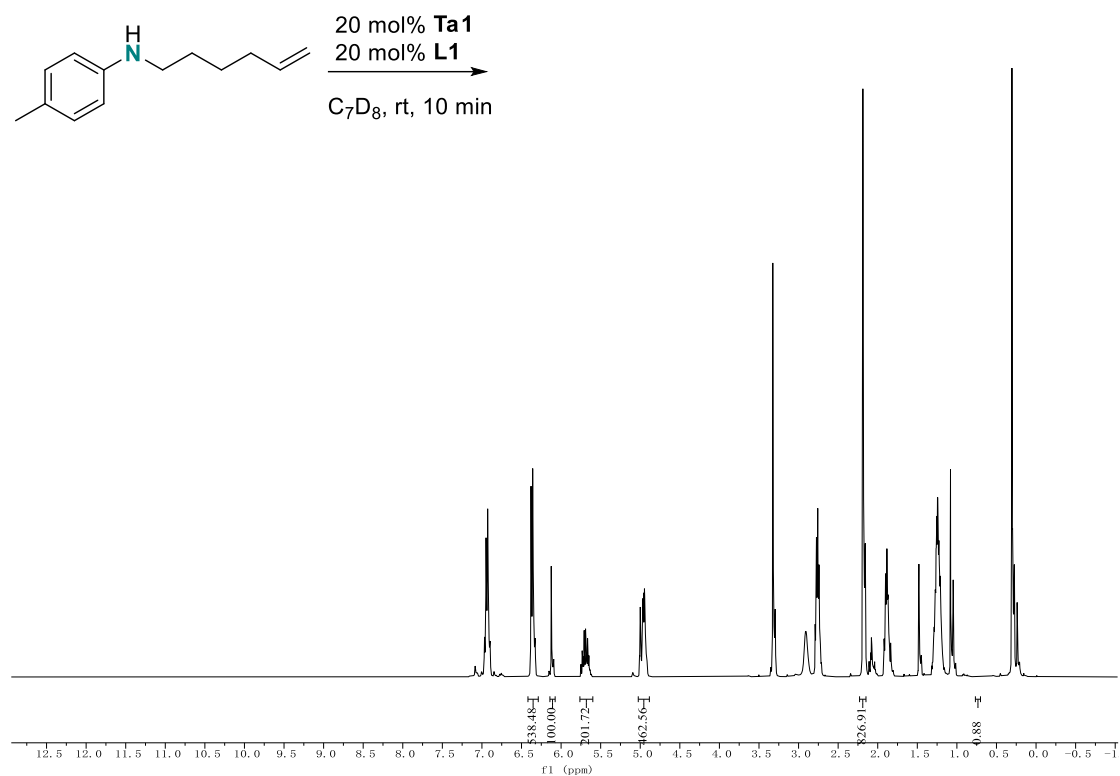


Figure S79

^1H NMR spectrum of reaction of N-(hex-5-en-1-yl)-4-methylaniline with 20 mol% TaL1 after 10 min in C_7D_8 at RT

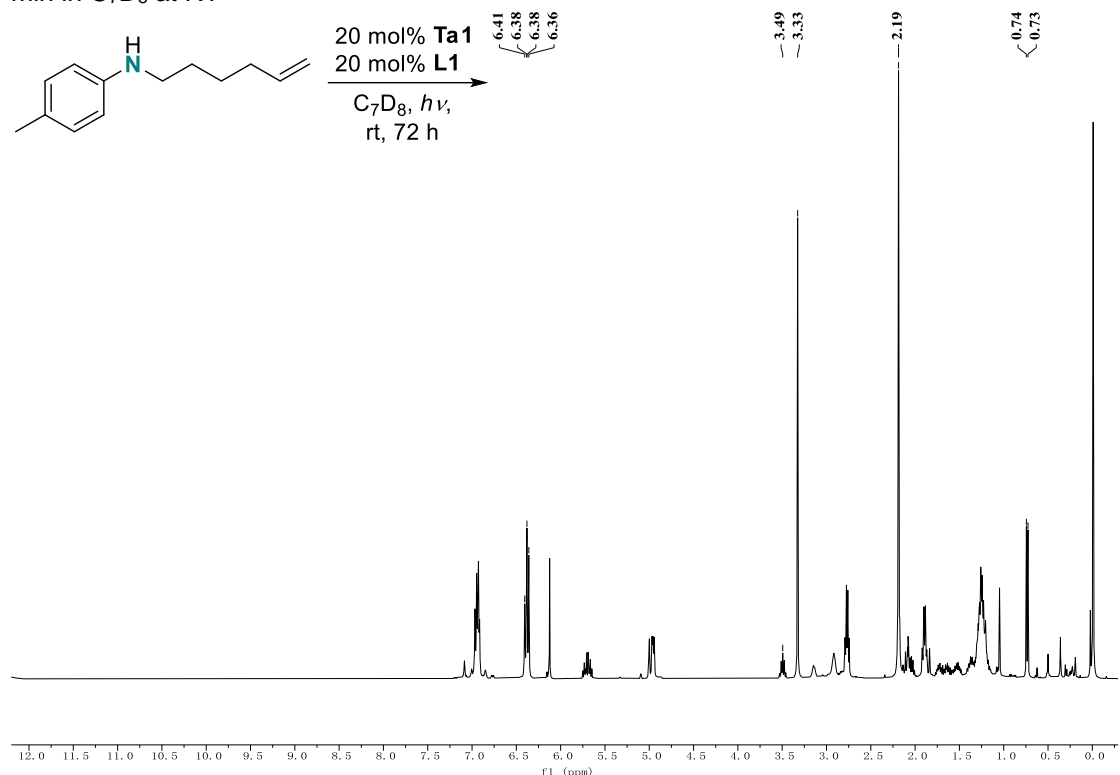


Figure S80

^1H NMR spectrum of reaction of N-(hex-5-en-1-yl)-4-methylaniline with 20 mol% TaL1 after 72 h irradiation in C_7D_8 at RT

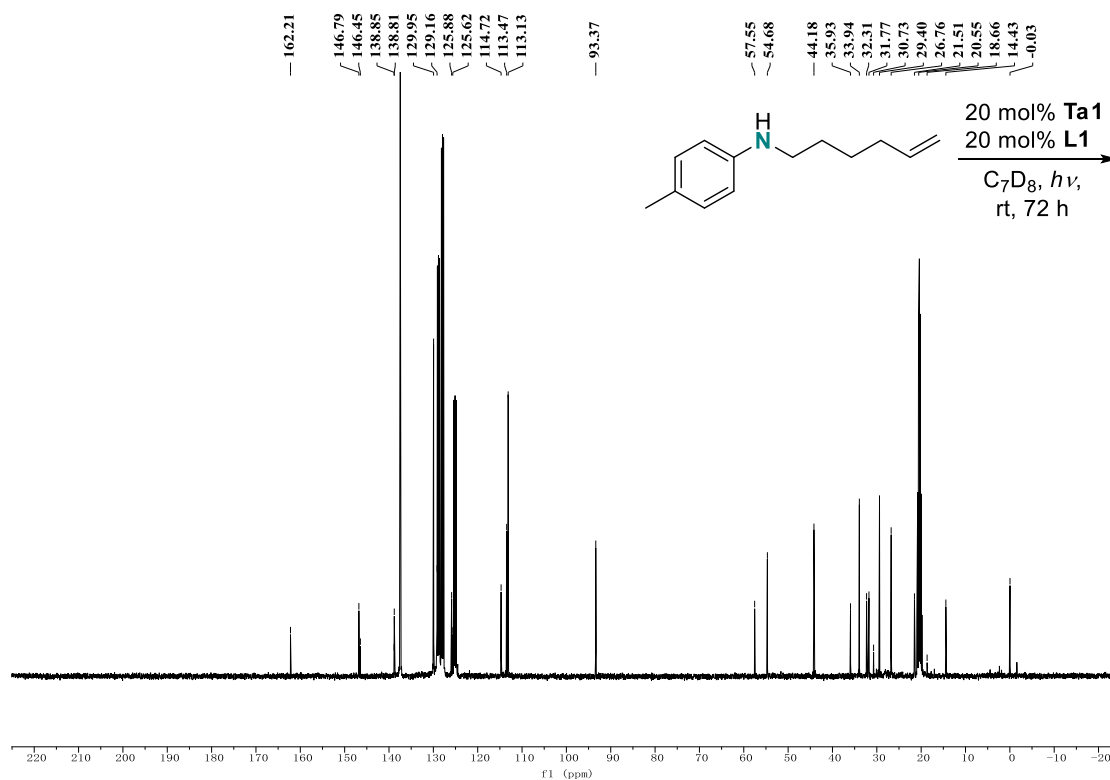


Figure S81

$^{13}C\{^1H\}$ NMR spectrum of reaction of N-(hex-5-en-1-yl)-4-methylaniline with 20 mol% TaL1 after 72 h irradiation in C_7D_8 at RT

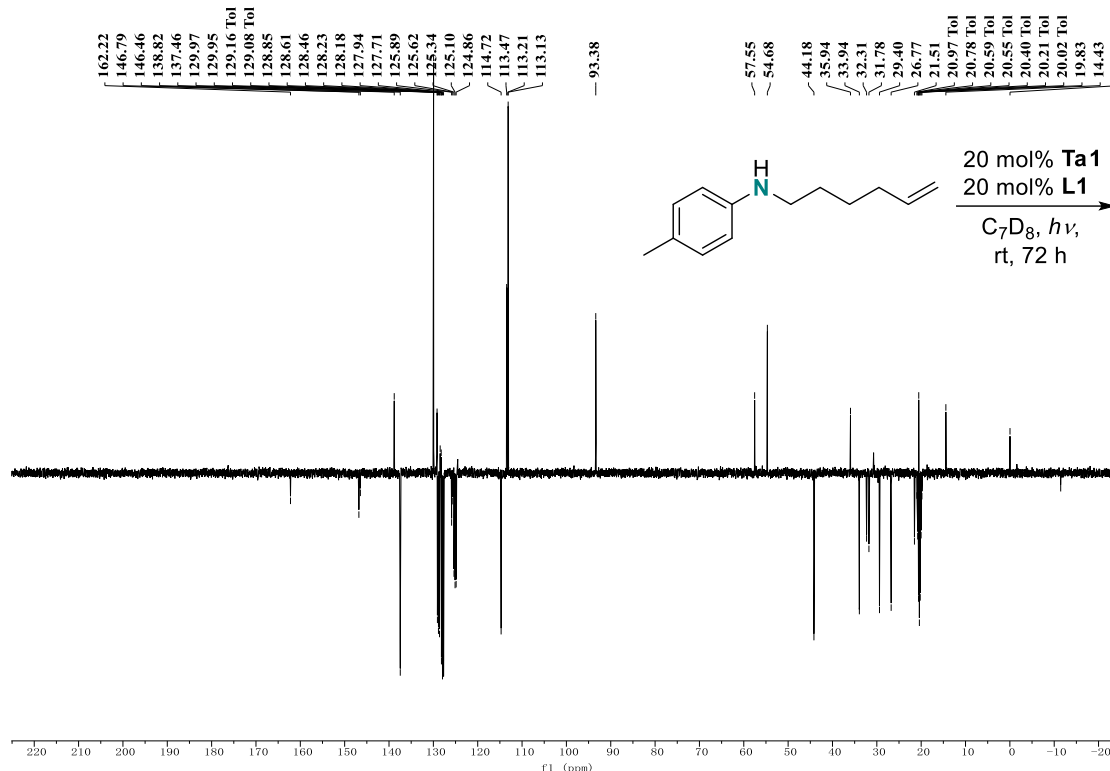


Figure S82

$^{13}C\{^1H\}$ -APT45 NMR spectrum of reaction of N-(hex-5-en-1-yl)-4-methylaniline with 20 mol% TaL1 after 72 h irradiation in C_7D_8 at RT

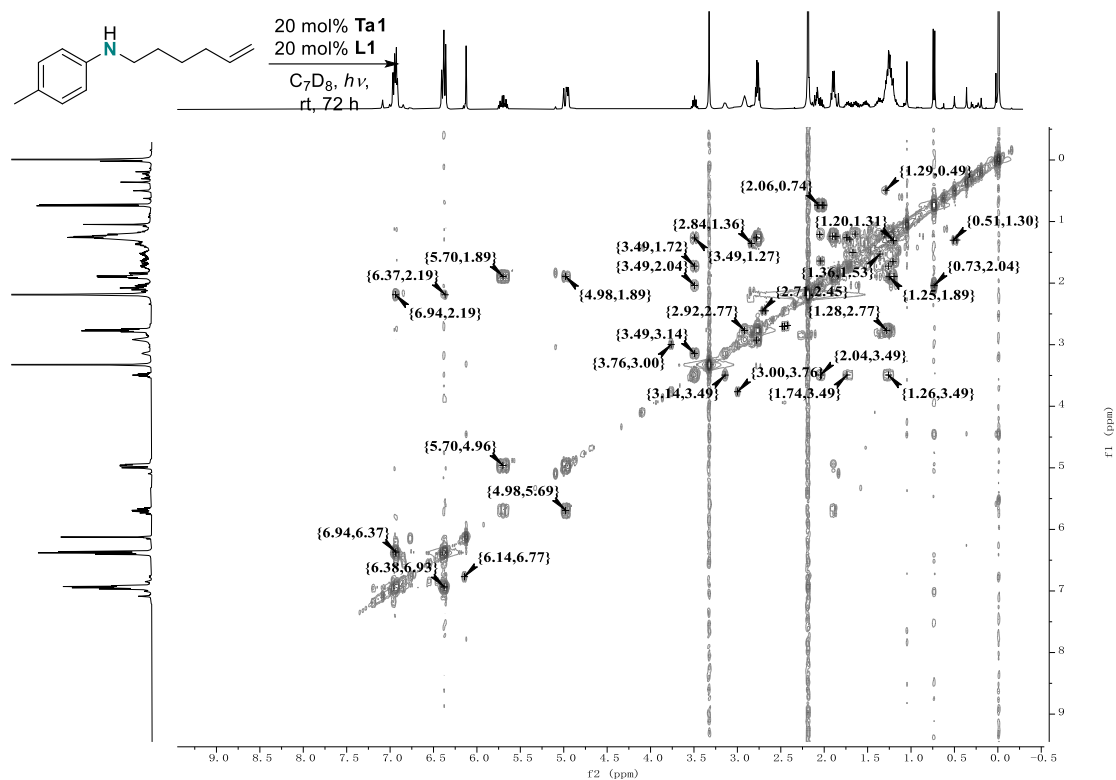


Figure S83

1H - 1H -COSY NMR spectrum of reaction of N-(hex-5-en-1-yl)-4-methylaniline with 20 mol% TaL1 after 72 h irradiation in C_7D_8 at RT

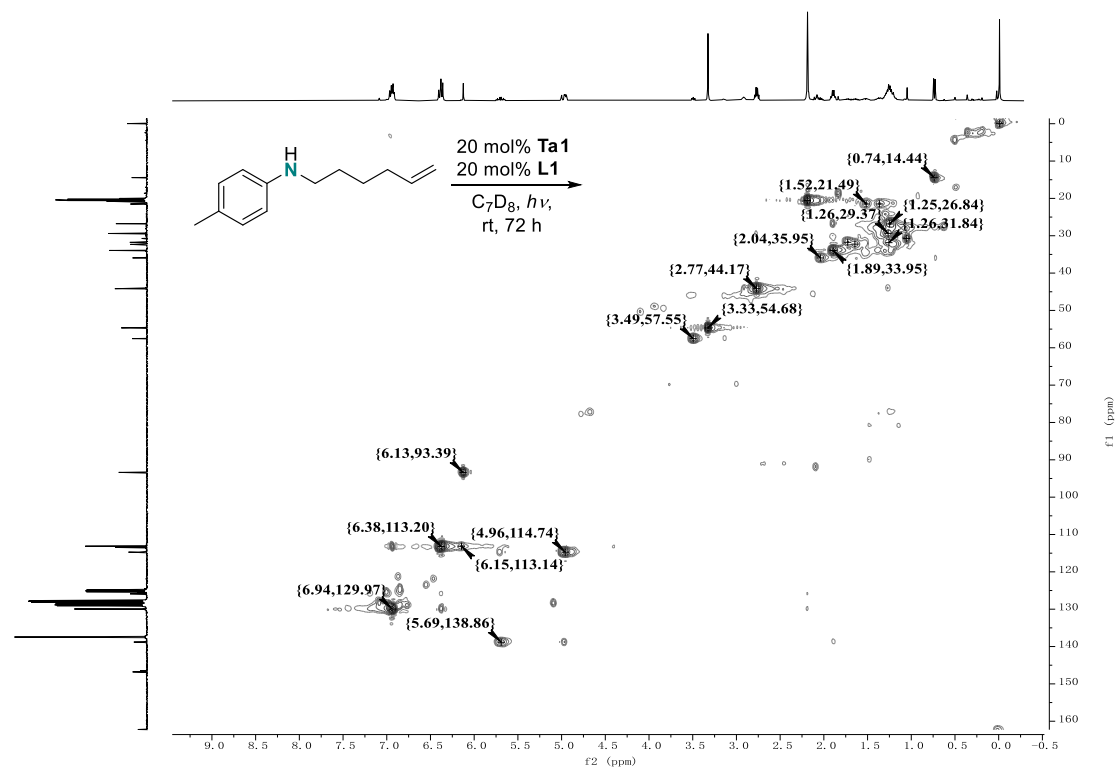


Figure S84

1H - ^{13}C -HSQC NMR spectrum of reaction of N-(hex-5-en-1-yl)-4-methylaniline with 20 mol% TaL1 after 72 h irradiation in C_7D_8 at RT

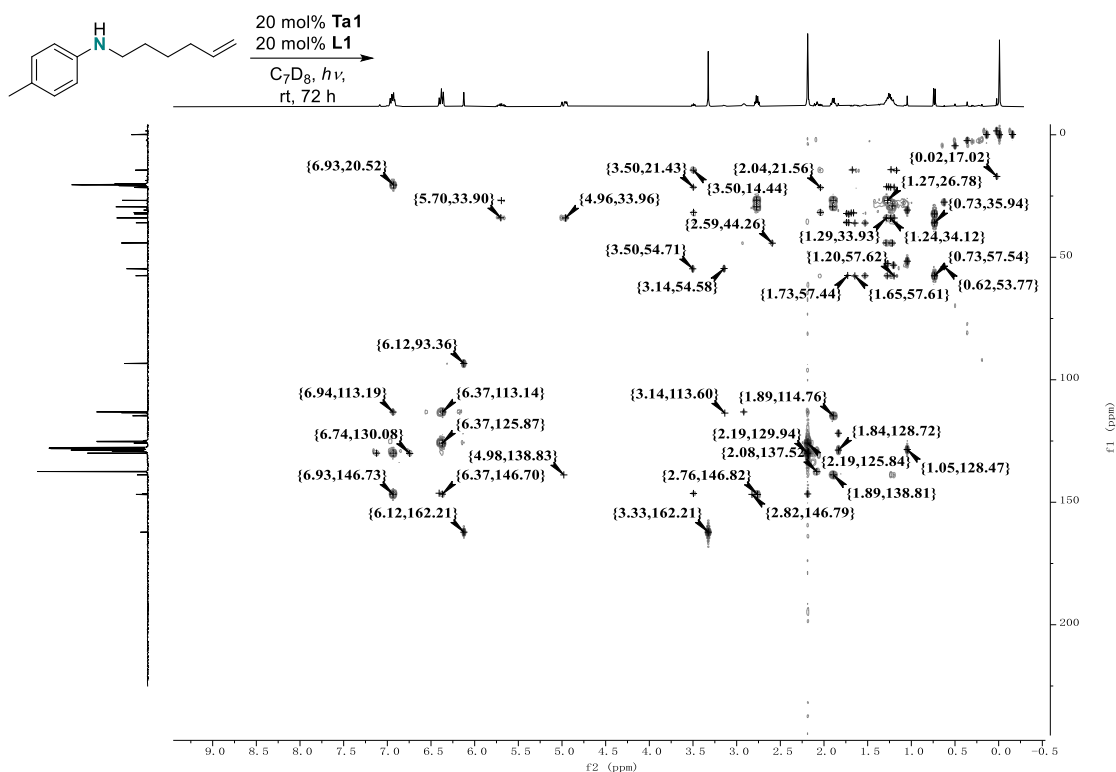


Figure S85

^1H - ^{13}C -HMBC NMR spectrum of reaction of N-(hex-5-en-1-yl)-4-methylaniline with 20 mol% TaL1 after 72 h irradiation in C_7D_8 at RT

Spectra rational:

Comparing the T_0 and $T_{72\text{h}}$ ^1H -NMR spectra (**Figure S79-80**), the integration of $-\text{CH}=\text{CH}_2$ signal at 5.70ppm decreases from 201 to 120 (TMB internal standard Ar-H = 100), overlapping toluyl group can be identified, with slightly down-field *N-ortho*-CH integrating to 168, double the decrease of $-\text{CH}=\text{CH}_2$, suggesting 1:1 formation of a new toluyl containing compound. A multiplet at 3.49ppm emerges and integrates to 82, same as decrease of $-\text{CH}=\text{CH}_2$ signal, and couples to 57.55ppm signal ^1H - ^{13}C -HSQC. In the ^1H - ^1H -COSY spectrum, it couples to multiple signals, including 3.14ppm and 2.04ppm. The 3.04ppm signal in the ^1H spectrum is a broad peak, and does not couple to any carbon in the ^1H - ^{13}C -HSQC, therefore assigned to a protic NH. The 2.04ppm signal couples to a sharp doublet at 0.73ppm in COSY spectrum, which integrates to 242 in ^1H spectrum. These two peaks are assigned to the methylidyne and methyl of a CHCH_3 moiety respectively. The 3.49ppm signal also couples to signals at 1.27ppm and 1.73ppm, which couple to the same carbon at 31.77ppm in ^1H - ^{13}C -HSQC. Combining these results, a R-NH-CH(CH₂-...)-CH(CH₃)-... substructure is proposed. (Chart S1 left)

In the ^{13}C -APT spectrum, three new CH₂ signals (negative phase) emerges at 32.31ppm, 31.77ppm and 21.51ppm. As mentioned ahead, the 31.77ppm signal is assigned the $-\text{CH}_2-$ beta- to the nitrogen. The rest two carbon signals couples to 1.65ppm/1.20ppm and 1.52ppm/1.36ppm in ^1H - ^{13}C -HSQC, and the corresponding ^1H signals couples to each other in COSY. The 32.31ppm signal couples to 1.73ppm and 0.73ppm signal in ^1H - ^{13}C -HMBC through 3J coupling, and the 21.51ppm signal couples to 3.49ppm and 2.04ppm signal through 3J coupling.

Summarizing the above rational, a 1-(toluyl-amino)-2-methyl-cyclopentane structure is proposed, which is the intramolecular hydroaminoalkylation cyclization product of N-(hex-5-en-1-yl)-4-methylaniline.

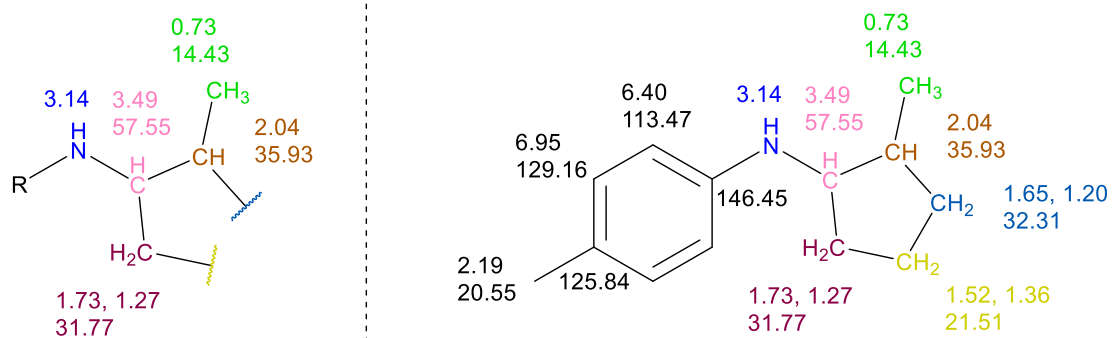


Chart 1

Structure rational of the major product of reaction of N-(hex-5-en-1-yl)-4-methylaniline with 20 mol% TaL1 after 72 h irradiation in C₇D₈ at RT

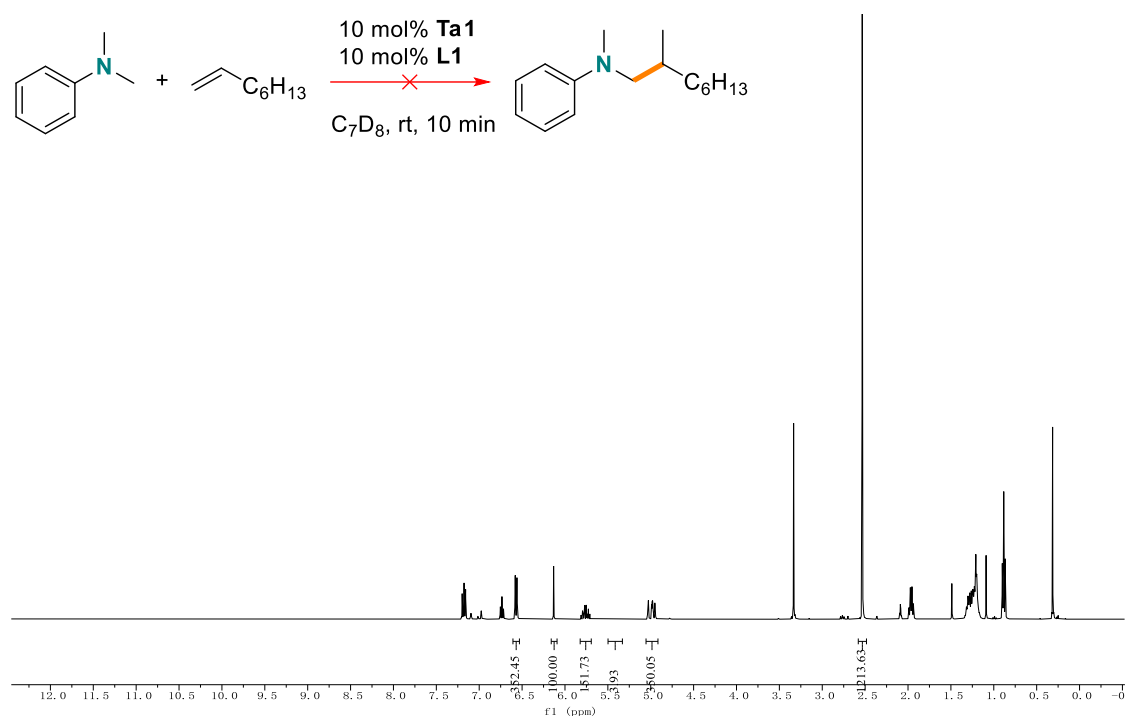


Figure S86

¹H NMR spectrum of reaction between 1-octene and N,N-dimethylaniline with 10 mol% TaL1 after 10 min in C₇D₈ at RT

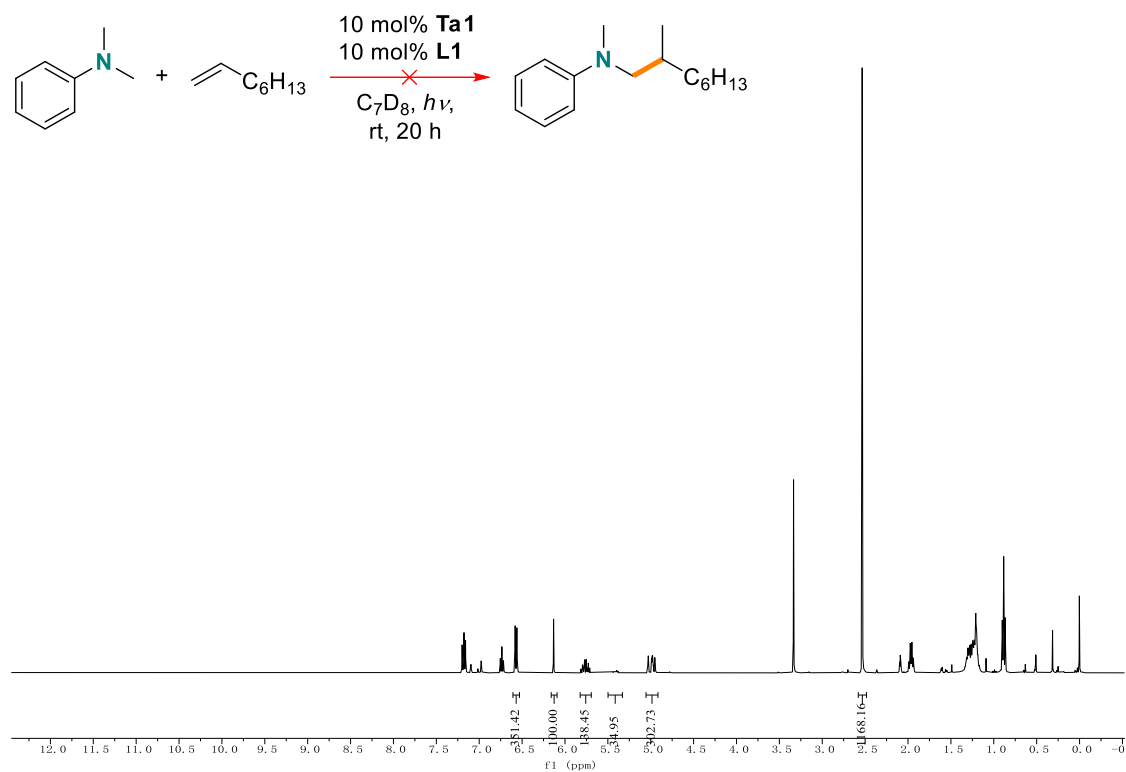


Figure S87

^1H NMR spectrum of reaction between 1-octene and N,N-dimethylaniline with 10 mol% TaL1 after 20h irradiation in C_7D_8 at RT

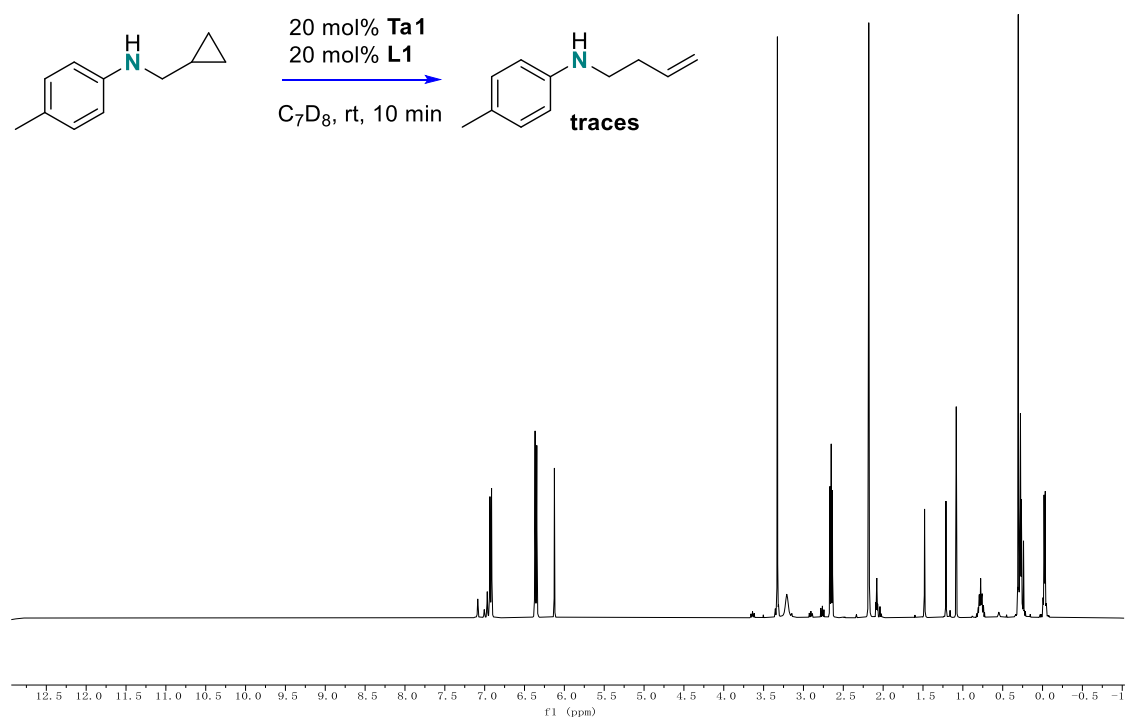


Figure S88

^1H NMR spectrum of reaction of N-(cyclopropylmethyl)-4-methylaniline with 20 mol% TaL1 after 10 min in C_7D_8 at RT

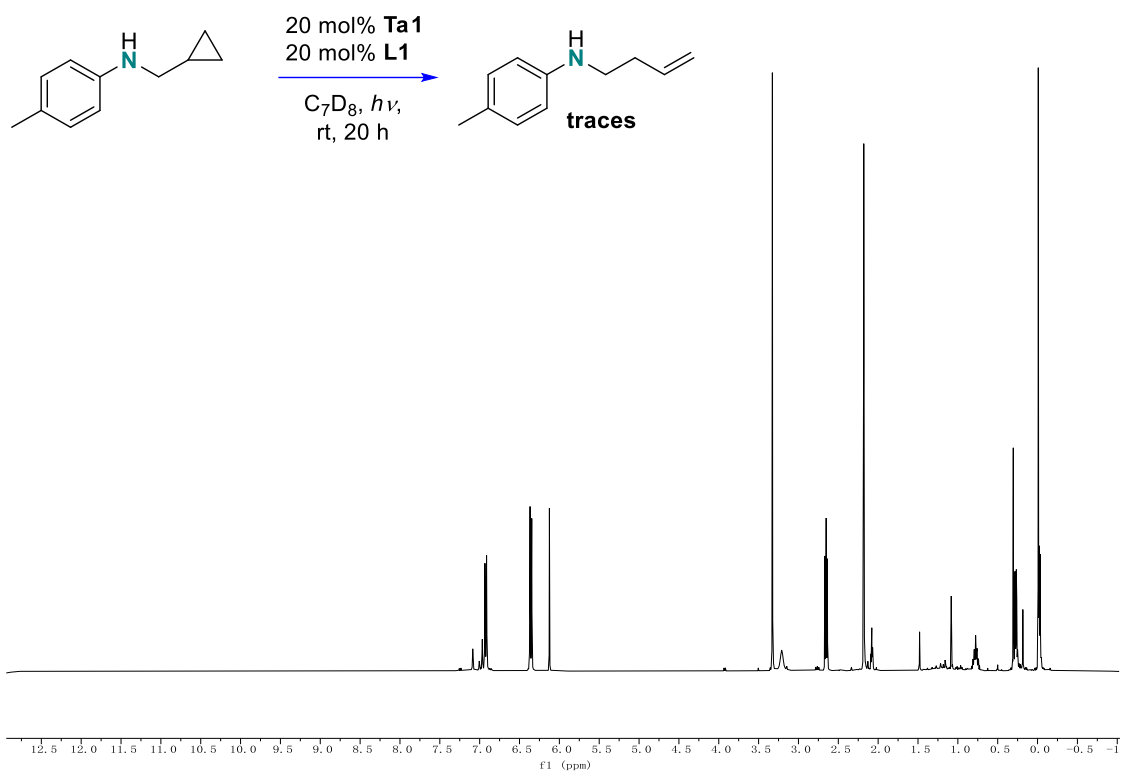


Figure S89

¹H NMR spectrum of reaction of N-(cyclopropylmethyl)-4-methylaniline with 20 mol% TaL1 after 20h irradiation in C₇D₈ at RT

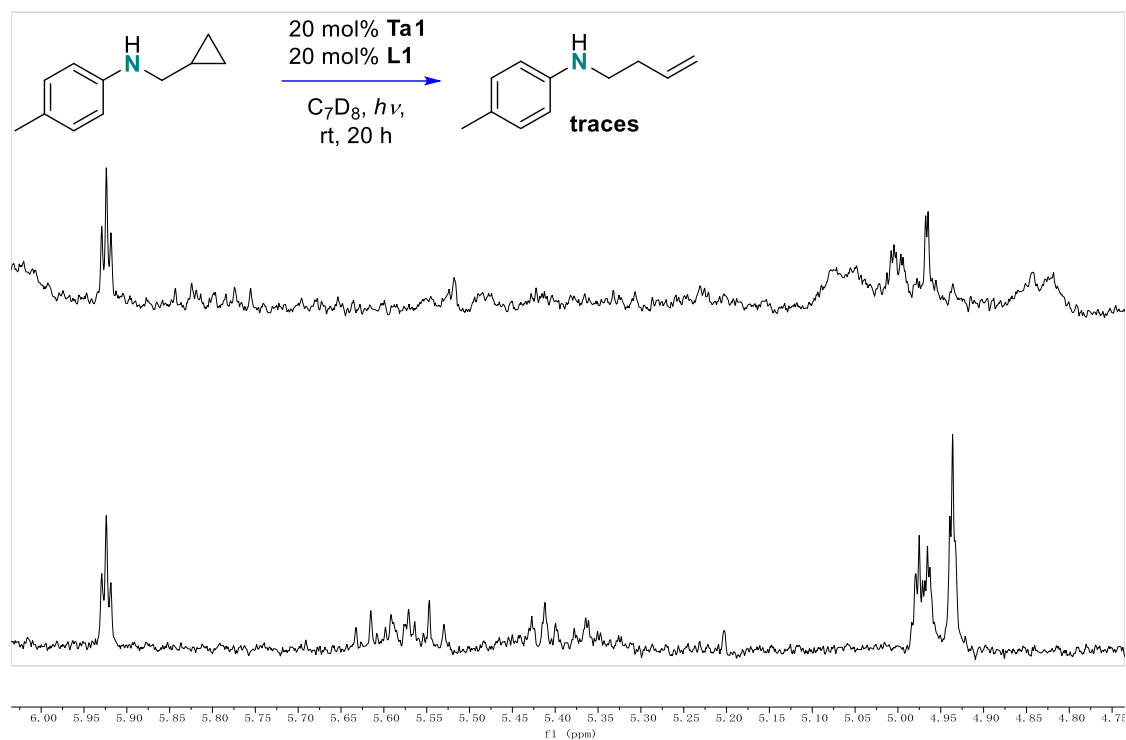


Figure S90

Comparison of ¹H NMR spectrum of reaction of N-(cyclopropylmethyl)-4-methylaniline with 20 mol% TaL1 after 10 min (bottom) and 20h irradiation (top) in C₇D₈ at RT. Peaks arising at 4.8 and 5.1 ppm are attributed to ring-opening products

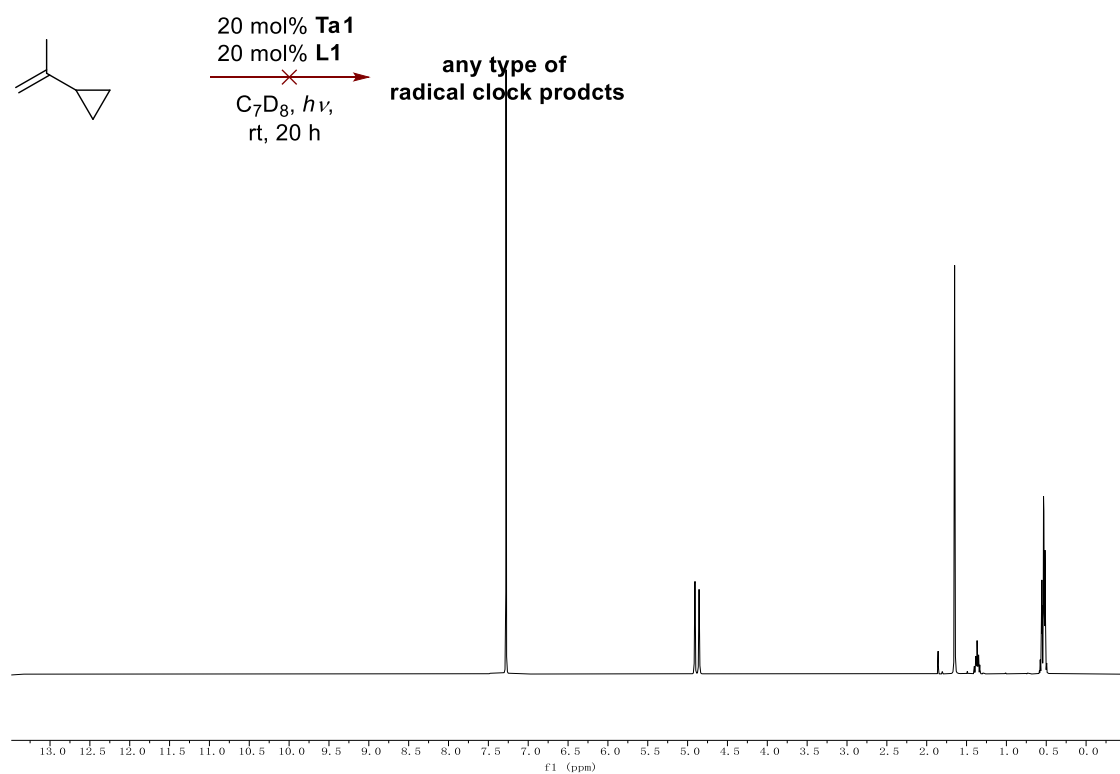


Figure S91

¹H NMR spectrum of reaction of prop-1-en-2-ylcyclopropane with 20 mol% TaL1 after 20 h in C₆D₆ at RT

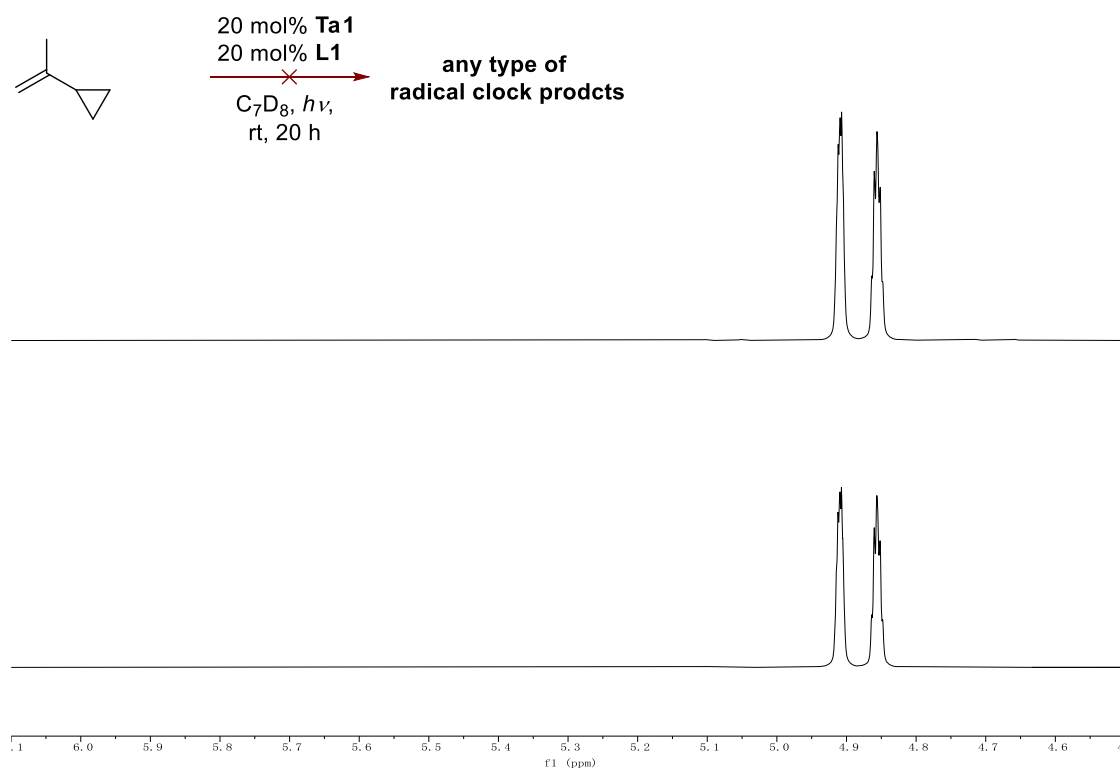


Figure S92

Comparison of ¹H NMR spectrum of reaction of prop-1-en-2-ylcyclopropane with 20 mol% TaL1 after 10 min (bottom) and 20h irradiation (top) in C₆D₆ at RT.

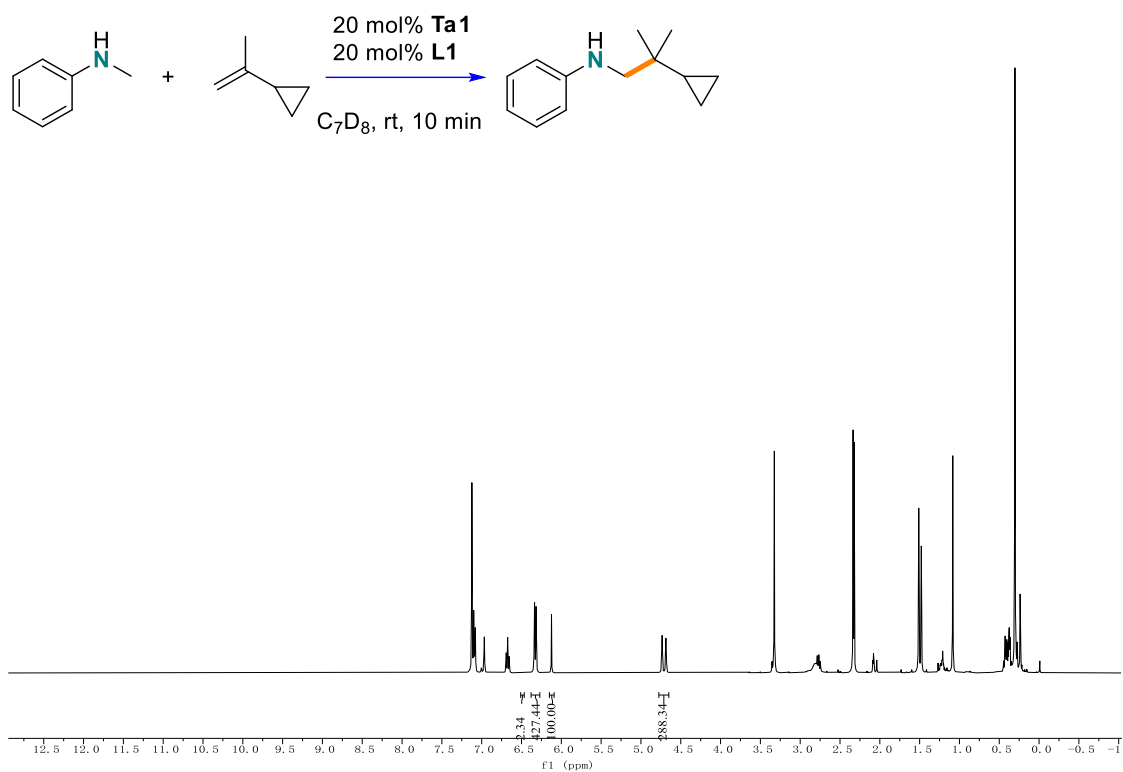


Figure S93

^1H NMR spectrum of reaction between prop-1-en-2-ylcyclopropane and N-methylaniline with 20 mol% TaL1 after 10 min in C_7D_8 at RT

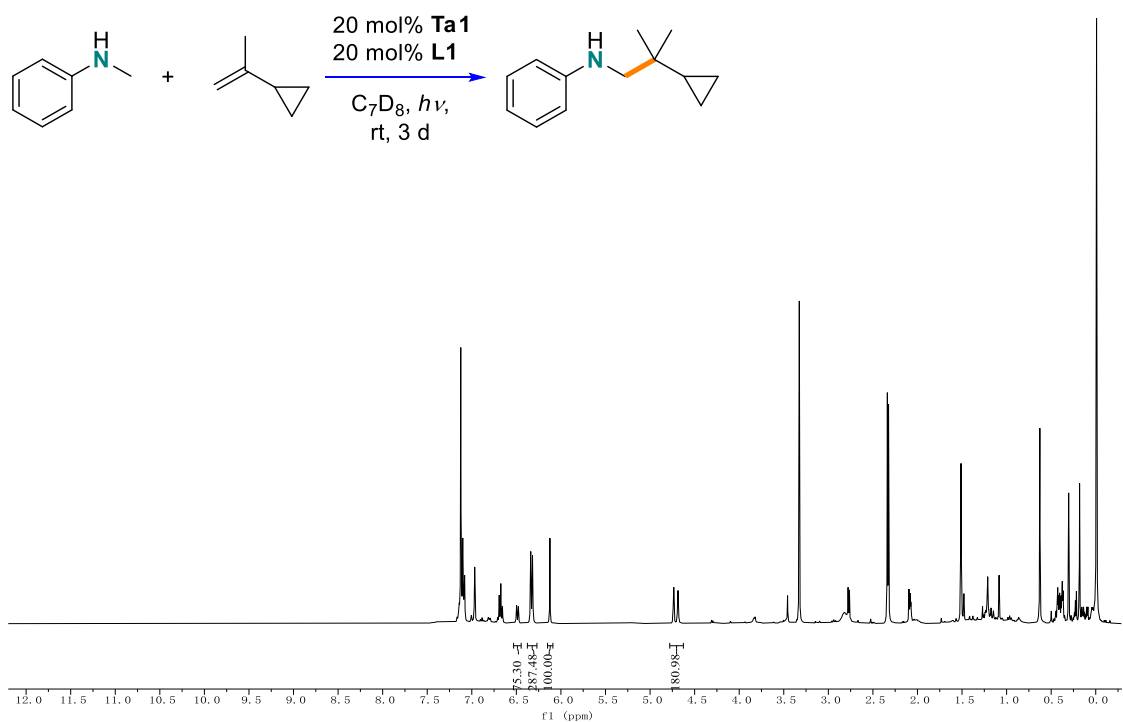


Figure S94

^1H NMR spectrum of reaction between prop-1-en-2-ylcyclopropane and N-methylaniline with 20 mol% TaL1 after 3 d irradiation in C_7D_8 at RT

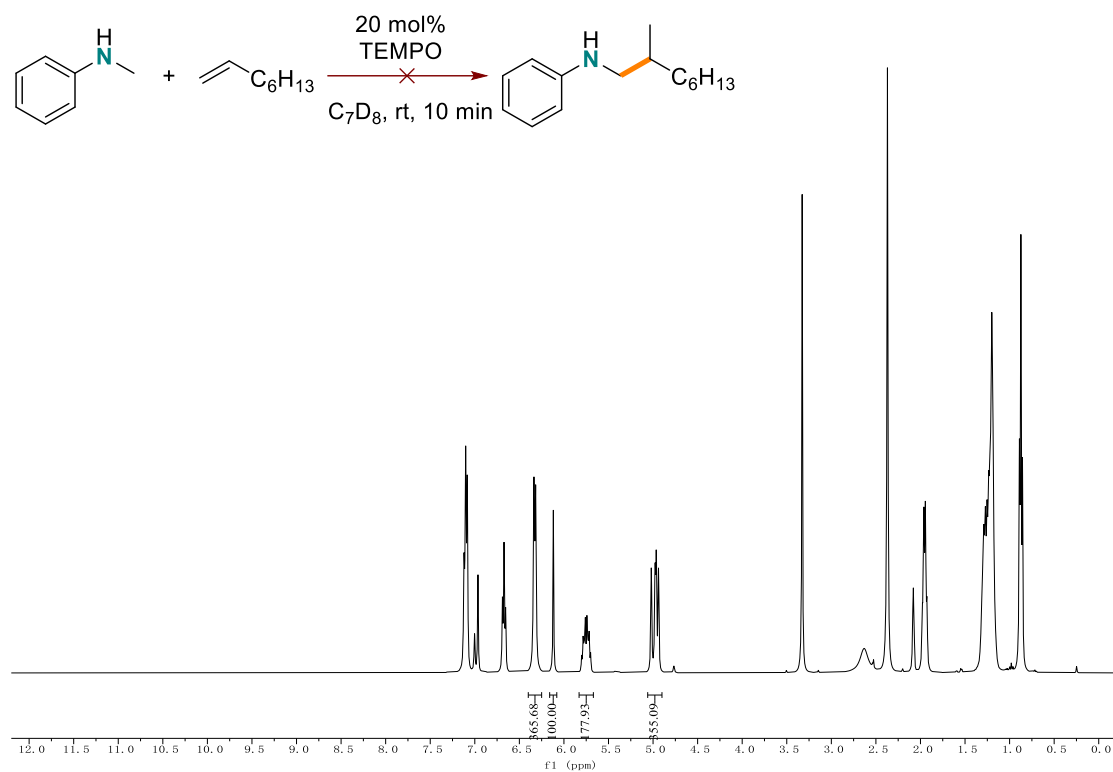


Figure S95

^1H NMR spectrum of reaction between 1-octene and N-methylaniline with 20 mol% TEMPO after 10 min in C_7D_8 at RT

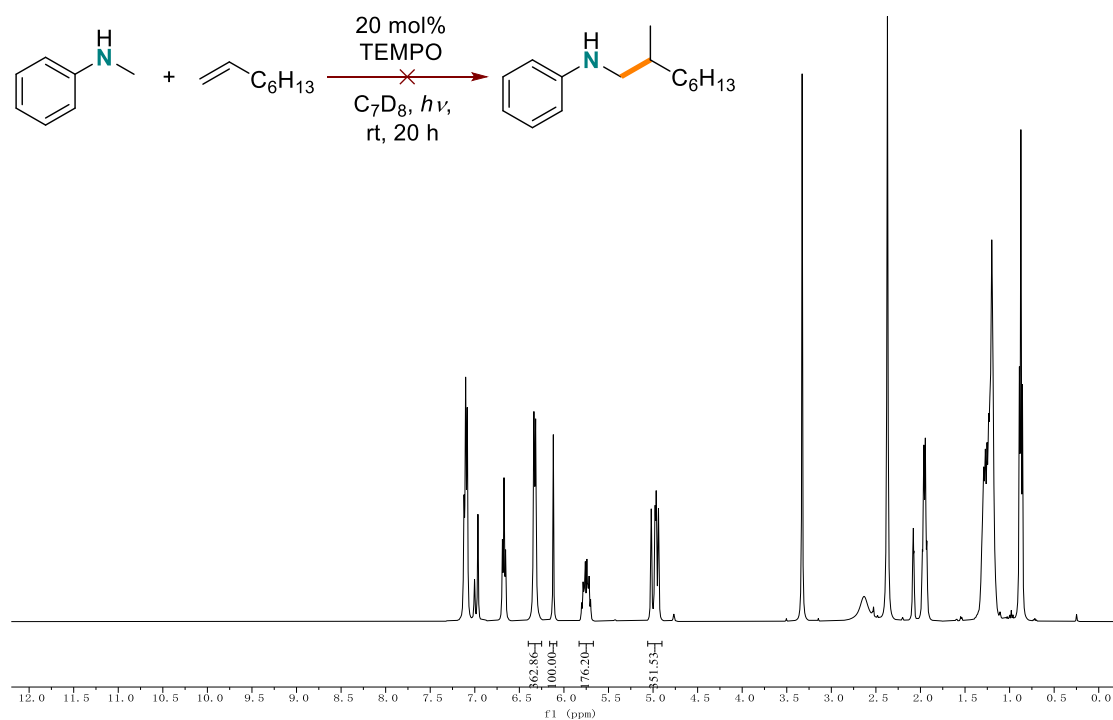


Figure S96

^1H NMR spectrum of reaction between 1-octene and N-methylaniline with 20 mol% TEMPO after 20 h irradiation in C_7D_8 at RT

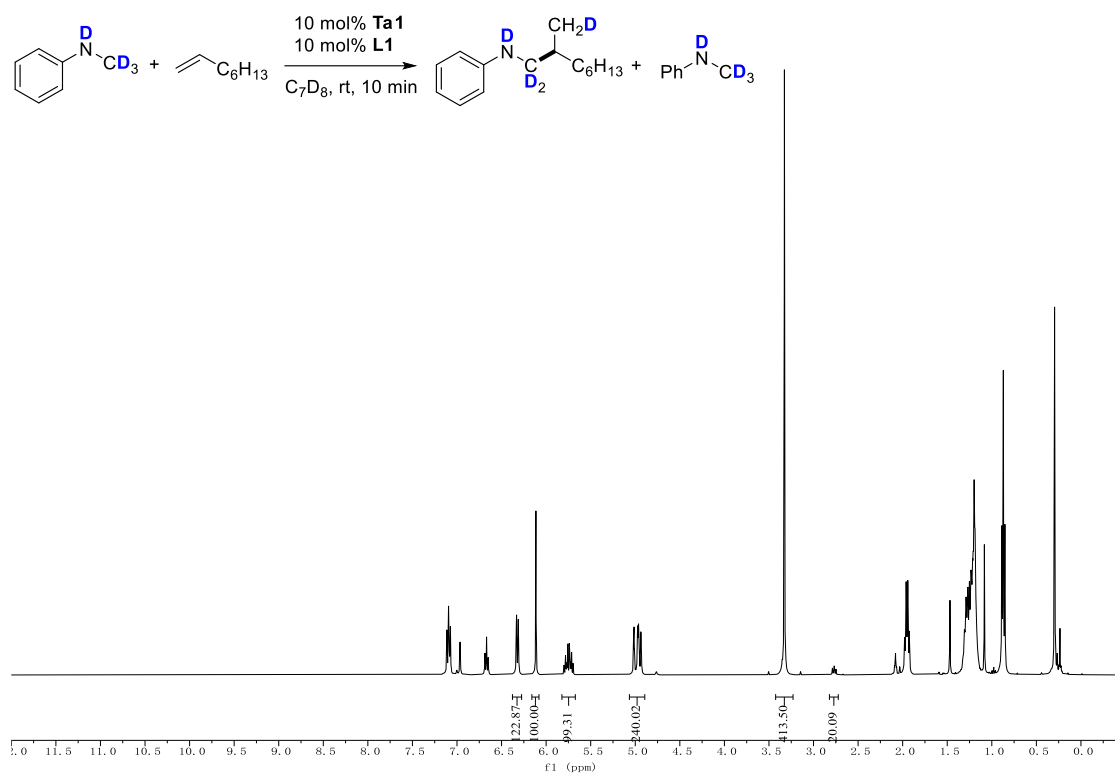


Figure S97

^1H NMR spectrum of reaction between 1-octene and PhNDCD_3 with 10 mol% TaL1 after 10 min in C_7D_8 at RT

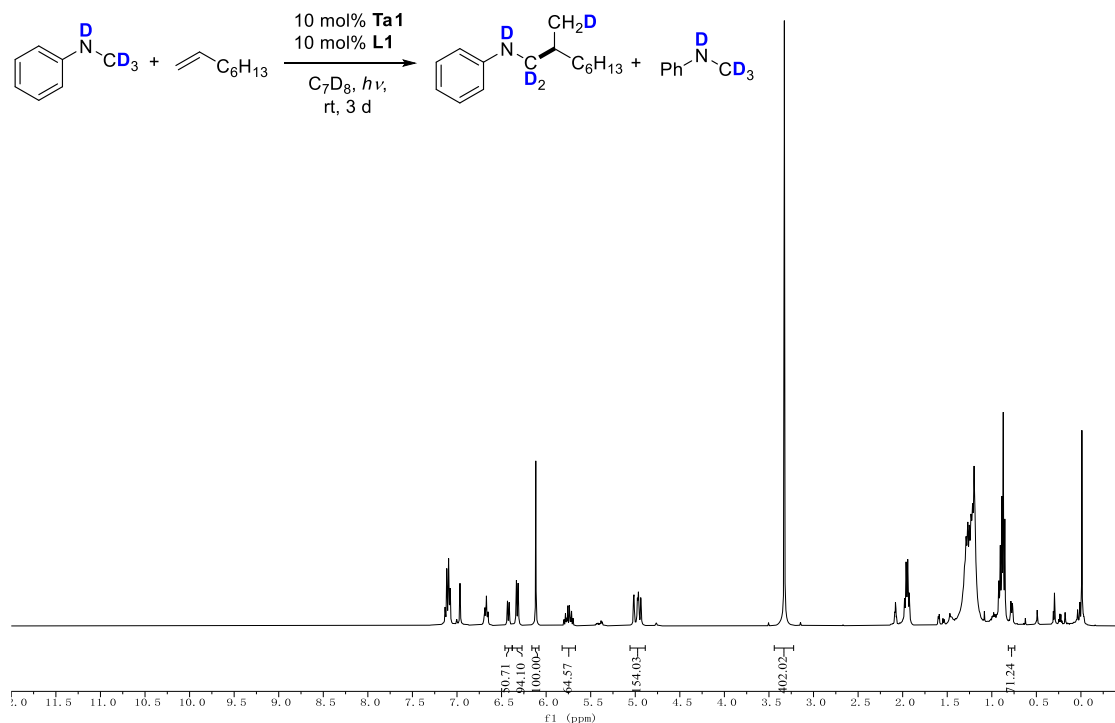


Figure S98

^1H NMR spectrum of reaction between 1-octene and PhNDCD_3 with 10 mol% TaL1 after 3 d irradiation in C_7D_8 at RT

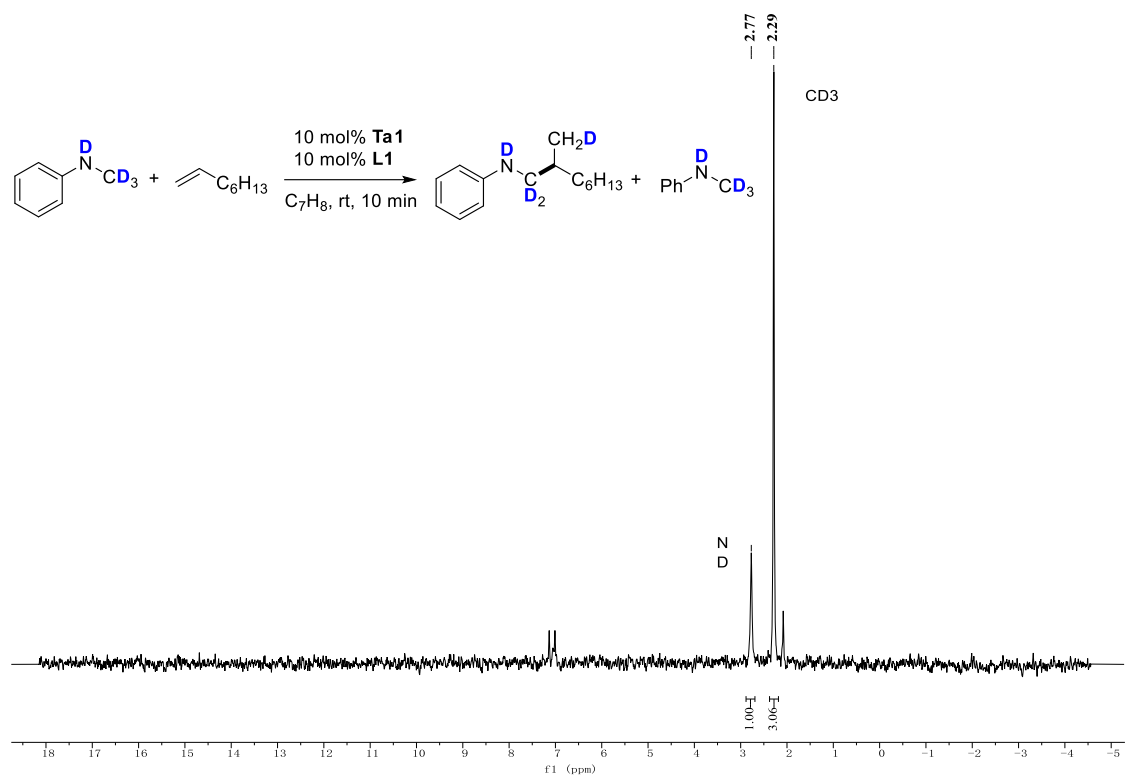


Figure S99

^2H NMR spectrum of reaction between 1-octene and PhNDCD_3 with 10 mol% TaL1 after 10 min in toluene (with C_7D_8 reference) at RT

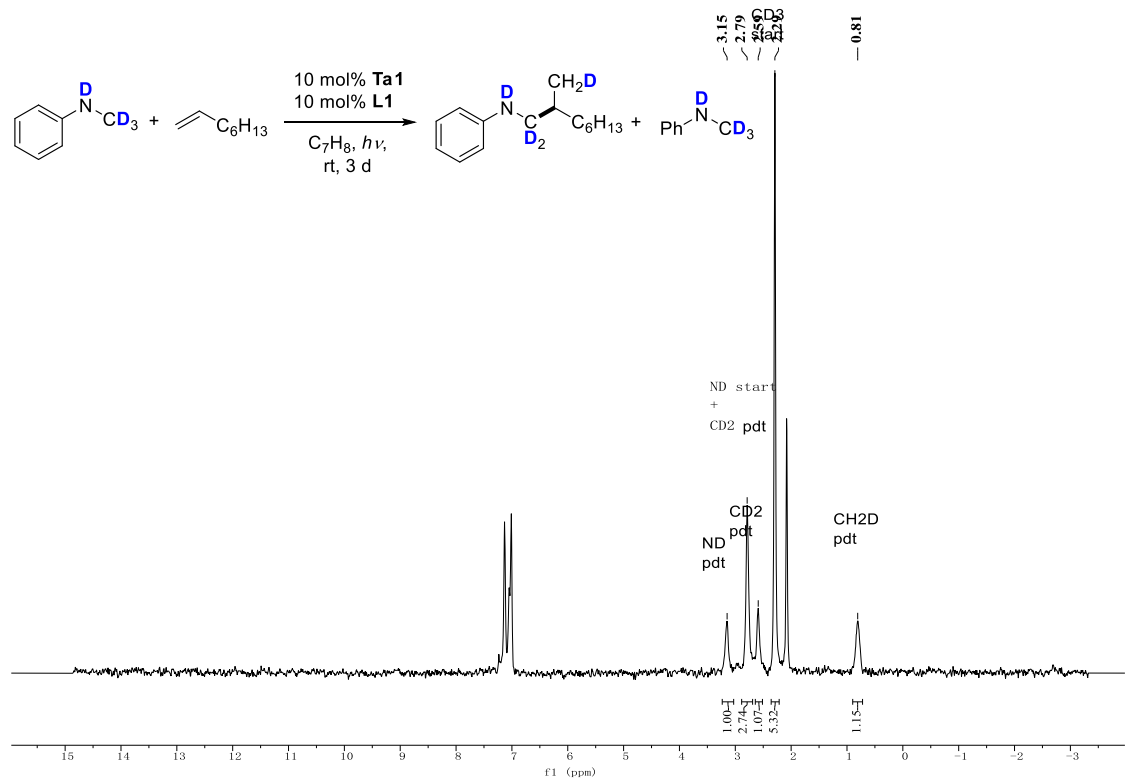


Figure S100

^2H NMR spectrum of reaction between 1-octene and PhNDCD_3 with 10 mol% TaL1 after 3 d irradiation in toluene (with C_7D_8 reference) at RT

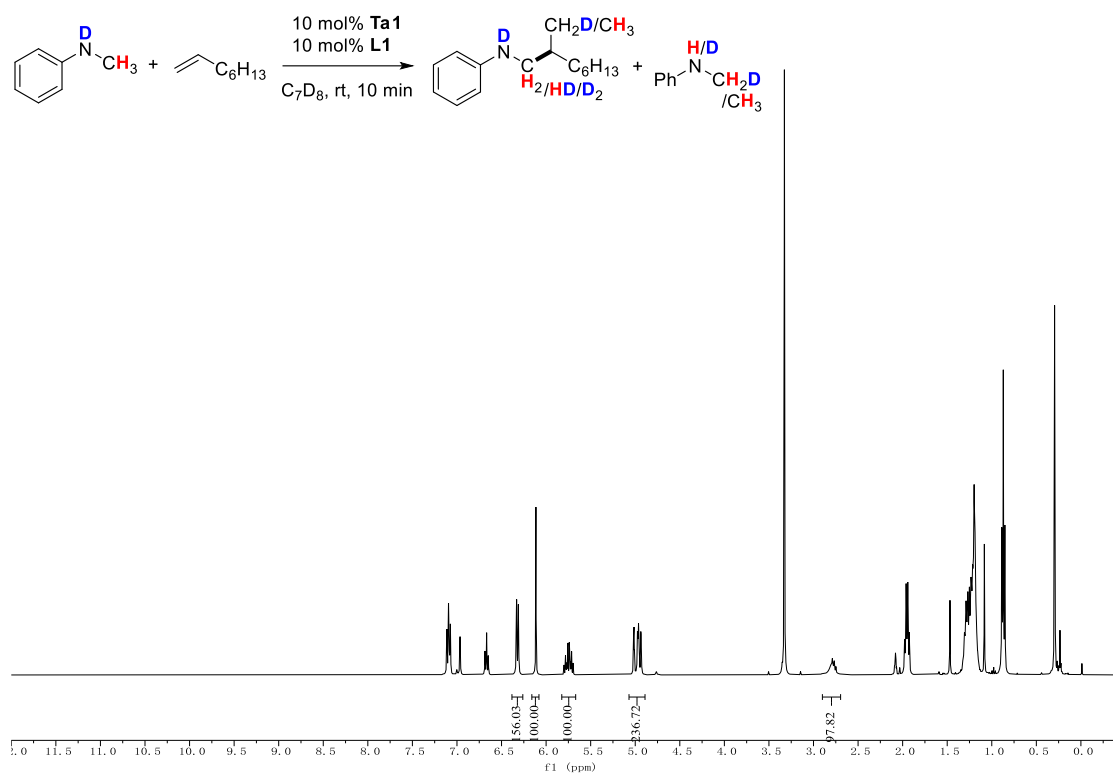


Figure S101

^1H NMR spectrum of reaction between 1-octene and PhNHCD_3 with 10 mol% TaL1 after 10 min in C_7D_8 at RT

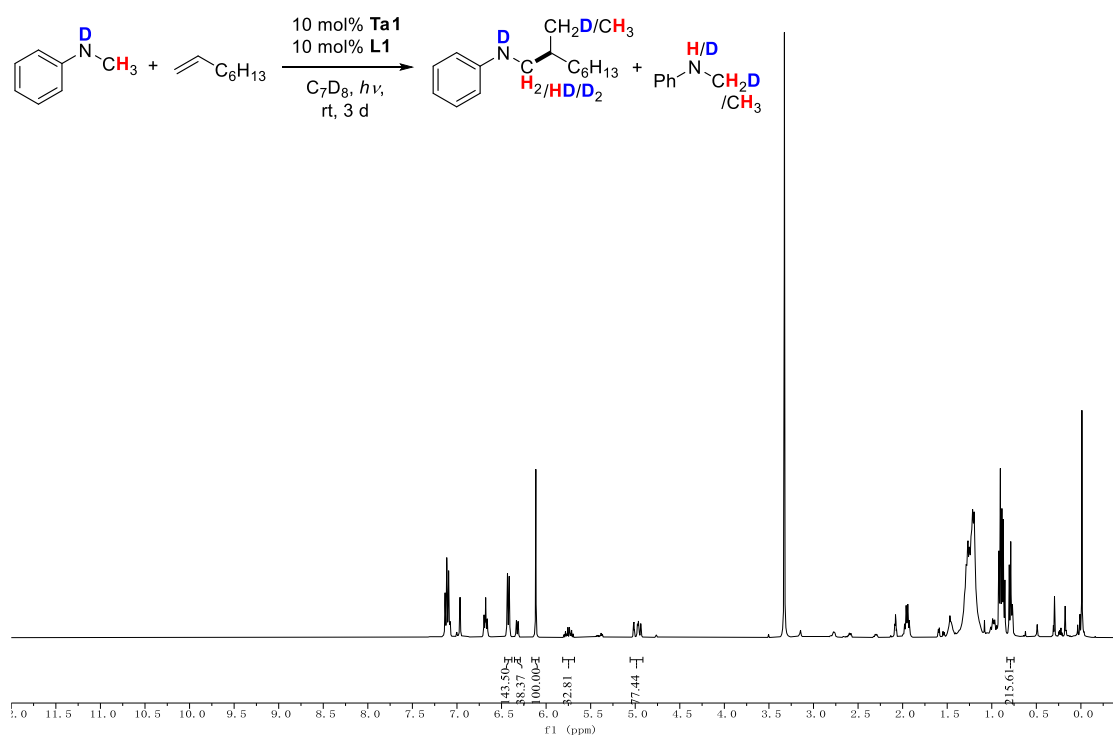


Figure S102

^1H NMR spectrum of reaction between 1-octene and PhNHCD_3 with 10 mol% TaL1 after 3 d irradiation in C_7D_8 at RT

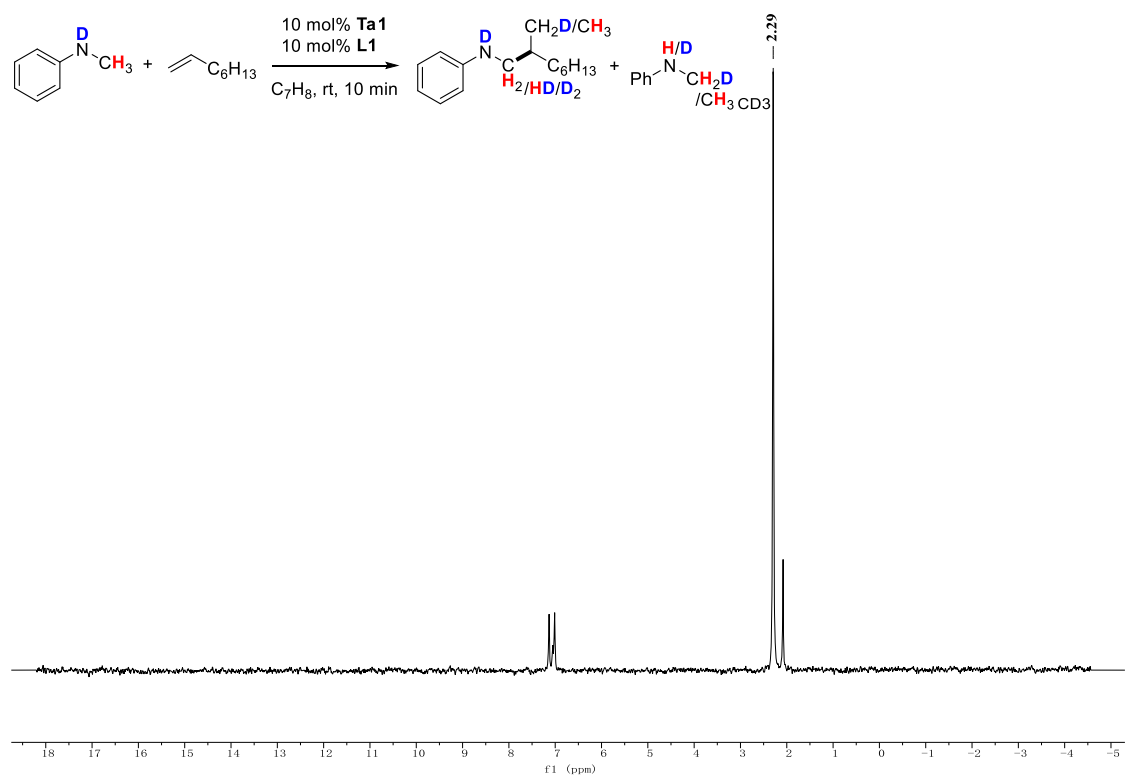


Figure S103

^{2}H NMR spectrum of reaction between 1-octene and PhNHCD_3 with 10 mol% TaL1 after 10 min in toluene (with C_7D_8 reference) at RT

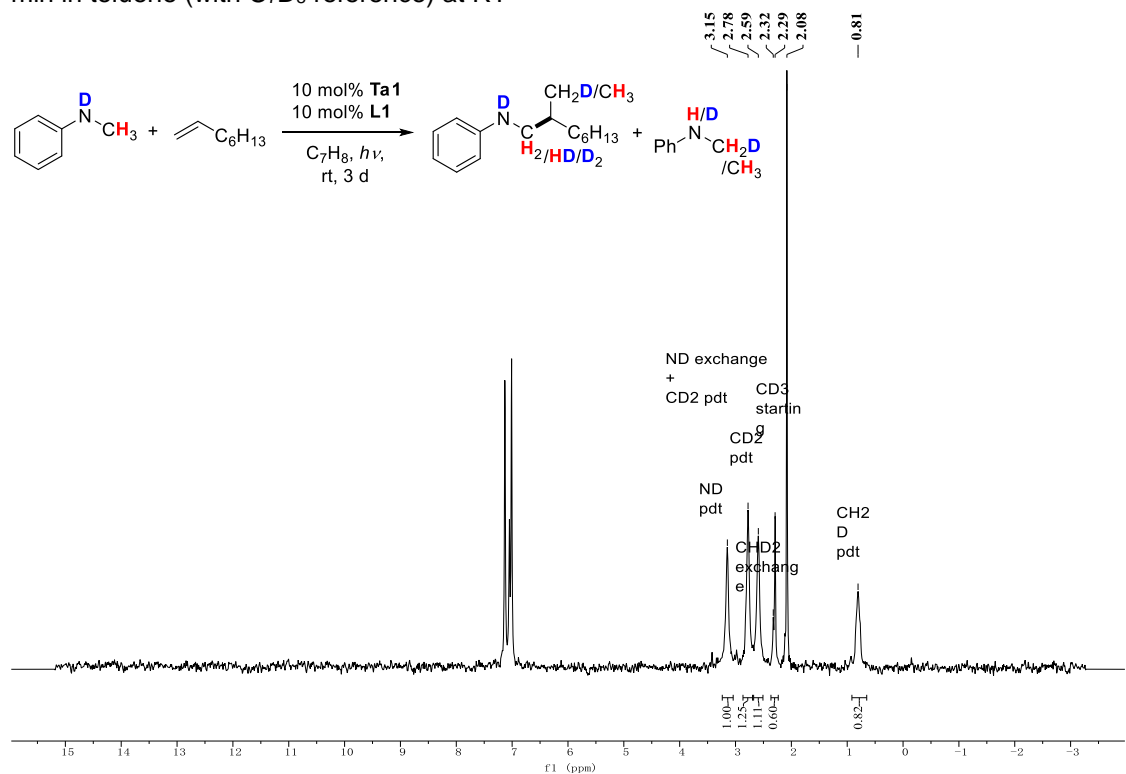


Figure S104

^{2}H NMR spectrum of reaction between 1-octene and PhNHCD_3 with 10 mol% TaL1 after 3 d irradiation in toluene (with C_7D_8 reference) at RT

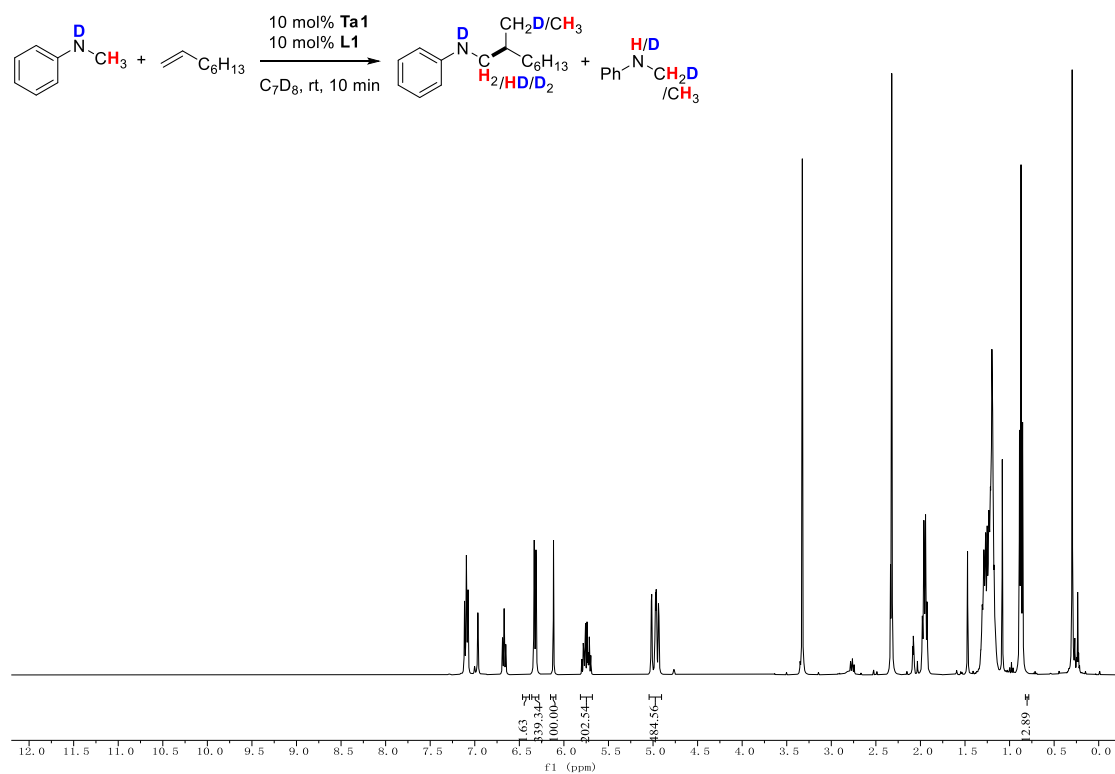


Figure S105

^1H NMR spectrum of reaction between 1-octene and PhNDCH₃ with 10 mol% TaL1 after 10 min in C₇D₈ at RT

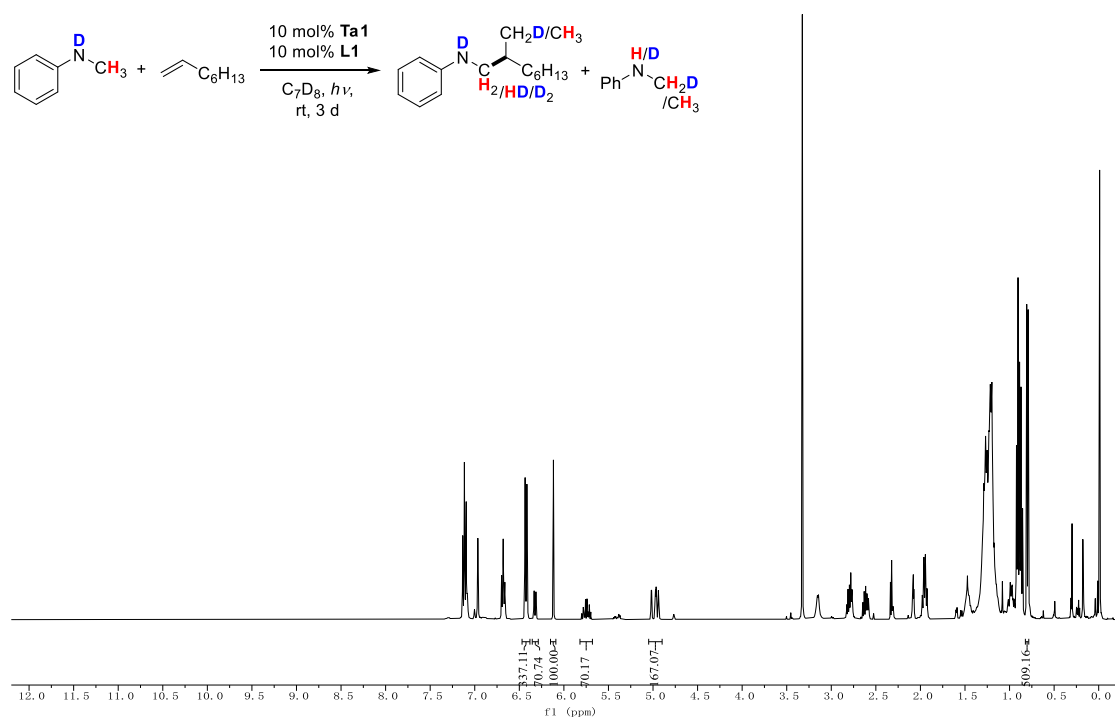


Figure S106

^1H NMR spectrum of reaction between 1-octene and PhNDCH₃ with 10 mol% TaL1 after 3 d irradiation in C₇D₈ at RT

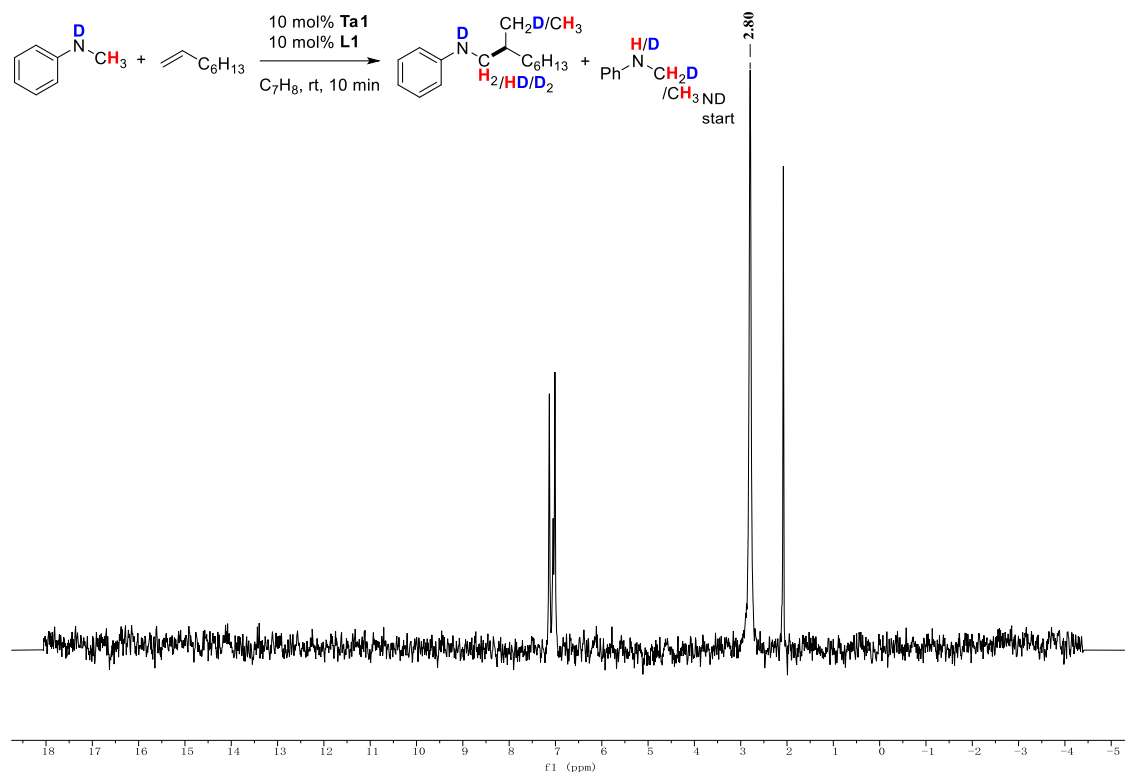


Figure S107

^2H NMR spectrum of reaction between 1-octene and PhNDCH_3 with 10 mol% TaL1 after 10 min in toluene (with C_7D_8 reference) at RT

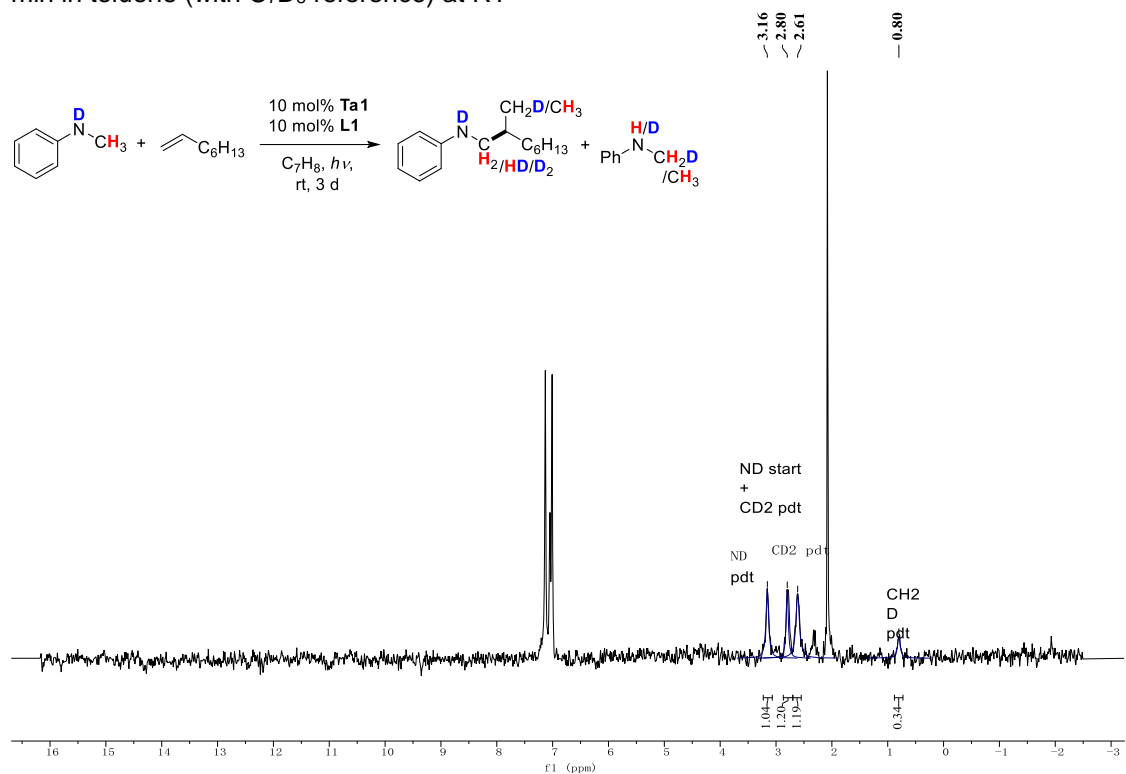
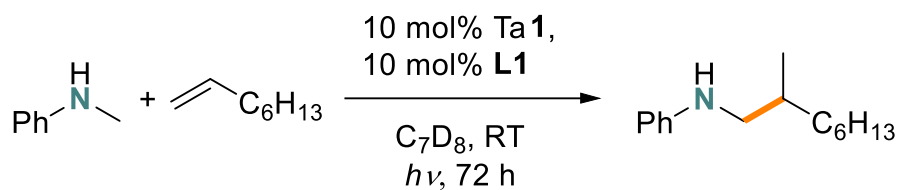


Figure S108

^2H NMR spectrum of reaction between 1-octene and PhNDCH_3 with 10 mol% TaL1 after 3 d irradiation in toluene (with C_7D_8 reference) at RT

S8. GC-MS Reports

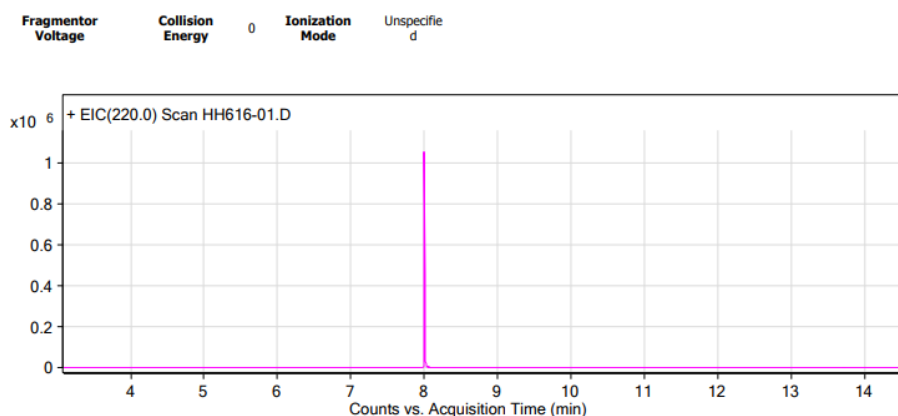
S8.1



Qualitative Analysis Report

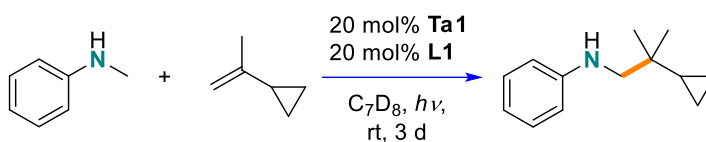
Data File	HH616-01.D	Sample Name	HH616-01
Sample Type		Position	26
Instrument Name	GCMS	User Name	
Acq Method	SCHAFFER.M	Acquired Time	8/7/2020 2:25:23 PM
IRM Calibration Status	Not Applicable	DA Method	default.m
Comment		Sample Amount	
Expected Barcode		TuneName	PCICH4.U
Dual Inj Vol	1	TuneDateStamp	Thursday, June 11, 2020 4:26:59 PM (UTC-07:00)
TunePath	D:\MassHunter\GCMS\1\5977\	OperatorName	
MSFirmwareVersion	6.00.30	Acquisition SW Version	MassHunter GC/MS Acquisition B.07.04.2260 28-Oct-2015 Copyright © 1989-2014 Agilent Technologies, Inc.
RunCompletedFlag	True		

User Chromatograms



--- End Of Report ---

S8.2

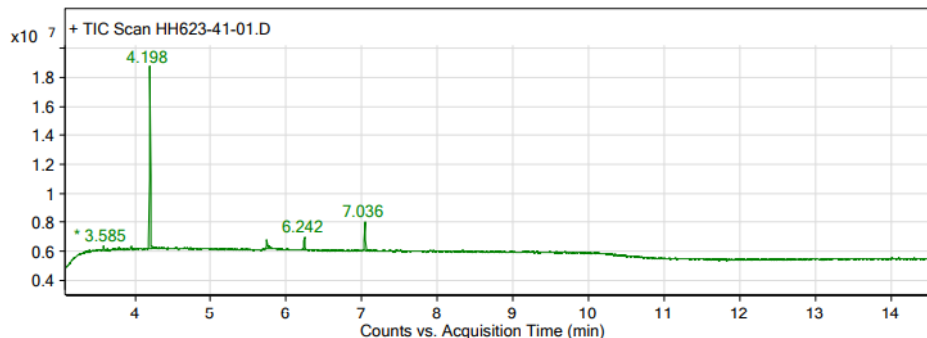


Qualitative Analysis Report

Data File	HH623-41-01.D	Sample Name	HH623-41-01
Sample Type		Position	31
Instrument Name	GCMS	User Name	
Acq Method	SCHAFFER.M	Acquired Time	9/29/2020 4:36:35 PM
IRM Calibration Status	Not Applicable	DA Method	default.m
Comment		Sample Amount	
Expected Barcode		TuneName	PCICH4.U
Dual Inj Vol	1	TuneDateStamp	Tuesday, August 11, 2020 2:58:16 PM (UTC-07:00)
TunePath	D:\MassHunter\GCMS\1\5977\	OperatorName	
MSFirmwareVersion	6.00.30	Acquisition SW Version	MassHunter GC/MS Acquisition B.07.04.2260 28-Oct-2015 Copyright © 1989-2014 Agilent Technologies, Inc.
RunCompletedFlag	True		

User Chromatograms

Fragmentor Voltage Collision Energy 0 Ionization Mode Unspecified

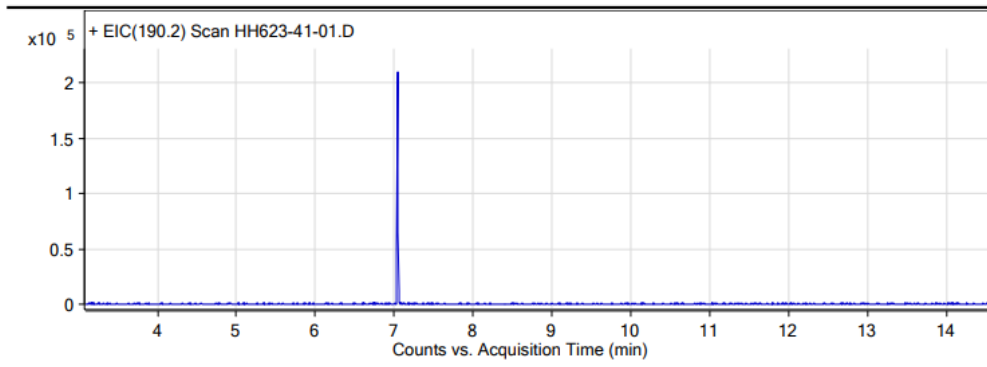


Integration Peak List

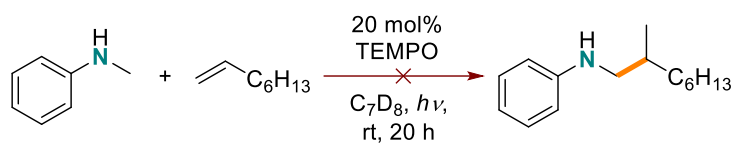
Peak	Start	RT	End	Height	Area	Area %
1	3.497	3.585	3.673	341127.91	770592.25	6.64
2	4.175	4.198	4.234	12609696.26	11596912.8	100
3	5.729	5.744	5.811	614203.73	1009783.09	8.71
4	6.226	6.242	6.257	913956.33	726330.4	6.26
5	7.02	7.036	7.067	1955924.82	1711275.7	14.76

Fragmentor Voltage Collision Energy 0 Ionization Mode Unspecified

Qualitative Analysis Report



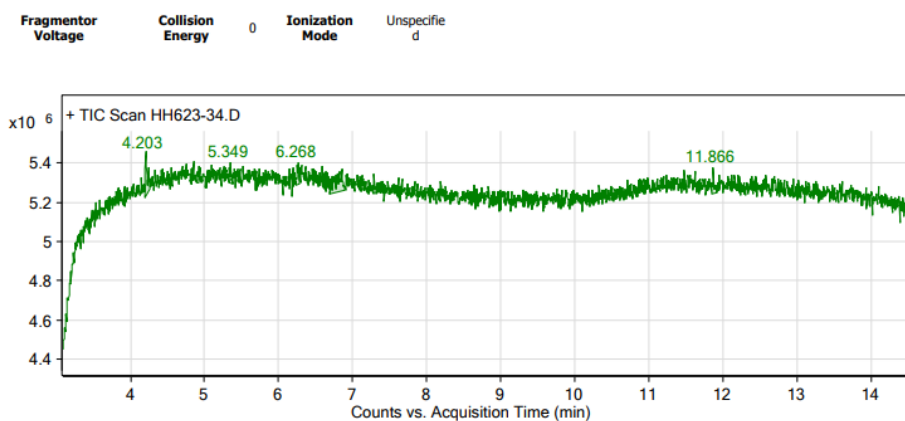
S8.3



Qualitative Analysis Report

Data File	HH623-34.D	Sample Name	HH623-34
Sample Type		Position	34
Instrument Name	GCMS	User Name	
Acq Method	SCHAFER.M	Acquired Time	8/20/2020 7:10:38 PM
IRM Calibration Status	Not Applicable	DA Method	default.m
Comment			
Expected Barcode		Sample Amount	
Dual Inj Vol	1	TuneName	PCICH4.U
TunePath	D:\MassHunter\GCMS\1\5977\	TuneDateStamp	Tuesday, August 11, 2020 2:58:16 PM (UTC-07:00)
MSFirmwareVersion	6.00.30	OperatorName	
RunCompletedFlag	True	Acquisition SW Version	MassHunter GC/MS Acquisition B.07.04.2260 28-Oct-2015 Copyright © 1989-2014 Agilent Technologies, Inc.

User Chromatograms



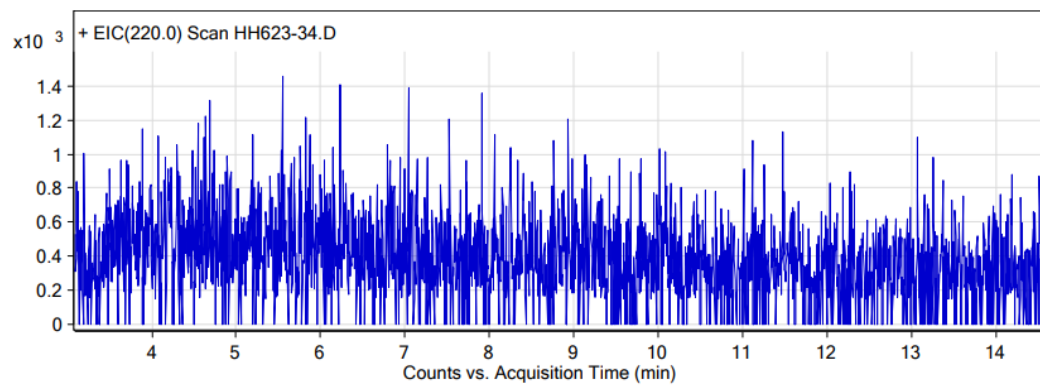
Integration Peak List

Peak	Start	RT	End	Height	Area	Area %
1	4.192	4.203	4.265	230690.11	447471.04	65.43
2	4.893	4.924	4.929	86873.23	96221.2	14.07
3	5.323	5.349	5.375	101007	139823.38	20.44
4	6.231	6.268	6.278	110415.14	184728.48	27.01
5	6.693	6.854	6.89	111378.58	683902.15	100
6	11.84	11.866	11.918	130462.33	186551.87	27.28

User Spectra

Spectrum Source	Fragmentor Voltage	Collision Energy	Ionization Mode
-----------------	--------------------	------------------	-----------------





--- End Of Report ---

S9. Literature

- (1) Gaussian 09, Revision D.01, M. J. Frisch, G. W. Trucks, H. B. Schlegel, G. E. Scuseria, M. A. Robb, J. R. Cheeseman, G. Scalmani, V. Barone, B. Mennucci, G. A. Petersson, H. Nakatsuji, M. Caricato, X. Li, H. P. Hratchian, A. F. Izmaylov, J. Bloino, G. Zheng, J. L. Sonnenberg, M. Hada, M. Ehara, K. Toyota, R. Fukuda, J. Hasegawa, M. Ishida, T. Nakajima, Y. Honda, O. Kitao, H. Nakai, T. Vreven, J. A. Montgomery, Jr., J. E. Peralta, F. Ogliaro, M. Bearpark, J. J. Heyd, E. Brothers, K. N. Kudin, V. N. Staroverov, T. Keith, R. Kobayashi, J. Normand, K. Raghavachari, A. Rendell, J. C. Burant, S. S. Iyengar, J. Tomasi, M. Cossi, N. Rega, J. M. Millam, M. Klene, J. E. Knox, J. B. Cross, V. Bakken, C. Adamo, J. Jaramillo, R. Gomperts, R. E. Stratmann, O. Yazyev, A. J. Austin, R. Cammi, C. Pomelli, J. W. Ochterski, R. L. Martin, K. Morokuma, V. G. Zakrzewski, G. A. Voth, P. Salvador, J. J. Dannenberg, S. Dapprich, A. D. Daniels, O. Farkas, J. B. Foresman, J. V. Ortiz, J. Cioslowski, and D. J. Fox, Gaussian, Inc., Wallingford CT, **2013**.
- (2) Zhao, Y.; Truhlar, D. G. *J. Chem. Phys.*, **2006**, *125*, 194101.
- (3) Weigend, F. Ahlrichs, R. *Phys. Chem. Chem. Phys.*, **2005**, *7*, 3297-3305.
- (4) Marenich, A. V.; Cramer, C. J.; Truhlar, D. G. *J. Phys. Chem. B* **2009**, *113*, 6378-6396
- (5) Lu, T.; Chen, F. *J. Comput. Chem.* **2012**, *33*, 580-592.
- (6) Humphrey, W., Dalke, A.; Schulten, K. *J. Molec. Graphics* **1996**, *14*, 33-38.
- (7) Daneshmand, P.; Rosca, S.-C.; Dalhoff, R.; Yin, K.; DiPucchio, R. C.; Ivanovich, R. A.; Polat, D. E.; Beauchemin, A. M.; Schafer, L. L. *J. Am. Chem. Soc.* **2020**, *142*, 15740–15750.
- (8) DiPucchio, R. C.; Rosca, S.-C.; Schafer, L. L. *Angew. Chem. Int. Ed.* **2018**, *57*, 3469–3472
- (9) Chong, E.; Brandt, J.W.; Schafer, L.L. *J. Am. Chem. Soc.* **2014**, *136*, 10898-10901.
- (10) Eisenberger, P.; Ayinla, R. O.; Lauzon, J. M. P.; Schafer, L. L. *Angew. Chem. Int. Ed.* **2009**, *48*, 8361-8365.
- (11) Quast, H.; Nahr, U. *Chem. Ber.* **1984**, *117*, 2761-2778.
- (12) Feng, Y.; Hussian, M.; Zhang, X.; Shi, J.; Hu, W.; Xiong, Y. *Tetrahedron* **2018**, *74*, 2669-2676

- (13) Knoke, M.; Meijere, A. *Eur. J. Org. Chem.* **2005**, *11*, 2471-2482.
- (14) Ebule, R. ; Mudshinge, S. ; Nantz, M. H. ; Mashuta, M. S. ; Hammond, G. B. ; Xu, B. *J. Org. Chem.* **2019**, *84*, 3249-3259.